National Library of Canada
Bibliothèque nationale du Canada

Canadian Theses Service
Service des thèses canadiennes

Ottawa, Canada
K1A 0N4

## NOTICE

The quality of this microform is heavily dependent upon the quality of the original thesis submitted for microfilming. Every effort has been made to ensure the highest quality of reproduction possible.

If pages are missing, contact the university which granted the degree.

Some pages may have indistinct print especially if the original pages were typed with a poor typewriter ribbon or if the university sent us an inferior photocopy.

Reproduction in full or in part of this microform is governed by the Canadian Copyright Act, R.S.C. 1970, c. C-30, and subsequent amendments.

## AVIS

La qualité de cette microforme dépend grandement de la qualité de la thèse soumise au microfilmage. Nous avons tout fait pour assurer une qualité supérieure de reproduction.

S'il manque des pages, veuillez communiquer avec l'université qui a conféré le grade.

La qualité d'impression de certaines pages peut laisser à désirer, surtout si les pages originales ont été dactylographiées à l'aide d'un ruban usé ou si l'université nous a fait parvenir une photocopie de qualité inférieure.

La reproduction, même partielle, de cette microforme est soumise à la Loi canadienne sur le droit d'auteur, SRC 1970, c. C-30, et ses amendements subséquents.

NL-339 (r. 88/04) c

Canada

UNIVERSITY OF ALBERTA

# MEASUREMENT AND EXPLOITATION OF ISCHEMIA INDUCED BY PHOTODYNAMIC THERAPY OF SOLID TUMORS

BY

RONALD B. MOORE

A THESIS

SUBMITTED TO THE FACULTY OF GRADUATE STUDIES AND RESEARCH

IN PARTIAL FULFILMENT OF THE REQUIREMENTS FOR THE DEGREE OF

DOCTOR OF PHILOSOPHY

IN

EXPERIMENTAL SURGERY

DEPARTMENT OF SURGERY

EDMONTON, ALBERTA

FALL, 1991

National Library of Canada
Bibliothèque nationale du Canada

Canadian Theses Service
Service des thèses canadiennes

Ottawa, Canada
K1A 0N4

The author has granted an irrevocable non-exclusive licence allowing the National Library of Canada to reproduce, loan, distribute or sell copies of his/her thesis by any means and in any form or format, making this thesis available to interested persons.

The author retains ownership of the copyright in his/her thesis. Neither the thesis nor substantial extracts from it may be printed or otherwise reproduced without his/her permission.

L'auteur a accordé une licence irrévocable et non exclusive permettant à la Bibliothèque nationale du Canada de reproduire, prêter, distribuer ou vendre des copies de sa thèse de quelque manière et sous quelque forme que ce soit pour mettre des exemplaires de cette thèse à la disposition des personnes intéressées.

L'auteur conserve la propriété du droit d'auteur qui protège sa thèse. Ni la thèse ni des extraits substantiels de celle-ci ne doivent être imprimés ou autrement reproduits sans son autorisation.

ISBN 0-315-70122-6

Canada

UNIVERSITY OF ALBERTA

RELEASE FORM

NAME OF AUTHOR Ronald B. Moore

TITLE OF THESIS Measurement and Exploitation of Ischemia Induced By Photodynamic Therapy of Solid Tumors

DEGREE FOR WHICH THESIS WAS PRESENTED Doctor of Philosophy

YEAR THIS DEGREE GRANTED 1991

Permission is hereby granted to THE UNIVERSITY OF ALBERTA LIBRARY to reproduce single copies of this thesis and to lend or sell such copies for private, scholarly or scientific research purposes only.

The author reserves other publication rights, and neither the thesis nor extensive extracts from it may be printed or otherwise reproduced without the author's written permission.

(SIGNED) Ronald B Moore

PERMANENT ADDRESS

4015 - 89 Street

EDMONTON, Alberta

Canada T6K 1G2

DATED: September 27, 1991

Running Title: Photodynamic Therapy - Induced Ischemia

THE UNIVERSITY OF ALBERTA

FACULTY OF GRADUATE STUDIES AND RESEARCH

The undersigned certify they have read and recommend to the Faculty of Graduate Studies and Research for acceptance, a thesis entitled "Measurement and Exploitation of Ischemia Induced by Photodynamic Therapy of Solid Tumors" submitted by Ronald B. Moore in partial fulfilment of the requirements for the degree of Doctor of Philosophy in Medical Sciences (Surgery).

J. Donald Chapman, Supervisor

Malcolm S. McPhee

James C. Russell

Alexander J. McEwan

A. Michael Rauth

Date June 21, 1991

**DEDICATION**

To My Family
And Many Mentors
Who Have
Supported
Shaped
And Guided
My Education

## 0.1 ABSTRACT

Photodynamic therapy (PDT) defines the localized treatment of neoplastic disease with "visible" light following the systemic administration of a photosensitizing drug. The photosensitizer currently undergoing Phase III Clinical Trials is Photofrin ($P_{II}$). Activation of $P_{II}$ by light results in the generation of reactive oxygen species. Recent studies have shown both direct and indirect means of cell killing resulting from membrane oxidation. The studies in this thesis investigate tumor response and indirect cell killing by the induction of tumor ischemia.

The effect of PDT on tumor perfusion in both the anaplastic (R3327-AT) and the well differentiated (R3327-H) Dunning prostatic tumor models was studied using the radiopharmaceutical, $^{99m}Tc$ hexamethylpropyleneamine oxime ($^{99m}TcHMPAO$). Scintigraphy yielded qualitative and quantitative data on tumor infarction which were light dose- and time-dependent. Regional differences in perfusion within treated and non-treated tumors were also investigated using tomography. Again light-dose-dependent volumes of infarction were demonstrated and related to measured light dosimetry.

The induction of tumor hypoxia by PDT was studied in the R3327-AT tumor using the radiopharmaceutical $^{123}I$-iodoazomycin arabinoside ($^{123}I$-IAZA). Measurements of PDT-

induced tumor hypoxia and tumor perfusion were compared. An inverse correlation of $^{99m}$TcHMPAO and $^{123}$I-IAZA signals from PDT treated tumors was demonstrated. The images obtained with $^{123}$I-IAZA demonstrate that this radiolabelled bioreductive alkylating agent (BRAA) may have clinical potential for monitoring hypoxia in tumor and other tissues. It also demonstrates that BRAAs can be targeted at PDT-induced hypoxia as adjuvant chemotherapy if administered at cytotoxic doses.

Potentiation of PDT by BRAAs was investigated. EMT-6 tumors growing in BALB/c mice were treated with PDT in the presence or absence of Etanidazole (ETAN), misonidazole (MISO), SR4233 and RSU1069. Tumor was assayed *in-vitro* for clonogenicity to quantitate the potentiation. There was little or no cell killing if the tumors were removed immediately after PDT. However, if the tumors were left *in-situ* for 24 hr prior to excision and assay, there was a light-dose-dependent cell kill that was potentiated by all the BRAAs tested. At approximately equal toxicity, ETAN was as good as any of the BRAAs studied.

*In-vitro* characterization of PDT was carried out with isolated murine endothelial and murine tumor cells using a clonogenic assay. The endothelial cells were not significantly more sensitive to PDT. Survival curves as a function of light dose demonstrated an initial shoulder

followed by exponential cell killing, both of which were dependent upon the concentration of photosensitizer and oxygen. Correlations between *in-vitro* photobiology measurements and tumor response are discussed.

Histological studies were performed on *in-vivo* and *in-vitro*, treated and non-treated R3327-AT tumor tissue. Transmission electron microscopy revealed mitochondrial changes in treated tissue when compared to non-treated tissue. Mitochondrial changes were evident in both endothelial and tumor cells and were present in both *in-vivo* and *in-vitro* specimens supporting previous hypothesis that mitochondria are a sensitive target for direct cell killing.

Overall these studies demonstrate that *in-vivo* tumor response and cell kill is secondary to ischemia after PDT with $P_{II}$ and that this ischemia can be targeted for monitoring and therapeutic gain.

**ACKNOWLEDGEMENT**

In keeping with the complexity of Photodynamic Therapy and the multidisciplinary approach at the Cross Cancer Institute, this project was made possible through the contributions of many people who willingly shared their time and expertise. I would especially like to thank my two supervisors, Drs J.D. Chapman and M.S. McPhee, for the opportunity to train in the Departments of Radiobiology and Surgery. These two people have been monumental in shaping my field of study, by examples set. Dr Chapman's boundless energy, creative ideas and formulated approach to research were inspiring. His departure to the Fox Chase Cancer Center is a big loss to the research community in Edmonton. Dr. McPhee's steadfast pursuit of excellence in research and its application to clinical medicine were motivational for this project.

Dr. A.J. McEwan and his staff in the Nuclear Medicine Department generously provided their time, expertise and equipment to allow the imaging of nearly 200 rats, that required coordinated radioisotope delivery and camera and computer time.

Drs. J.R. Mercer and R.H. Mannan collaborated by synthesizing the $^{123}$I-IAZA to study hypoxia induction by PDT.

Drs J. Tulip and M. Arnfield provided their expertise in lasers, optics and photodosimetry.

Dr. Poppema and his staff in the Pathology Department generously provided their expertise and time. Special thanks are extended to: Jan Spivak-Steele who did histological sectioning, Laith Dabbagh who did immuno-cytology, Jay Babiak who did flowcytometry and Richard Vriend who did electron microscopy for this project.

A special note of thanks goes to Dr. T. Shnitka who provided his expert opinion in the interpretation of the electron micrographs.

I would also like to thank Bert Meeker, Andrew Mokrzanowski, Kevin Small, Corrine Stobbe, Doreen Buryn and Jane Lee, who provided much-appreciated assistance with various technical aspects of the project.

I am especially grateful to Cindy Johns and Bev Chapman for typing the manuscript and Frank LoCicero for the photography.

Financial support for this research project was provided by the Alberta Cancer Board, the Northern Alberta Urology Foundation and the Alberta Heritage Foundation for Medical Research (AHFMR), by an AHFMR Scholarship.

## TABLE OF CONTENTS


CHAPTER I INTRODUCTION ..... 1

CHAPTER II NUCLEAR MEDICINE ASSAYS OF PDT-INDUCED PERFUSION SHUTDOWN..... 18

2.1 INTRODUCTION..... 18

2.2 MATERIALS AND METHODS..... 20
2.2.1 TUMOR MODEL..... 20
2.2.2 ANAESTHETICS..... 22
2.2.3 PHOTOSENSITIZER..... 23
2.2.4 INTERSTITIAL PHOTOTHERAPY..... 24
2.2.5 TUMOR TEMPERATURE..... 24
2.2.6 RADIOPHARMACEUTICALS..... 26
2.2.7 SCINTIGRAPHY..... 27
2.2.8 TOMOGRAPHIC IMAGING..... 28
2.2.9 DOSIMETRY..... 28
2.2.10 EXPERIMENTAL PROTOCOL..... 29
2.2.10.1 PERFUSION STUDIES..... 29
2.2.10.2 HYPOXIA STUDIES..... 29
2.2.11 STATISTICAL ANALYSIS..... 30

2.3 RESULTS..... 30
2.3.1 PERFUSION STUDIES..... 30
2.3.2 HYPOXIA STUDIES..... 42

2.4 DISCUSSION..... 48
2.4.1 PERFUSION STUDIES..... 48
2.4.2 HYPOXIA STUDIES..... 52

2.5 CONCLUSION..... 57

CHAPTER III POTENTIATION OF PDT WITH BIOREDUCTIVE ALKYLATING AGENTS..... 59

3.1 INTRODUCTION..... 59

3.2 MATERIALS AND METHODS..... 60
3.2.1 TUMOR MODEL..... 60
3.2.2 ANAESTHETICS..... 61
3.2.3 PHOTOSENSITIZER..... 61
3.2.4 BIOREDUCTIVE ALKYLATING AGENTS... 62
3.2.5 INTERSTITIAL PHOTOTHERAPY..... 62
3.2.6 *IN-VITRO* CLONOGENIC ASSAY..... 63
3.2.7 EXPERIMENTAL PROTOCOL..... 65

3.3 RESULTS..... 66

3.4 DISCUSSION..... 71

3.5 CONCLUSION..... 74

CHAPTER IV *IN-VITRO* PHOTOBIOLOGY..... 76

4.1 INTRODUCTION..... 76

4.2 MATERIALS AND METHODS..... 78
4.2.1 CELL CULTURE..... 78
4.2.2 CELL CHARACTERIZATION..... 81
4.2.3 PHOTOSENSITIZER..... 84
4.2.4 PHOTOSENSITIZER UPTAKE..... 84
4.2.5 PHOTODYNAMIC TREATMENT..... 86
4.2.6 CLONOGENIC CELL SURVIVAL..... 87

4.3 RESULTS..... 89
4.3.1 CELL CHARACTERIZATION..... 89
4.3.2 PHOTOFRIN UPTAKE..... 91
4.3.3 CLONOGENIC CELL SURVIVAL (PHOTOFRIN UPTAKE)..... 95
4.3.4 CLONOGENIC CELL SURVIVAL ($O_2$ DEPENDENCY)..... 98

4.4 DISCUSSION..... 102

4.5 CONCLUSIONS..... 107

CHAPTER V GROSS AND MICROSCOPIC PATHOLOGY OF CELLULAR DAMAGE BY PDT..... 108

5.1 INTRODUCTION..... 108

5.2 MATERIALS AND METHODS..... 109
5.2.1 TUMOR MODEL..... 109
5.2.2 PHOTOSENSITIZER..... 109
5.2.3 LIGHT MICROSCOPY..... 109
5.2.4 ELECTRON MICROSCOPY..... 110
5.2.5 EXPERIMENTAL PROTOCOL..... 111

5.3 RESULTS..... 111
5.3.1 GROSS MORPHOLOGICAL DESCRIPTION... 111
5.3.2 MICROSCOPIC DESCRIPTION..... 112

5.4 DISCUSSION..... 121

5.5 CONCLUSIONS..... 123

CHAPTER VI GENERAL DISCUSSION..... 124

BIBLIOGRAPHY..... 132

VITA..... 154

## LIST OF TABLES

Table 2.1 Tumor/brain ratios comparing perfusion of Dunning R3327-H and R3327-AT tumors.

Table 2.2 Light dose dependent growth delay of R3327-AT tumor following PDT.

Table 2.3 Comparison of perfusion shutdown with PDT at 2 or 24 hr following $P_{II}$ administration.

Table 3.1 Cell yield and plating efficiencies of EMT-6 tumor cells after *in-vivo* PDT, with or without adjuvant bioreductive chemotherapy.

Table 4.1 Characterization of R3327-AT, EMT-6 and UNA-ME cells.

Table 4.2 *In-vitro* inactivation rates for R3327-AT, EMT-6 and UNA-ME cells.

## LIST OF FIGURES

Figure 2.1 Light micrograph of the well differentiated R3327-H tumor.

Figure 2.2 Light micrograph of the anaplastic R3327-AT tumor.

Figure 2.3 Photograph of experimental setup for treating the Dunning rat tumors.

Figure 2.4 Pre- and post-PDT $^{99m}$TcHMPAO scintigrams of the well perfused R3327-H tumor.

Figure 2.5 Pre- and post-PDT $^{99m}$TcHMPAO scintigrams of the poorly perfused R3327-AT tumor.

Figure 2.6 Region of interest (ROI) $^{99m}$TcHMPAO scintigrams demonstrating the difference in tumor perfusion.

Figure 2.7 Light dose dependency of perfusion shutdown for both the Dunning R3327-AT and R3327-H tumor.

Figure 2.8 Time dependency of perfusion shutdown for both the Dunning R3327-AT and R3327-H tumor.

Figure 2.9 Tomographic studies of perfusion shutdown and light dosimetry.

Figure 2.10 $^{99m}$TcHMPAO and $^{123}$I-IAZA scintigrams of a rat with bilateral flank tumors, treated and non-treated with PDT, comparing labels in the same animal.

Figure 2.11 $^{123}$I-IAZA scintigram of a rat bearing a large tumor of which only the caudal portion has been treated.

Figure 2.12 Tomographic scintigrams of the tumor removed from the rat in Figure 2.11 demonstrating selective intra-tumor retention of $^{123}$I-IAZA.

Figure 2.13 Linear regression plot of tumor/brain ratios of $^{123}$I-IAZA vs $^{99m}$TcHMPAO demonstrating the negative correlation in labelling.

Figure 2.14 $^{123}$I-IAZA scintigrams demonstrating the time dependency of biodistribution and hypoxia labelling.

Figure 2.15 Graph of relative tissue concentrations as a function of time and T½ of clearance.

Figure 3.1 Photograph of experimental setup for treating mice with PDT.

Figure 3.2 Graph of cell yield following PDT *in-vivo*, with or without the addition of BRAAs, as a function of light dose.

Figure 3.3 Graph of plating efficiencies as a function of light dose, with or without the addition of BRAAs.

Figure 3.4 Graph of clonogens as a function of light dose, with or without the addition of BRAAs.

Figure 4.1 Scanning electron micrograph of Dunning R3327-AT spheroid.

Figure 4.2 Photograph of *in-vitro* photo-irradiation setup.

Figure 4.3 Graph of *in-vitro* cellular $P_{II}$ uptake as a function of time.

Figure 4.4 Bar graph of *in-vivo* cellular $P_{II}$ uptake comparing the two methods of cell isolation.

Figure 4.5 *In-vitro* PDT survival curves for R3327-AT cells as a function of $P_{II}$ concentration and light exposure.

Figure 4.6 Graph of $1/D_{50}$ for UNA-ME and R3327-AT cells as a function of cellular $P_{II}$ concentration and 2 hr or 24 hr incubation.

Figure 4.7 *In-vitro* PDT survival curves for UNA-ME cells as a function of $O_2$ concentration and light exposure.

Figure 4.8 $O_2$ Km plot for UNA-ME cells.

Figure 5.1 Postmortem photograph of a rat sacrificed 24 hr post-PDT.

Figure 5.2 Postmortem photograph of a rat that died 3 days post-PDT.

Figure 5.3 Transmission electron micrographs of *in-vivo* PDT treated and non-treated R3327-AT tumor tissue (magnification: A x 3000; B x 3000).

Figure 5.4 Transmission electron micrographs of *in-vivo* PDT treated and non-treated R3327-AT tumor tissue (magnification: A x 9000; B x 4500).

Figure 5.5 Transmission electron micrographs of *in-vitro* PDT treated and non-treated R3327-AT tumor cells (magnification: A x 4500; B x 4500).

Figure 5.6 Transmission electon micrographs of *in-vitro* PDT treated and non-treated R3327-AT tumor cells (magnification: A x 10500; B x 10500).

Figure 5.7 Transmission electron micrographs of *in-vitro* PDT treated R3327-AT tumor cells receiving 3.0 $J/cm^2$ (magnification: A x 4500; B x 45000).

Figure 6.1 Graph of 630 nm and 789 nm light attenuation in Dunning R3327-H and R3327-AT tumors.

## LIST OF ABBREVIATIONS

| | |
|---|---|
| ADP | adenosine diphosphate |
| ATP | adenosine triphosphate |
| BME | Eagle's basal medium |
| BRAA | bioreductive alkylating agent |
| $dH_2O$ | distilled water |
| DHE | dihematoporphyrin ether/ester |
| DTNB | Ellman's Reagent 5,5-Dithiobis-(2-nitrobenzioc acid) |
| EM | electon microscopy |
| EMT-6 | experimental mammary tumor |
| ER | enhancement ratio |
| ETAN | etanidazole |
| FCS | fetal calf serum |
| GBq | gigabecqueral |
| GSH | glutathione |
| HBSS | Hank's balanced salt solution |
| HDL | high density lipoprotein |
| HMPAO | hexamethylpropyleneamine oxime |
| HP | hematoporphyrin |
| HpD | hematoporphyrin derivative |
| HVD | hydroxyethylvinyldeuteroporphyrin |
| IAZA | iodoazomycin arabinoside |
| KeV | kiloelectron volts |
| LDL | low density lipoprotein |
| MBq | megabecqueral |
| MEM | minimal essential media |
| MISO | misonidazole |
| NADPH | nicotinamide-adenine dinucleotide phosphate |
| NSAID | non-steroidal anti-inflamatory drug |
| $P_{II}$ | photofrin |
| PBS | phosphate buffered saline |
| PDT | photodynamic therapy |
| RBC | red blood cell |
| RIF | radiation induced fibrosarcoma |
| ROI | region of interest |
| SDS | sodium dodecyl sulphate |
| SOD | superoxide dismutase |
| SPECT | single photon emission computed tomography |
| TCA | trichloroacetic acid |

# CHAPTER I

## INTRODUCTION

One goal of oncology is to develop a selective treatment for cancer. Currently many localized tumors can be treated by surgery and/or ionizing radiation. Certain systemic cancers can be treated by potent cytotoxins. These modalities of therapy are limited by access and host tolerance to damage of normal tissue. Current treatment regimes are striving to selectively target these relatively non-selective therapies thus sparing normal host tissue. Photodynamic therapy (PDT) is an experimental cancer treatment modality which employs tumor-localizing photosensitizers, mostly porphyrins, and their subsequent activation by light (Dougherty, 1987). Because of the reported selective nature of this form of therapy it has recently attracted a great deal of clinical interest.

To date more than 3000 patients have undergone PDT for malignant disease (Gomer *et al.*, 1989). Most patients have been advanced cases who have failed all conventional therapy and follow-up has been short-term. The major reported side effect has been cutaneous photosensitivity up to 6 weeks post-PDT (Dougherty *et al.*, 1990). A large number of reported cases come from China (Li *et al.*, 1990) and the USA (Dougherty, 1987). Although anecdotal cases of PDT for almost any anatomical site, histological grade and stage can

be found, PDT appears to be most promising for superficial disease and areas that can be reached by endoscopic means.

The most encouraging clinical results are for treatments of diffuse carcinoma *in-situ* and recurrent superficial transitional cell carcinoma of the bladder which can be effectively treated by endoscopic means (Prout *et al.*, 1987; Nseyo *et al.*, 1987; Shumaker and Hetzel, 1987; Benson, 1985). Similarly there have been preliminary reports on the use of PDT for malignant mesothelioma (Lofgren *et al.*, 1991; Pass *et al.*, 1990). Endobronchial tumors and early lung cancer have responded favorably (Balchum *et al.*, 1984a; Lam *et al.*, 1986; Edell and Cortese, 1987). Chest wall metastasis from breast cancer following surgery and radiotherapy can be treated (Dougherty *et al.*, 1978; 1979). Cutaneous and subcutaneous malignant neoplasms have a good response rate dependent on their size (McCaughan *et al.*, 1989). Kennedy *et al.* (1990) have treated 82 patients with basal cell carcinoma using topical application of the porphyrin precursor 5-aminolevulinic acid with a 90% complete response at 3-4 months.

PDT requires 3 components for cytotoxicity; (1) An adequate amount of photosensitizer (Henderson *et al.*, 1983; Chapman *et al.*, 1991c), (2) the simultaneous presence of an adequate amount of oxygen in target cells (Moan and Sommer, 1985; Mitchell *et al.*, 1985; Chapman *et al.*, 1991b) and (3) an

adequate exposure to activating light (Wilson *et al.*, 1986). Visible light initially interacts with photosensitizers to produce an excited energy state by electron spin changes. Excited heterocyclic molecules, such as porphyrins, can interact with biomolecules by both Type I and Type II photochemical pathways (Foote, 1984). Type I interactions involve free radical production as a result of electron or hydrogen transfer. These radicals can react with oxygen to produce peroxides, hydroxyl radicals and superoxide ion (Buettner and Need, 1985). Type II interactions result in singlet oxygen ($^1O_2$) generation via energy transfer to ground state $O_2$ from the excited triplet state photosensitizer. The lifetime of $^1O_2$ varies from $10^{-6}$ sec in an aqueous environment to $10^{-4}$ sec in hydrophobic environments (Wilkinson and Brummer, 1981). The involvement of $^1O_2$ in PDT has been demonstrated using $^1O_2$ quenchers such as tryptophan and 1,3-diphenylisobenzofuran (Henderson and Miller, 1986; Wieshaupt *et al.*, 1976). In these experiments the investigators demonstrated no cell kill in the presence of adequate scavenger. Intracellular protection from $^1O_2$ has also been demonstrated to result from thiols (Miller and Henderson, 1986).

Although reports of photo-inactivation date back to the frequently cited work of Raab (1900), who observed paramecium inactivation with acridine dye and light, the recent emergence of research interest in this field can

largely be attributed to Dougherty and colleagues (Dougherty, 1984a). The development of porphyrins as photosensitizers was largely their doing, in fact they are responsible for developing the only clinically approved photosensitizer today, which is, dihematoporphyrin ether (DHE).

The first account of porphyrin photosensitization dates back to Meyer-Betz (1913) who in the advancement of science injected himself and mice with hematoporphyrin and demonstrated cutaneous photosensitivity.

Hematoporphyrin (Hp) was initially used for neoplastic diagnosis. Following systemic administration Hp was shown to be selectively retained in embryonic, traumatized and tumor tissue (Figge *et al.*, 1948). These lesions were visualized by fluorescence when exposed to ultraviolet light. Lipson *et al.* (1961) working at the Mayo Clinic, improved tumor localization by acetylating Hp in 5% $H_2SO_4$ and then reducing the final product in base. The resulting mixture was termed hematoporphyrin derivative (HpD) and was used in many subsequent tumor localizing studies (Balchum *et al.*, 1984b; Benson *et al.*, 1982; Gregorie *et al.*, 1968).

In the early 1970's the photosensitizers Hp and HpD were documented as being effective in photo-inactivation of experimental rat gliomas (Diamond *et al.*, 1972) and DBA/2

Ha-SMT mice mammary tumors (Dougherty *et al.*, 1975). This led to many studies in various laboratories using locally synthesized HpD (from Lipson's description) of which the active chemical composition was unknown. Thus there was no standardization by which these early experiments could be compared. Despite the unknown chemical composition of the drug, Dougherty *et al.* (1978) initiated clinical studies of efficacy because of the dramatic response observed in experimental tumor models. In this initial study they reported a complete and partial response rate of 111 out of 113 patients with cutaneous lesions of various histology.

Eventually it was shown that HpD contains several porphyrin monomers including Hp, hydroxyethylvinyldeuteroporphyrin (HVD) and protoporphyrin, as well as an aggregated hydrophobic fraction (Dougherty *et al.*, 1984b; Kessel and Chou, 1983; Moan *et al.*, 1982; Berenbaum *et al.*, 1982). The monomers were not active in *in-vivo* biological assays and the aggregated fraction was shown to be responsible for tumor localization and photosensitization. The composition of this hydrophobic fraction has been the subject of much debate and continues to be debated. The current concensus is that it is a complex mixture of hematoporphyrin dimer, trimer, tetramer, pentamer, hexamer and their dehydration products joined by ether, ester, or carbon-carbon linkages (Bonnett and Berenbaum, 1983; Kessel, 1986b; Scourides *et al.*, 1987; Byrne *et al.*, 1990; Bonnett and Berenbaum, 1989;

Pandy and Dougherty, 1989; Pandy *et al.*, 1991). A purified form of HpD is now marketed as Photofrin$^{Tm}$ II by Quadralogic Technologies (Vancouver, BC) in conjunction with Lederle, American Cyanimid Company (Pearl River, NY). Prior to this the patent had changed hands several times. Photofrin II ($P_{II}$) contains 15-20% monomers (Hp, HVD, and Protoporphyrin) as compared to the 50% reported in crude HpD (Dougherty, 1987).

The pharmacokinetics of HpD and $P_{II}$ in mice have been studied using $^{3}H$- and $^{14}C$-labelled drug (Gomer and Dougherty, 1979; Bellnier *et al.*, 1989). $P_{II}$ and HpD are not selectively taken up by tumor tissue as often stated. These drugs are taken up by all cells, but are preferentially retained by the reticuloendothelial system where porphyrins undergo normal degradation to biliverdin and eventually to bilirubin for excretion by the hepatobiliary system. Fifty-nine percent of the drug is recovered from the feces within 48 hr. The drug is retained in experimental tumors to higher degrees than in skin, brain, lungs and muscle, with muscle retaining the least amount. Excretion of monomers and low molecular weight components is more rapid than the oligomers. Serum clearance is multiphasic with an initial rapid clearance ($T_{½}$-1 hr), an intermediate clearance ($T_{½}$-10 hr) and a slow clearance ($T_{½}$-200 hr). The slow clearance most likely represents enterohepatic circulation. The dark $LD_{50}$ in mice is about 275 mg/kg for Hpd and about half that

for $P_{II}$. The believed cause of death is liver toxicity (Dougherty, 1987). With total body light exposure the animals die from systemic shock at much lower drug doses. Initially these hydrophobic compounds are bound to albumin and demonstrate preferential binding to lipoproteins especially HDL and LDL (Kessel, 1986a). Intracellular delivery is believed to be dependent on the LDL pathway (Candide *et al.*, 1986).

Hp, HpD and $P_{II}$ have an intense absorption in the blue region of the electromagnetic spectrum (~400 nm) termed the Soret band. In addition they have 4 other absorption peaks, of decreasing magnitude, at 500 nm, 530 nm, 577 nm and 630 nm. The 400 nm absorption band is 20 times greater than the absorption at 630 nm and is more efficient at exciting the porphyrins *in-vitro*. The longer wavelength however, has better tissue penetration and is therefore more efficient *in-vivo*. Optical penetration depths, which are defined as I/Io=1/e (37%), are tissue-dependent and typically <1 mm for wavelengths <600 nm and ~ 2-4 mm at wavelengths 700-800 nm with a sharp increase at 600 nm (Wilson *et al.*, 1985). The absorption of red light in tissue is mainly by porphyrins and melanin. Therefore, lasers generating 625 - 635 nm light are used for *in-vivo* porphyrin PDT (Gomer *et al.*, 1984).

Although no one primary target has been identified at the molecular or cellular level, numerous mechanisms of *in-vitro*

cell inactivation by porphyrin PDT have been postulated. These lipophilic drugs tend to localize to membranes based on their partition coefficient, with the more lipophilic drugs being more active (Kessel, 1977, 1984). Using microspectrofluorometry porphyrins have been shown to localize to mitochondria and lysosomes (Berns *et al.*, 1982; Reyftmann *et al.*, 1986). The delivery of porphyrin to these organelles is believed to occur via LDL transport. Singlet $O_2$ generation results in lipid peroxidation of unsaturated bonds which can be protected against by various $O_2$ radical scavengers (Thomas and Girotti, 1989; Athar *et al.*, 1988). Singlet $O_2$ can also cause protein damage by covalent cross-linking, oxidation of cystine, histidine, tryptophan, methionine and tyrosine residues, with resultant loss of function (Prinsze *et al.*, 1990). Lipid peroxidation and protein oxidation cause biomembranes to leak (Grossweiner, 1984; Dubbelman and van Steveninck, 1984). This membrane damage causes autolysis from leaking lysosomal membranes which has been observed in photosensitized cells using microspectrofluorometry (Santus *et al.*, 1983). Perlin *et al.* (1985) and Hilf *et al.* (1986) have demonstrated membrane damage to mitochondria resulting in disruption of oxidative phosphorylation as measured by inhibition of proton-ATPase transport, electron transport, cytochrome c oxidase, and succinate dehydrogenase. These studies taken together suggest that membrane damage, including fatty acids and

proteins are major targets of PDT and that mitochondria and lysosomes are important intracellular targets.

Damage to DNA has also been reported following PDT. Gomer (1980; 1983) has reported the induction of sister chromatid exchanges and single strand breaks in Chinese hamster cells. Purines, especially guanine, have been shown to be susceptible to photo-oxidation and diene degradation (Foote, 1984). This damage to DNA however, is not mutagenic when compared to UV irradiation, gamma irradiation or 3-methylochlanthrene exposure (Gomer *et al.*, 1988b). In fact DNA repair deficient human fibroblasts from ataxia telangiectasia and xeroderma pigmentosum patients had the same sensitivity to *in-vitro* PDT as fibroblasts from normal patients not afflicted with these conditions (Gomer *et al.*, 1988a). The phenotypic expression of cellular inactivation is not like that observed after ionizing radiation suggesting a different primary site of inactivation, other than DNA. Thus it appears that membrane damage, in particular mitochondrial and lysosomal membranes, plays a primary role in direct PDT cytotoxicity and that cell kill is abrupt unlike mitotic cell death observed after ionizing radiation.

The mechanism of tumor response *in-vivo* however, appears to be indirect. In the early 1960's Castellani *et al.* (1963) with cinematography recorded agglutination of red blood

cells and vascular stasis in transparent frog tongue and the rat mesentery following Hp PDT. A more recent study by Star *et al.* (1986) used sandwich observation chambers to observe a light dose dependent vascular stasis in an experimental rat mammary tumor (3 mm in dia) with HpD PDT. It was noted that if stasis was not also observed in the surrounding normal tissue there was tumor regrowth. Using radiolabelled microspheres Selman *et al.* (1984) quantitatively demonstrated almost complete infarction of experimental rat bladder tumors (1 cm dia) 10 min and 24 hr post-HpD PDT. Subsequent morphological studies of this tumor model using electron microscopy and lanthanum have demonstrated loss of the endocapillary layer suggesting endothelium as a sensitive tumor target (Chaudhuri *et al.*, 1987). Henderson *et al.* (1985) assayed tumor cell clonogenicity in 2 experimental mouse tumors (5-8 mm dia) at various times post *in-vivo* PDT with $P_{II}$. If the tumors were removed immediately after treatment there was no cell kill. A time dependent decrease in clonogenicity was observed depending on the time the tumor remained *in-situ* post-PDT. The decrease in clonogenicity with time coincided with that observed for non-treated tumors made hypoxic by sacrificing the host (postmortem *in-situ* time). A subsequent study (Henderson and Fingar, 1987) estimated the degree of hypoxia by assaying for radiosensitivity post-PDT. Using fluorescein dye exclusion as a marker of perfusion Fingar and Henderson (1987) demonstrated the reciprocity of light and $P_{II}$ dose

and the need to infarct surrounding normal tissue to obtain tumor cures. Gonzalez *et al.* (1986) demonstrated potentiation of HpD PDT with the hypoxic cytotoxin misonidazole (MISO). Subsequent experiments confirmed this synergistic potentiation and demonstrated a light dose dependent binding of the $^{3}$H-MISO to tumor and normal tissue (Hirsch *et al.*, 1987). Taken together these studies indicate that tumor response is secondary to infarction.

If the vasculature is indeed the target for PDT induced response in solid tumors, experimental systems for testing new photosensitizers and for optimizing PDT must take this tumor target into account. The current trend of research is to isolate the various biological components and study them individually *in-vitro*. Such trends in photobiology have lead many investigators to predict direct mechanisms of cell killing when in fact the mechanism appears to be indirect. Another example of *in-vivo/in-vitro* discrepancy is the *in-vitro* protection of PDT cell kill by MISO (Santus *et al.*, 1991) and its *in-vivo* potentiation of tumor response (Gonzalez *et al.*, 1986). Such findings reinforce the need for whole animal models in conjunction with *in-vitro* models to study the complex nature of PDT. One experimental system which can assay PDT optimization is *in-vivo* treatment with explantation and *in-vitro* measurement of tumor cell response as described by Henderson *et al.* (1985). A second

experimental system would be the non-invasive or invasive monitoring of the degree and extent of tumor infarction.

Because the primary cellular target of PDT is not DNA, it may prove useful for treating drug and radiation resistant tumors. One such tumor is anaplastic prostate cancer. Research at the Cross Cancer Institute (CCI) has utilized the Dunning rat prostate tumor model for several years. Initial studies looked at response of the well differentiated R3327-H tumor to radiotherapy and chemotherapy. This tumor was shown to be extremely resistant to several chemotherapeutic drugs but responsive to ionizing radiation, with 25 Gy inhibiting growth (Mador *et al.*, 1982). The anaplastic R3327-AT tumor was found to be relatively resistant to radiotherapy with doses up to 50 Gy (single fraction) producing little growth delay (Thorndyke *et al.*, 1985). Preliminary studies with PDT treatment of both the R3327-H and R3327-AT tumors were dramatic, demonstrating its ability to cure even R3327-AT tumors (McPhee *et al.*, 1984). At that time it was envisioned that PDT could be applied to human prostate cancer using interstitial techniques similar to those in use for brachytherapy. Because of the volume of human prostate cancer at the time of diagnosis (>1 cm dia) and the limited penetration of 630 nm light in tissue it was realized that multiple light sources and optical dosimetry would be needed. Towards this goal multiple cylindrical fibers and

optical dosimetry have been developed to optimize the spatial geometry of light delivery (Arnfield *et al.*, 1986; 1989).

A special area of research interest at the CCI has been oxygen mimetic nitroimidazoles and tumor oxygenation status. Nitroimadazoles were initially investigated for selective radiosensitization of hypoxic cells. Subsequent clinical studies with the prototype radiosensitizer MISO revealed dose limiting neurotoxicity with little or no clinical benefit. Spin-offs of radiosensitizer investigations include the development of potent hypoxic cytotoxins and hypoxic markers (Chapman *et al.*, 1989).

The hypoxic radiosensitizer MISO was shown to potentiate ionizing radiotherapy of the R3327-AT tumor. Autoradiography with $^{14}$C-MISO demonstrated a 15-20% hypoxic fraction in the R3327-AT tumors and no evidence of hypoxia in the R3327-H tumors of similar size (Thorndyke *et al.*, 1985). The radioresistance of the R3327-AT tumor was attributed, in part, to this hypoxic fraction. Subsequent PDT studies revealed potentiation with the addition of the hypoxic cytotoxin MISO (Gonzalez *et al.*, 1986). These studies were confirmed by Hirsch *et al.* (1987) who demonstrated a 53% cure rate in the R3327-AT tumor with the addition of MISO and a 0% cure rate without. Increased binding of $^{3}$H-MISO to PDT-treated tissue was demonstrated by liquid scintillation counting and was found to be light dose dependent.

These studies prompted a study comparing NMR spectroscopy and sensitizer adduct measurements of PDT induced ischemia (Chapman et al., 1991a). $^{31}$P-NMR spectra of PDT treated tumors revealed a decrease in phosphocreatine, $\alpha$-ATP, $\beta$-ATP and $\gamma$-ATP, with an accompanying increase in inorganic phosphate (Pi). Sensitizer-adduct formation was found to correlate with [Pi]/[$\beta$-ATP] ratios, both presumably measures of tissue oxygenation status. The precision of these procedures for measuring tumor hypoxia had a limitation of ± 15%.

At the same time *in-vitro* photobiology experiments with EMT-6 tumor cells were conducted to evaluate the oxygen and photosensitizer requirement of PDT and their interaction with various nitroimidazoles. These studies established a competitive inhibition of the phototoxic process by nitroimidazoles (Santus *et al.* 1991) and demonstrated intracellular compartmentalization of $P_{II}$ requiring different $P_{II}$ and $O_2$ concentrations for cell kill (Chapman *et al.*, 1991c; 1991b).

Elsewhere on the University of Alberta campus, in collaboration with the radiobiology group at the CCI, a radio-iodinated nitroimidazole ($^{123}$I-Iodoazomycin arabinoside) was being developed to non-invasively monitor tumor hypoxia using scintigraphy (Mannan *et al.*, 1991).

The well equipped Nuclear Medicine Department at the CCI was studying cerebral perfusion using the novel marker $^{99m}$Tc-hexamethylpropyleneamine oxime (HMPAO) which had recently been shown by Hammersley *et al.* (1987) to be a good marker of tumor perfusion.

Consequently, using the available technologies this thesis project sought to answer several questions.

A. Can the extent of vascular damage induced by interstitial PDT in solid tumors be qualitatively and quantitatively measured by non-invasive nuclear medicine assays?

A non-invasive assay which can provide both functional and morphological information on PDT response is needed for clinical application of interstitial PDT. One such assay is radionuclide imaging. If the mechanism of cell death is tumor infarction then radiopharmaceuticals that monitor perfusion or hypoxia should provide the needed information. A study was therefore designed to examine the utility of $^{99m}$TcHMPAO and $^{123}$I-IAZA in monitoring PDT in both the anaplastic and well differentiated Dunning prostatic tumor models.

B. Can both first and second generation BRAAs potentiate tumor cell killing induced by PDT? And if so, which of the currently available BRAAs is most effective?

Initial studies demonstrating potentiation used MISO, which is no longer available for clinical studies because of its demonstrated neurotoxicity. Recent *in-vitro* studies have demonstrated photo-protection by BRAAs, dependent upon their lipophilicity. Second generation BRAAs are reportedly more potent hypoxic cytotoxins. Therefore an experiment that treated tumors *in-vivo* and assayed for tumor cell clonogenicity *in-vitro* was employed to quantitate the potentiation of cell killing by several currently available BRAAs.

C. Are mouse vascular endothelial cells more sensitive to PDT *in-vitro* than mouse tumor cells?

Two recent *in-vitro* studies have reported that endothelial cells are more sensitive to PDT than vascular myocytes and fibroblasts, and tumor cells. The one study looked at only the various vascular elements of bovine origin and concluded that the endothelial cells were the most sensitive component (Gomer *et al.*, 1988a). The other study compared bovine endothelial cells with human tumor cells (West *et al.*, 1990). To determine if endothelial cells are truly more sensitive than tumor cells a study was designed to compare mouse endothelial with mouse tumor cells. If endothelial cells are intrinsically more sensitive this could explain why the vasculature is the most sensitive target within tumors.

D. Can *in-vitro* photobiology data for the R3327-AT tumor cells predict tumor response *in-vivo*?

Knowing the intrinsic sensitivity of the tumor cells, as determined under strictly controlled *in-vitro* assays, may allow determination of the proportion of indirect and direct tumor cell kill *in-vivo*. A study was therefore designed to characterize the photosensitivity of the Dunning R3327-AT cells and compare them to *in-vivo* treatment parameters.

E. What can be learned by histological studies looking at early cellular events after PDT treatments *in-vivo* and *in-vitro*?

Previous histological studies described cytological changes that could occur by both direct and indirect means (ie tumor hypoxia). By comparing histological findings of tumor treated *in-vivo* and *in-vitro* the histological findings associated with direct cell kill could be discerned.

The overall aim of this project was to examine the indirect cell killing of PDT and means of potentiating this mechanism of tumor response. In addition the development of non-invasive nuclear medicine probes for monitoring PDT outcome would be most useful in rationally extending these techniques to human protocols.

# CHAPTER II

## NUCLEAR MEDICINE ASSAYS OF PDT-INDUCED PERFUSION SHUTDOWN

### 2.1 INTRODUCTION

Photodynamic therapy (PDT) has been shown to kill cells by both direct and indirect means. Direct cell killing *in-vitro* is believed to result from singlet oxygen damage to biomembranes (Bertoloni *et al.*, 1984; Grossweiner, 1984). Experimental models using erythrocytes (Deuticke *et al.*, 1988) and planar lipid bilayers (Stozhkova and Mirskii, 1990) have shown that photo-peroxidation results in leaky membranes. Thus, damage to lysosomes (Torinuki *et al.*, 1980; Volden *et al.*, 1981; Santus *et al.*, 1983 and Reyftmann *et al.*, 1986) results in cellular autolysis and damage to mitochondria (Sandberg *et al.*, 1982; Berns *et al.*, 1982 and Singh *et al.*, 1987) results in the disruption of oxidative phosphorylation. Indirect killing of cells *in-vivo* probably results from microvascular damage causing cessation in blood flow and secondary ischemic cell death (Henderson *et al.*, 1985; Selman *et al.*, 1984 and Star *et al.*, 1986).

This tumor infarction can be targeted to enhance treatments and to monitor solid tumor response to PDT. Previous studies have shown that adjuvant chemotherapy with bioreductive alkylating agents (BRAAs) potentiated tumor response to PDT (Gonzalez *et al.*, 1986; Graschew and Shopova, 1986; Hirsch *et al.*, 1987; Henry and Issacs, 1989). PDT effectiveness for producing tumor ischemia has been estimated by $^{31}$P-NMR

spectroscopy (Hilf *et al.*, 1987; Chopp *et al.*, 1990), experimental radiobiology techniques (Henderson and Fingar, 1987), blood flow measurements (Selman *et al.*, 1984; Wieman *et al.*, 1988) and sensitizer adduct formation (Hirsch *et al.*, 1987; Chapman *et al.*, 1991a).

If PDT is to become a clinical modality for solid tumor therapy, non-invasive assays which can measure the extent and degree of PDT-induced ischemia could play a major role in its development. One such technique is radionuclide imaging. The radiopharmaceutical $^{99m}$Technetium hexamethylpropyleneamine oxime ($^{99m}$TcHMPAO) was shown by Hammersley *et al.* (1987) to be a good marker of tumor perfusion in experimental animals and was used by Rowell *et al.* (1989) to assess blood flow in human lung tumors. $^{123}$Iodine-labelled iodoazomycin arabinoside ($^{123}$I-IAZA) is a radiolabelled BRAA that was shown to label hypoxic cells in mice (Mercer *et al.*, 1990). This marker is currently being evaluated for its utility as a marker of hypoxia in human cancers (Parliament *et al.*, 1991).

A study was therefore designed utilizing $^{99m}$TcHMPAO and $^{123}$I-IAZA to investigate PDT-induced ischemia in the Dunning prostatic tumors.

## 2.2 MATERIALS AND METHODS

### 2.2.1 TUMOR MODEL

The Dunning rat prostate tumor model was initially isolated by Dr. W.H. Dunning when it occurred spontaneously in a breeder rat (Dunning, 1963). Since initial isolation several sublines have been developed and well characterized (Issacs, 1987). The two sublines used in this study, designated R3327-H and R3327-AT, express the extremes of differentiation when grown as solid tumors. The R3327-H tumor was obtained from the Papinicolaou Institute (Miami, FL). It is well differentiated (Figure 2.1), hormonally sensitive, diploid and slow growing with a doubling time of 15-20 days. The R3327-AT tumor was obtained from Dr. D. Coffey of John Hopkins University (Baltimore, MD). It is anaplastic (Figure 2.2), hormonally insensitive, aneuploid and rapidly growing with a doubling time of 2-3 days.

The tumors were maintained by serial passage in F1 males from matings of Fisher 344 (female) X Copenhagen 2331 (male) rats. Ethics approval for all animal experimentation was obtained from the local animal care committee. The animals were bred by the University of Alberta Health Sciences Laboratory Animal Service from breeder stock obtained from Harlen Sprague, Dawley Inc. (Indianapolis, IN) and were cared for in accordance with the guidelines of the Canadian Council on Animal Care. Donor tumor tissue was selected from

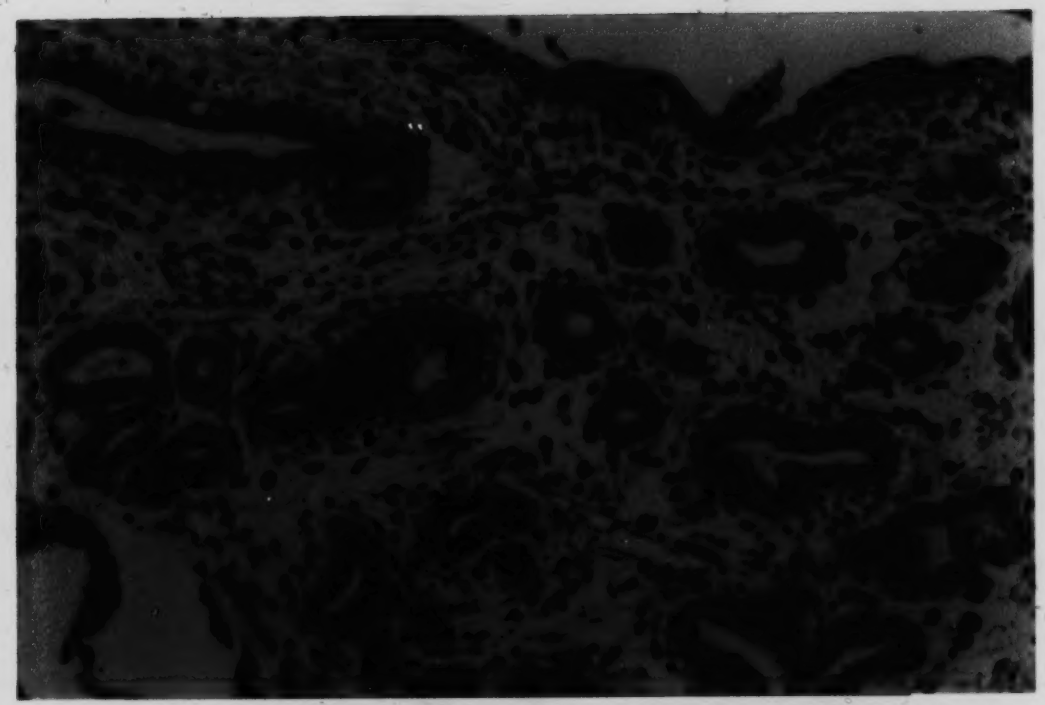

Figure 2.1: Light micrograph of the well differentiated R3327-H tumor (magnification x 160).

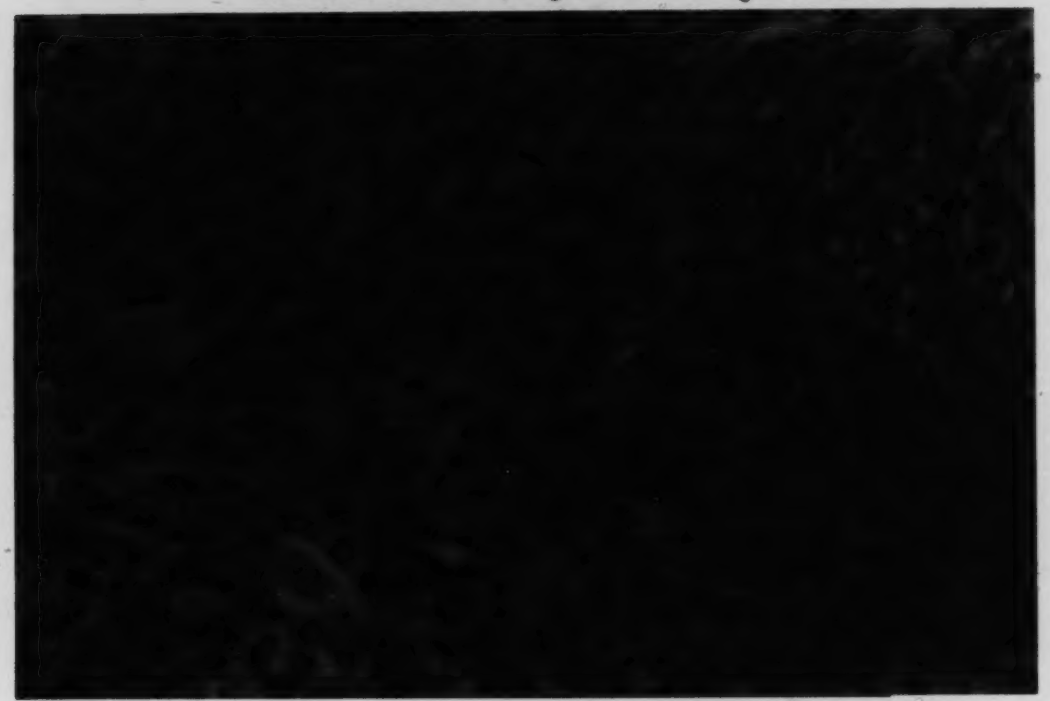

Figure 2.2: Light micrograph of the anaplastic R3327-AT tumor (magnification x 250).

tumors that had been monitored for growth characteristics and studied histologically in order to avoid tumor drift. Using aseptic techniques, selected tumor pieces of approximately 2 $mm^3$ were implanted surgically into the flanks of animals greater than 6 weeks of age as previously described (Thorndyke *et al.*, 1985). Following grafting there was a latency period of 1-2 weeks for the anaplastic tumor and 4-5 months for the well differentiated tumor. Tumor volumes were measured 3 times a week for the anaplastic tumor and once a week for the well differentiated tumor as described elsewhere (Mador *et al*, 1982). Briefly, tumor dimensions were measured with calipers in 3 mutually perpendicular directions while the animals were lightly anesthetized. Tumor volumes were then calculated using the ellipsoid formula $V = \pi/6 \times d1 \times d2 \times d3$ after a skin fold of 1.4 mm was subtracted from each diameter. Tumors were treated at volumes between 2-3 $cm^3$.

2.2.2 ANAESTHETICS

All procedures were performed under general anaesthesia. For short-term anaesthesia (for tumor measurement and tumor implantation) inhalation halothane was employed. For anaesthesia of intermediate duration (for tail vein catheterization) ketamine (75 mg/kg) and xylazine (7.5 mg/kg) were administered intraperitoneally. For long-term duration anaesthesia (for PDT and scintigraphy) the animals were induced with ketamine 12 mg/kg and xylazine 1 mg/kg IV

by an indwelling tail vein catheter and maintained with the constant infusion of ketamine (25 mg/kg per hr) and xylazine (2 mg/kg per hr). Animals undergoing long duration anaesthesia were also given atropine (0.05 mg/kg IM) to dry up their pulmonary secretions, and Lacralube$^{Tm}$ was placed in their eyes to prevent desiccation.

### 2.2.3 PHOTOSENSITIZER

Photofrin$^{Tm}$ II ($P_{II}$) was obtained from Quadrologic Technologies (Vancouver, Canada) in frozen isotonic saline (2.5 mg/ml). One bottle of this drug was thawed and dispensed into 2.5 ml aliquots and stored frozen protected from light until the time of use. $P_{II}$ was administered at 15 mg/kg IV 2 hr prior to PDT in all experiments except for those which compared the magnitude of perfusion shutdown at 2 or 24 hr following $P_{II}$ administration. The new lyophilized $P_{II}$ (lot number P89-0089) was obtained from Quadrologic Technologies (Vancouver, Canada) to replace the expended $P_{II}$ stock and was used in some of the later studies. These studies included; comparison of perfusion shutdown 2 or 24 hr post-$P_{II}$ administration and time dependency of perfusion shutdown for the H tumor. The lyophilized preparation was dissolved in 30 ml of sterile 5% dextrose and water to a final concentration of 2.5 mg/ml. It was also stored in frozen aliquots, however it was administered at 7.5 mg/kg because of its increased potency *in-vitro* (Chapman *et al.*, 1991c) and increased toxicity to mice (unpublished data).

2.2.4 INTERSTITIAL PHOTOTHERAPY

The light source used in these experiments was a Coherent CR-599 argon driven dye laser tuned to 630 nm with a maximum output of 4 watts. The monochromatic light beam from this laser was split into 8 separate beams and directed down 600 micron quartz optical fibers with 1.5 cm cylindrical diffusing tips (Arnfield *et al.*, 1986). Interstitial phototherapy was carried out using 7 of these fibers which were inserted into semi-transparent plastic needles. These needles were implanted into the tumor through a template, in a hexagonal pattern of equilateral triangles, 8 mm on edge (Figure 2.3). A Laser Guide$^{Tm}$ power meter was used to measure the power output of each fiber and to confirm the wave length, which was set using a SPEX$^{Tm}$ monochromator. The eighth fiber was then left in the power meter to continuously monitor the power output. The power output (dose rate) was kept constant at ~ 90 mW per fiber and the time of exposure varied to yield different doses as required.

2.2.5 TUMOR TEMPERATURE

Hyperthermia was shown by Kinsey *et al.* (1983) and others (Waldow and Dougherty, 1984) to potentiate photodynamic therapy. Therefore to exclude a hyperthermic effect a 27 gauge copper constantan thermocouple (Omega$^{Tm}$) was inserted into the tumor and the temperature continuously monitored during phototherapy to ensure the tumor core temperature

Figure 2.3: Photograph of experimental setup for treating the Dunning rat tumor. The infusion pump is administering ketamine and xylazine, with heparin via a lateral tail vein. Seven optical fibers with cylindrical diffusing tips are implanted through the template in pattern of equilateral triangles. A thermocouple is also inserted into the tumor.

did not exceed 40°C. Tumor heating was not a problem with a dose rate of 90 mW per fiber. However on the rare occasion when it did exceed 40°C external cooling with 70% isopropyl alcohol was employed (Gonzalez *et al.*, 1986).

2.2.6 RADIOPHARMACEUTICALS

$^{99m}$TcHMPAO was prepared from a kit (Ceretec$^{Tm}$, Amersham International) by adding 5 ml of second elution $^{99m}$Tc sodium pertechnatate at 90 MBq/ml to a lyophilized preparation of HMPAO (0.5 mg) and stannus chloride (7.6 μg). Labelling efficiency of the lipid soluble complex was assayed by a 2 phase immiscible partition of 0.9% saline and ethyl acetate (Ballinger *et al.*, 1988). A lipid phase containing greater than 90% activity was considered acceptable and the preparation was used within 30 min of preparation. One ml of the radiopharmaceutical was administered via an indwelling tail vein catheter and the catheter flushed with 1 ml of normal saline. Following administration of this marker a minimum interval of 5 min was allowed for biodistribution. HMPAO is a diastereoisomer. The lipophilic complex that forms with $^{99m}$Tc converts with time to a less lipophilic complex. This complex is retained in the tissue resulting in essentially first pass labelling with rapid clearance of the unbound drug, principally in the urine, but also by the hepatobiliary system (Neirinckx *et al.*, 1987).

The radiolabelled BRAA, $^{123}$I-IAZA was prepared by Drs. Mannan and Mercer as described elsewhere (Mannan *et al.*, 1991). Briefly, $^{123}$I-IAZA was prepared the day of administration from non-labelled IAZA using an iodine exchange reaction with sodium $^{123}$Iodide (Nordion International Inc., Vancouver, Canada). The reaction mixture was purified by radio-HPLC, with a radiochemical purity of 95-99%. Specific radioactivity ranged from 20-100 GBq/mM. The final dry product was dissolved in sterile 0.9% saline at 20-80 MBq/ml. One ml of the radiopharmaceutical was administered IV via an indwelling tail vein catheter at the time of PDT and the catheter flushed with 1 ml of 0.9% saline.

2.2.7 SCINTIGRAPHY

Static planar images were obtained by placing the animals both supine and prone onto the low energy, high resolution collimator of a General Electric (Starport$^{Tm}$) 400 AC gamma camera using windows of 129-151 KeV for $^{99m}$Tc and 148-172 KeV for the $^{123}$Iodine. Digitized images were then acquired on a Picker PCS 512 computer using a 128-128 matrix. Quantitative data on regional activity were obtained from the digitized image using the region of interest (ROI) program. When comparing ROIs the pixel area was kept constant and the posterior and anterior images were averaged to reduce subjective error as well as error resulting from overlying activity from other organs.

### 2.2.8 TOMOGRAPHIC IMAGING

To better understand local failures following interstitial PDT, tomographic imaging was performed to investigate regional differences in perfusion and hypoxia within treated and non-treated tumors. Since single photon emission computed tomography (SPECT) has a limit of resolution of about 1.5 cm, tumors were excised, solidified in a slurry of dry ice plus 70% isopropyl alcohol and serially sectioned into 2 mm slices. The slices were then placed in their proper orientation, directly on the low energy, high resolution collimator of the gamma camera and images acquired for 30 min to produce tomograms of the tumor.

### 2.2.9 DOSIMETRY

Dosimetry of light in tumors used for tomographic studies was performed to compare the delivered light dose and the regional volume of perfusion shutdown. Dosimetry measurements were obtained with a miniature light detector placed at known depths within the acetal plastic needles immediately prior to PDT. These data were interpolated by computer to produce isodose plots at several planes, perpendicular to the cylindrical diffusing fibers (Arnfield *et al.*, 1989).

2.2.10 EXPERIMENTAL PROTOCOL

2.2.10.1 Perfusion Studies

Animals in these studies had tumor implanted in the left flank only. They were randomized to specific treatments when their tumors reached volumes of 2-3 cubic cm. A lateral tail vein was cannulated percutaneously with a 24 gauge (Baxter$^{Tm}$) Teflon catheter. The catheter was capped with a PRN$^{Tm}$ heparin lock and the tail covered with a protective copper-tinned coaxial sheath.

Each animal served as its own control by being imaged with $^{99m}$TcHMPAO before PDT. Following pre-treatment imaging the tail vein catheters were injected with 0.3 cc of heparin (100 units/ml) and the rats placed in metabolic isolation cages. Eight half-lives ($T_{\frac{1}{2}}$ = 6.05 hr) of decay were allowed to pass prior to PDT and repeat imaging. Animals in the dose dependent studies were treated with PDT to varying light doses and imaged 1 hr post-treatment. Animals in the time dependency studies were treated with PDT at a constant dose of 1600 Joules and imaged at 1, 4, 8 and 24 hr post-PDT. A minimum of 3 animals were included in each group. Animals were followed post-PDT for tumor growth, except for those sacrificed for tomographic studies.

2.2.10.2 Hypoxia Studies

Animals in these studies had tumors implanted bilaterally into both flanks. Only one tumor per rat was treated and the

contralateral tumor served as a control. Animals were randomly assigned to 1 of 3 groups to be treated with PDT. Groups received 800 Joules (n=3), 1600 Joules (n=3) or 2400 Joules (n=3) when the tumors reached volumes of 2-3 $cm^3$. $^{123}$I-IAZA was administered at the time of PDT and a 10 min biodistribution image was obtained immediately post-PDT. Following imaging, the animals were placed in metabolic isolation cages to allow for the excretion of unbound $^{123}$I-IAZA and its metabolites from normal tissues. The animals were then imaged at 24 hr post-PDT for selective retention of this hypoxia marker. After the 24 hr $^{123}$I-IAZA images were acquired, animals were immediately given $^{99m}$TcHMPAO at a dose that would overwhelm the remaining $^{123}$I-IAZA activity and perfusion images acquired as previously described.

### 2.2.11 STATISTICAL ANALYSIS

All quantitative data is reported as means ± standard deviations as determined by a Texas Instruments$^{Tm}$ calculator. When required, the statistical significance between samples was determined using Students T test.

## 2.3 RESULTS

### 2.3.1 PERFUSION STUDIES

This study yielded both visual and quantitative data on PDT induced ischemia. A pre-PDT scintigram of a rat bearing the well differentiated R3327-H tumor in his left flank is shown in Figure 2.4A. This tumor is relatively well perfused when

(A) (B)

Figure 2.4: Digitized planar $^{99m}$TcHMPAO scintigrams of a rat bearing a R3327-H tumor in his left flank (A) pre-PDT and (B) 8 hr post-PDT 1600 Joules.

compared to the essential organs, with a tumor to brain ratio of ~ 0.7. Figure 2.4B is a post-PDT scintigram of the same animal 8 hr following 1600 Joules of PDT. There is virtually no perfusion to the tumor and perfusion to the surrounding normal tissue is also diminished. Likewise Figure 2.5A is a pre-PDT scintigram of a rat bearing the anaplastic R3327-AT tumor in its left flank. This tumor is less well perfused relative to the R3327-H tumor. Figure 2.5B is a post-PDT scintigram of the same animal 1 hr following 1600 Joules of PDT. Again there is a perfusion deficit observed involving the treated tumor and the surrounding normal tissue. Quantitative data on regional activity was obtained using the ROI program. Figures 2.6A and 2.6B demonstrate ROIs comparing the perfusion of the R3327-H and the R3327-AT, respectively, with brain tissue. Analyses of these tumor/brain ratios show that the well differentiated tumor, on average, is 1.75 X better perfused than the anaplastic tumor with statistical significance of $<0.001$ (Table 2.1). Quantitative analyses of pre- and post-PDT scintigrams demonstrated a light-dose-dependent and time-dependent vascular shutdown at 1 hr post-treatment for both the R3327-H and the R3327-AT tumors. Figure 2.7 shows the dose dependency of vascular shutdown for both the well differentiated and anaplastic tumor. This histogram demonstrates a stepwise decrease in percent initial perfusion as a function of increasing light dose for both tumors. Despite differences in tumor angiogenesis both

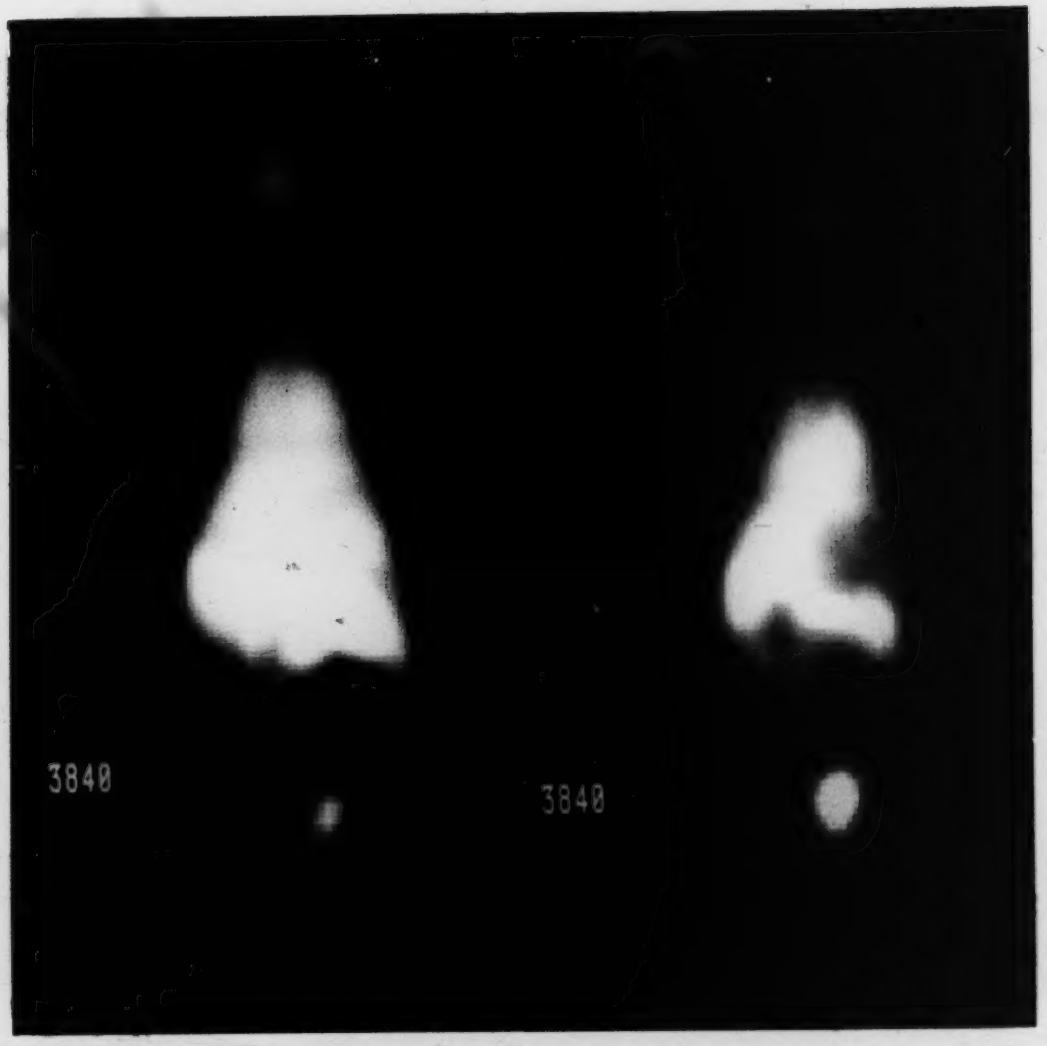


(A) (B)

Figure 2.5: Digitized planar $^{99m}$TcHMPAO scintigrams of a rat bearing a R3327-AT tumor in his left flank (A) pre-PDT and (B) 1 hr post-PDT 1600 Joules.

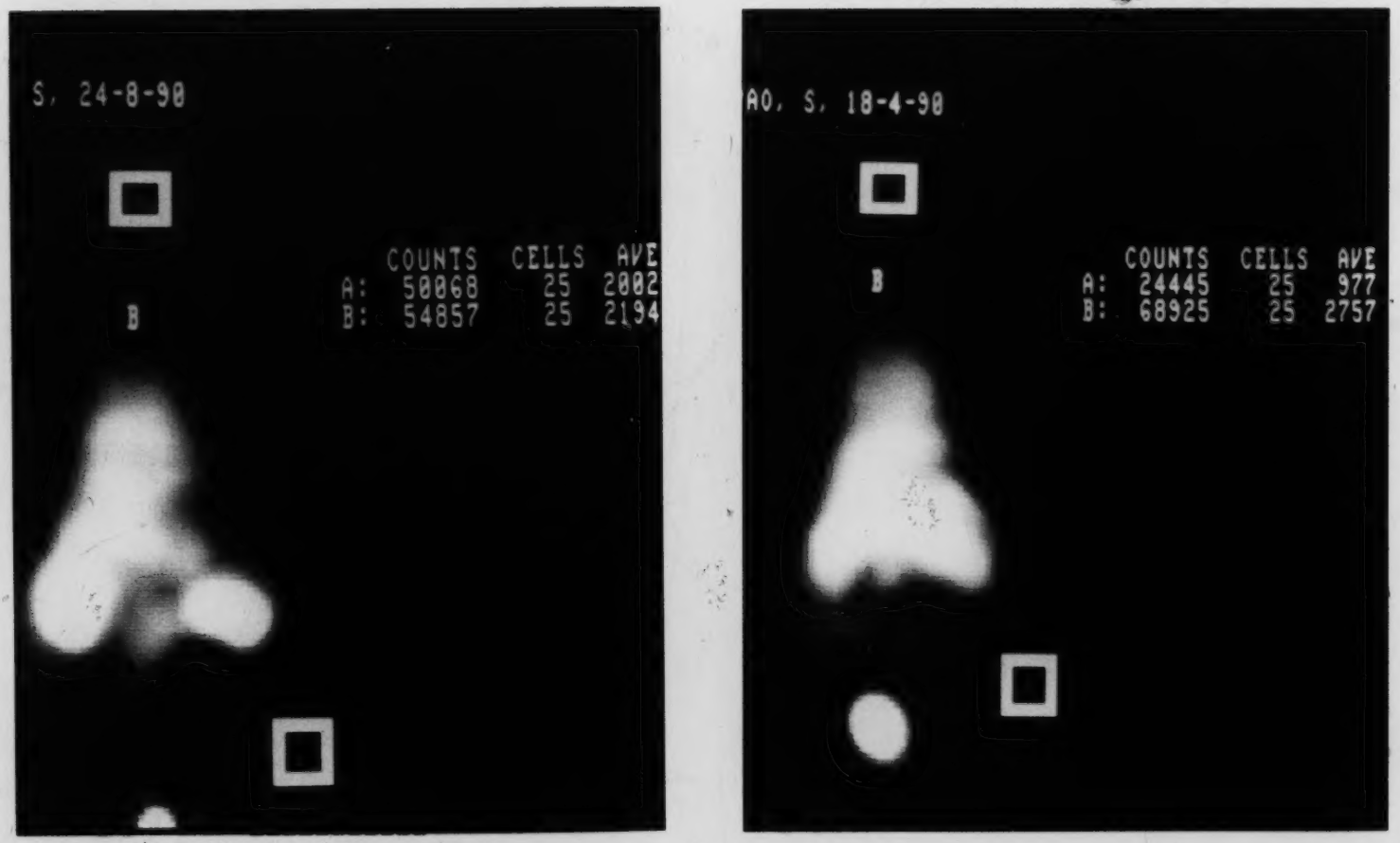


(A) (B)

Figure 2.6: Digitized planar $^{99m}$TcHMPAO scintigrams demonstrating the ROIs within tumor and brain. Comparision of tumor to brain ratios yield significant differences in perfusion of the R332/-H tumor (A) and R3327-AT tumor(B). On average the well differentiated tumor is 1.75 X better perfused than the anaplastic tumor.

TABLE 2.1

# TUMOR TO BRAIN RATIOS COMPARING PERFUSION OF R3327-AT AND R3327-H TUMORS

| R3327-H | R3327-AT |
|---|---|
| 0.623 | O.302 |
| 0.755 | 0.353 |
| 0.777 | 0.322 |
| 0.661 | 0.376 |
| 0.550 | 0.252 |
| 0.747 | 0.258 |
| 0.692 | 0.492 |
| 0.933 | 0.538 |
| 0.566 | 0.408 |
| 0.604 | 0.495 |
| 0.629 | 0.476 |

Student's t Statistic

Independent Samples n=11

| Variable: | R3327-H | R3327-AT |
|---|---|---|
| Mean: | 0.685 | 0.388 |
| Std. Deviation: | 0.112 | 0.101 |

| | | |
|---|---|---|
| Hypothesis: | t-statistic: | 6.890 |
| Ho: $\mu 1 = \mu 2$ | Degrees of Freedom: | 20 |
| Ha: $\mu 1 \neq \mu 2$ | Significance: | <0.001 |

Reject Null Hypothesis

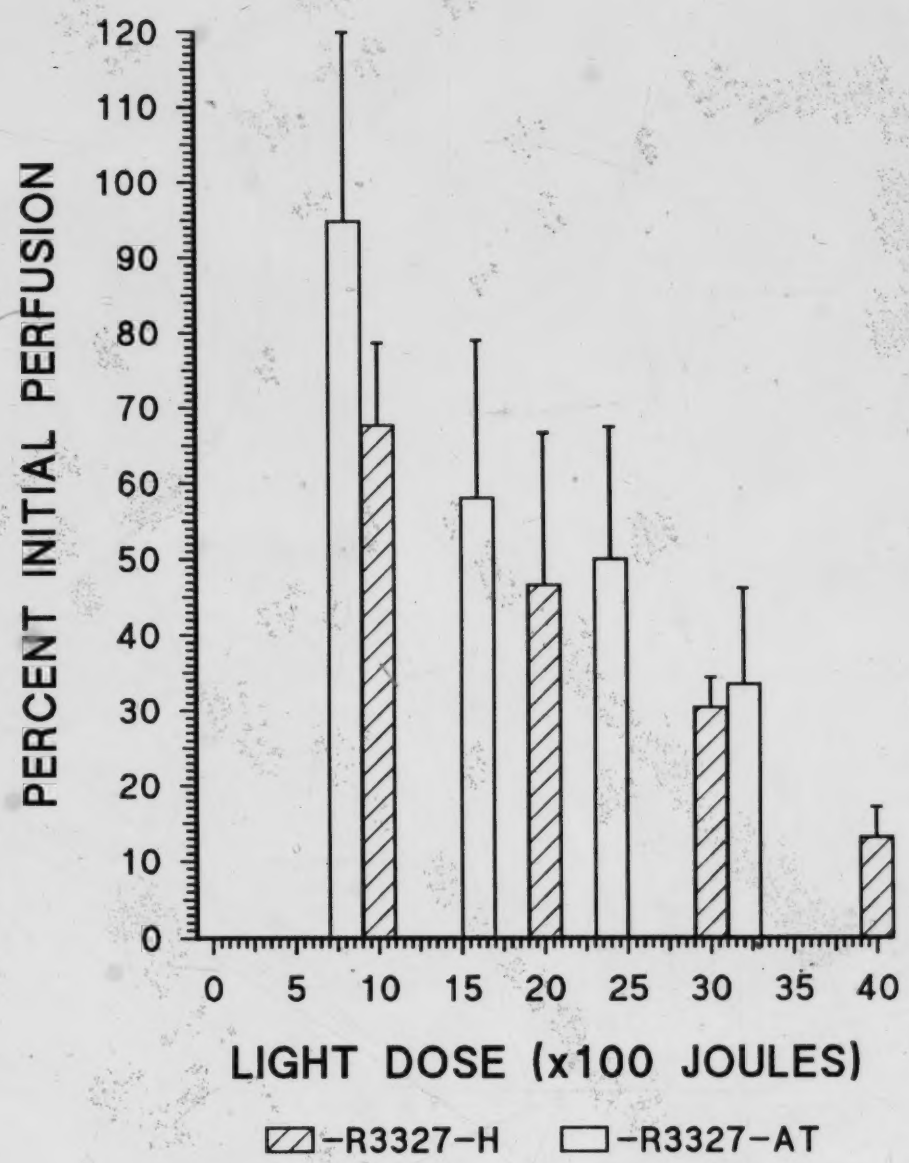


**Figure 2.7:** Histogram of percent initial perfusion (1 hr post-PDT) as a function of light-dose in the well differentiated R3327-H and anaplastic R3327-AT tumors. [error bars = sample standard deviation, minimum of three animals per group].

tumors demonstrate a similar light dose dependent vascular shutdown. An initial shoulder however, is suggested for the anaplastic tumor. This initial shoulder could be due to several factors. First, the initial dose and dose increments were decreased for the anaplastic tumor because of its increased light transmittance. Without this decrease a greater fluence would have reached the surrounding normal tissue resulting in animal morbidity. Another reason for this shoulder could be due to the increase in tumor volume between pre- and post-PDT scintigraphy in this rapidly growing tumor.

For the animals that were followed post-PDT for tumor growth the graded vascular shutdown coincided well with the observed tumor necrosis and growth delay for the R3327-AT tumor as depicted in Table 2.2.

The time dependency of perfusion shutdown was studied using both the anaplastic and well differentiated tumors. Tumors were treated at a constant light dose of 1600 Joules and imaged at various times post-PDT. The results are depicted in histogram form as percent initial perfusion versus time (Figure 2.8). Maximal shutdown occurs ~ 8 hr post-PDT and remains maximally infarcted at 24 hr.

Tomographic studies were performed on anaplastic tumors whose volumes were larger than 3 $cm^3$ so that boundaries and

TABLE 2.2

## R3327-AT GROWTH DELAY POST PDT
## TIME (DAYS) TO REACH 10X TREATMENT VOLUME

| CONTROL | 800 Joules | 1600 Joules | 2400 Joules | 3200 Joules |
|---|---|---|---|---|
| 14 | 27 | 42 | No Regrowth | No Regrowth |
| 17 | 18 | 42 | 40 | No Regrowth |
| 16 | 20 | 35 | 34 | 20 |
| 15 | 28 | 33 | 45 | |
| 17 | 42 | 22 | 45 | |
| 16 | 29 | 42 | | |
| 16 | 33 | 47 | | |
| 16 | 27 | 25 | | |
| 18 | | | | |
| 16 | | | | |
| 16 | | | | |
| 17 | | | | |
| 17 | | | | |
| 19 | | | | |
| Mean=16.3 | Mean=28.0 | Mean=36.0 | Mean=41.0<br>Cures=1 | Mean=20.0<br>Cures=2 |

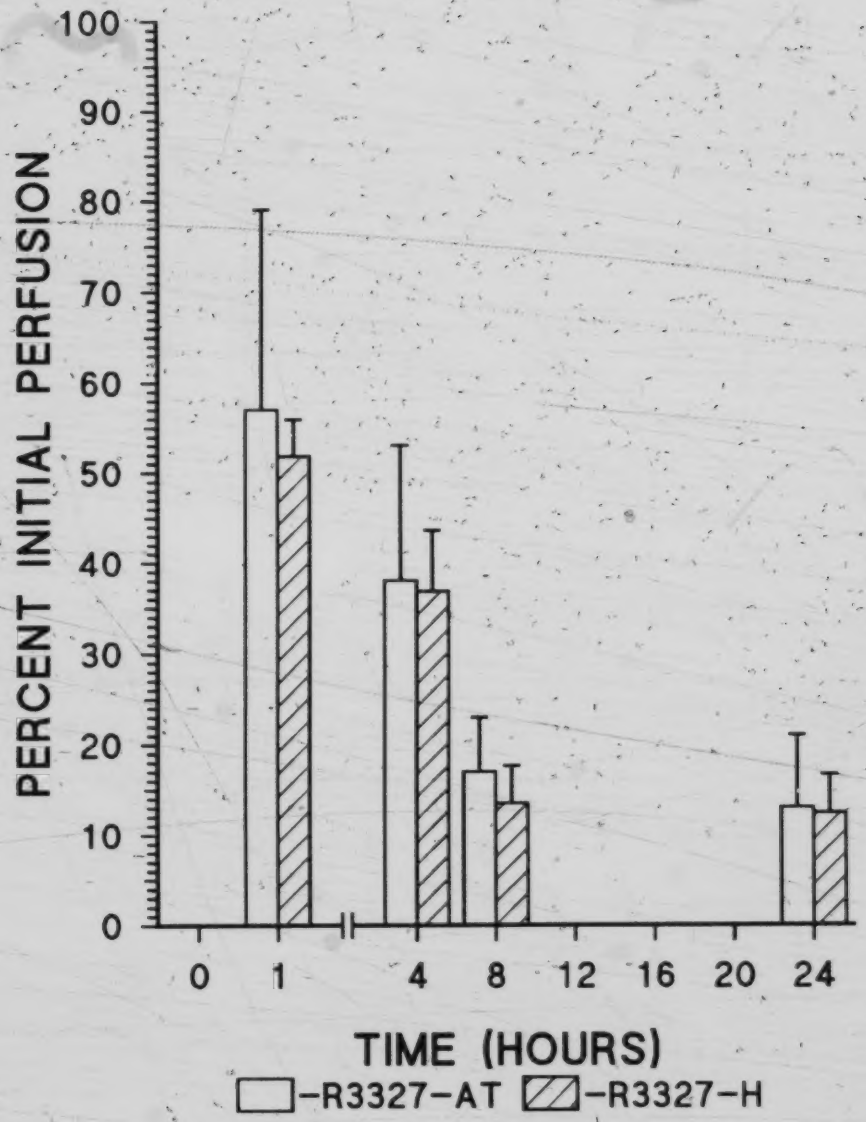


Figure 2.8: Histogram of percent initial perfusion as a function of time after PDT at a constant dose of 1600 J for both the R3327-AT and R3327-H tumors. [error bars = sample standard deviation, minimum of three animals per group].

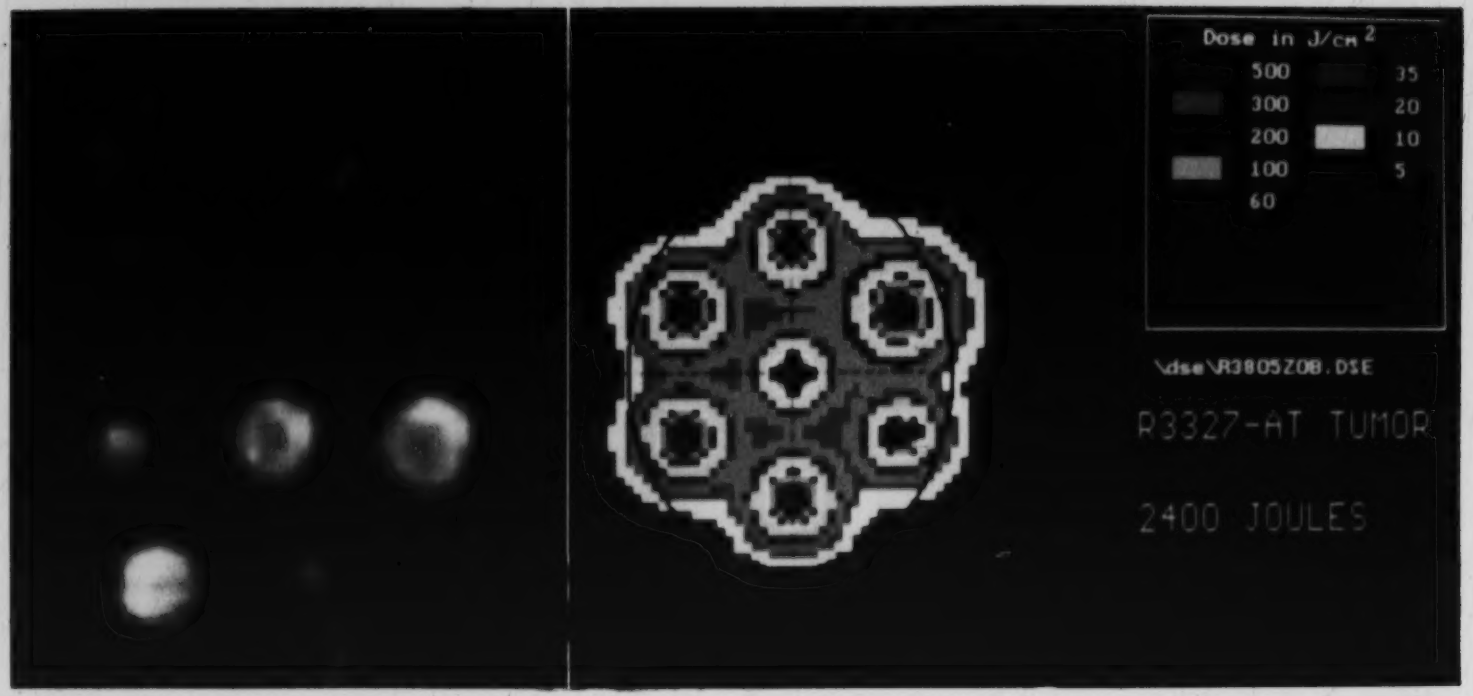


(A) (B)

Figure 2.9 (A) $^{99m}$TcHMPAO planar scintigrams of 2 mm tumor slices. The upper 2 rows are 5 sections from a tumor treated with PDT to 2400 Joules. The bottom 2 rows are 5 sections from a control tumor treated with light only. (B) Color coded isodose plot of the light dosimetry in the tumor comprising the sections in the upper 2 rows of (A). These measurements were taken in the middle of the tumor perpendicular to the diffusing fibers. The solid black line surrounding the isodose plots represents the tumor boundary.

regional differences in vascular perfusion might be observed. A control tumor receiving interstitial light only, (no photofrin) was included in each study for comparison. Both animals were treated with 2400 Joules and at 1 hr post-treatment received an equal dose of the radiopharmaceutical $^{99m}$TcHMPAO (prepared from the same kit) 1 hr post-PDT. Figure 2.9A is a scintigram of an untreated tumor (lower 2 rows) and a treated tumor (upper 2 rows). This scintigram shows a boundary of remaining perfusion in the treated tumor which probably represents the limitation of acute PDT effect within this tissue. The remaining peripheral perfusion is lower than that of untreated tumor and would be expected to decrease further with time, similar to results shown in Figure 2.8. Therefore the spatial geometry of 7 fibers in an icosohedral pattern, with the fibers 8 mm apart, will be limited to treating tumors of 2-3 $cm^3$. If $^{99m}$TcHMPAO can be considered a biological marker of "effective" light penetration, then the regional limitation of perfusion shutdown can be compared with the isodose plots of this tumor as shown in Figure 2.9B. The black line forming the ellipsoid shape around the isodose plots represents the tumor boundary as calculated from caliper measurements taken from the central needle to the periphery minus a skin flap of 0.7 mm. The minimum fluence to produce acute vascular shutdown (1 hr post-PDT) corresponds to the 35 Joules/$cm^2$ isodose plot. This limitation of "effective" 630 nm light penetration is less than 3 mm.

Since these studies were designed to measure optimal vascular damage, phototherapy was performed at 2 hr following administration of $P_{II}$ when the drug concentration is maximal in the blood pool as demonstrated by Paramsothy *et al.* (1989) using $^{99m}$TcHPD scintigraphy and Van Leengoed *et al.* (1990) using florescence angiography. However, phototherapy is normally applied 24-72 hr post-photosensitizer administration to allow for selective retention. Therefore perfusion shutdown was compared when phototherapy was applied at 2 or 24 hr following administration of $P_{II}$. Consistent with the reciprocity findings of Fingar *et al.* (1987) (ie. a ½ dose of photosensitizer requires a 2-fold increase in light-dose for equal effect and vis-a-vis) perfusion shutdown with phototherapy at 2 hr was on average 23% greater than that observed at 24 hr following the administration of $P_{II}$ (Table 2.3). The mean percent initial perfusion of the 2 treatments was significantly different by the Students T test of independent observations at a level of 0.02.

### 2.3.2 HYPOXIA STUDIES

$^{123}$I-IAZA scintigraphy also yielded qualitative and quantitative data. Figure 2.10A shows a typical color-coded $^{123}$I-IAZA scintigram 24 hr post-PDT of a rat in the prone position with bilateral R3327-AT tumors in its flanks. Very little radioactivity is retained except for the unblocked thyroid, the GI tract and the tumors. The tumor on the

TABLE 2.3

# PERCENT INITIAL PERFUSION OF R3327-AT TUMORS
## COMPARING PDT AT 2 AND 24 HR POST PII ADMINISTRATION

| 2 Hr | 24 Hr |
|---|---|
| 32.5 | 41.8 |
| 39.9 | 67.3 |
| 27.4 | 49.4 |
| 47.1 | 58.2 |
| 65.2 | 100 |
| 41.4 | 76.9 |
| 49.3 | 69.9 |

Student's t Statistic

Independent Samples n=7

| Variable: | 2 HOURS | 24 HOURS |
|---|---|---|
| Mean: | 43.3 | 66.2 |
| Std. Deviation: | 12.3 | 19.2 |

| | | |
|---|---|---|
| Hypothesis: | t-statistic: | 2.667 |
| Ho: $\mu 1 = \mu 2$ | Degrees of Freedom: | 12 |
| Ha: $\mu 1 \neq \mu 2$ | Significance: | 0.020 |

Reject Null Hypothesis

animal's left was treated to 2400 Joules and has a greater area and amount of activity, consistent with PDT-induced tumor ischemia. The control tumor on the animal's right contains a smaller amount of activity consistent with the naturally occurring hypoxic fraction of 15-25%, that contributes to the radioresistance observed for this tumor model (Thorndyke *et al.*, 1985). Figure 2.10B shows the $^{99m}$TcHMPAO perfusion scintigram of the same animal, obtained immediately after $^{123}$I-IAZA scintigraphy. The animal is in the prone position. There is virtually no activity in the treated left tumor (greater than 80% perfusion shutdown determined quantitatively). The right tumor is moderately perfused except for the central photopenic region that produces an inverse image to that obtained with $^{123}$I-IAZA.

Figure 2.11 is a $^{123}$I-IAZA scintigram of a large tumor (~ 8 $cm^3$) in the left flank. The caudad portion of this tumor has been treated with PDT to 2400 Joules and shows a greater retention of $^{123}$I-IAZA. Tomographic scintigrams of this same tumor are shown in Figure 2.12. Again greater amounts of $^{123}$I-IAZA are retained in the caudad pole of the tumor. The retention ratio of treated to non-treated tissue is ~ 2 as determined by ROI measurements.

Quantitative analysis of regional activity, 24 hr post-PDT failed to demonstrate a light dose dependent induction of tumor hypoxia as demonstrated in the perfusion study with

Right (A) Left Right (B) Left

Figure 2.10: (A) Color coded digitized scintigram of $^{123}$I-IAZA 24 hr post-PDT. The rat is prone on the collimator. The tumor in the rat's left flank has been treated with PDT to 2400 Joules. The control tumor in the right flank is untreated. (B) $^{99m}$TcHMPAO scintigram of the same animal in (A) obtained immediately after the $^{123}$I-IAZA acquisition. The rat is again prone on the collimator. The treated tumor is infarcted and not evident in the scintigram. The control tumor in the right flank is moderately perfused with a hypoxic center, producing an inverse image to that obtained with $^{123}$I-IAZA.

Figure 2.11: $^{123}$I-IAZA scintigram of a rat bearing a large R3327-AT tumor of which only the caudal portion has been treated with PDT 2400 Joules. This scintigram shows the selective retention in this region as well as activity in the unblocked thyroid and in the GI tract as a result of hepatobiliary clearance.

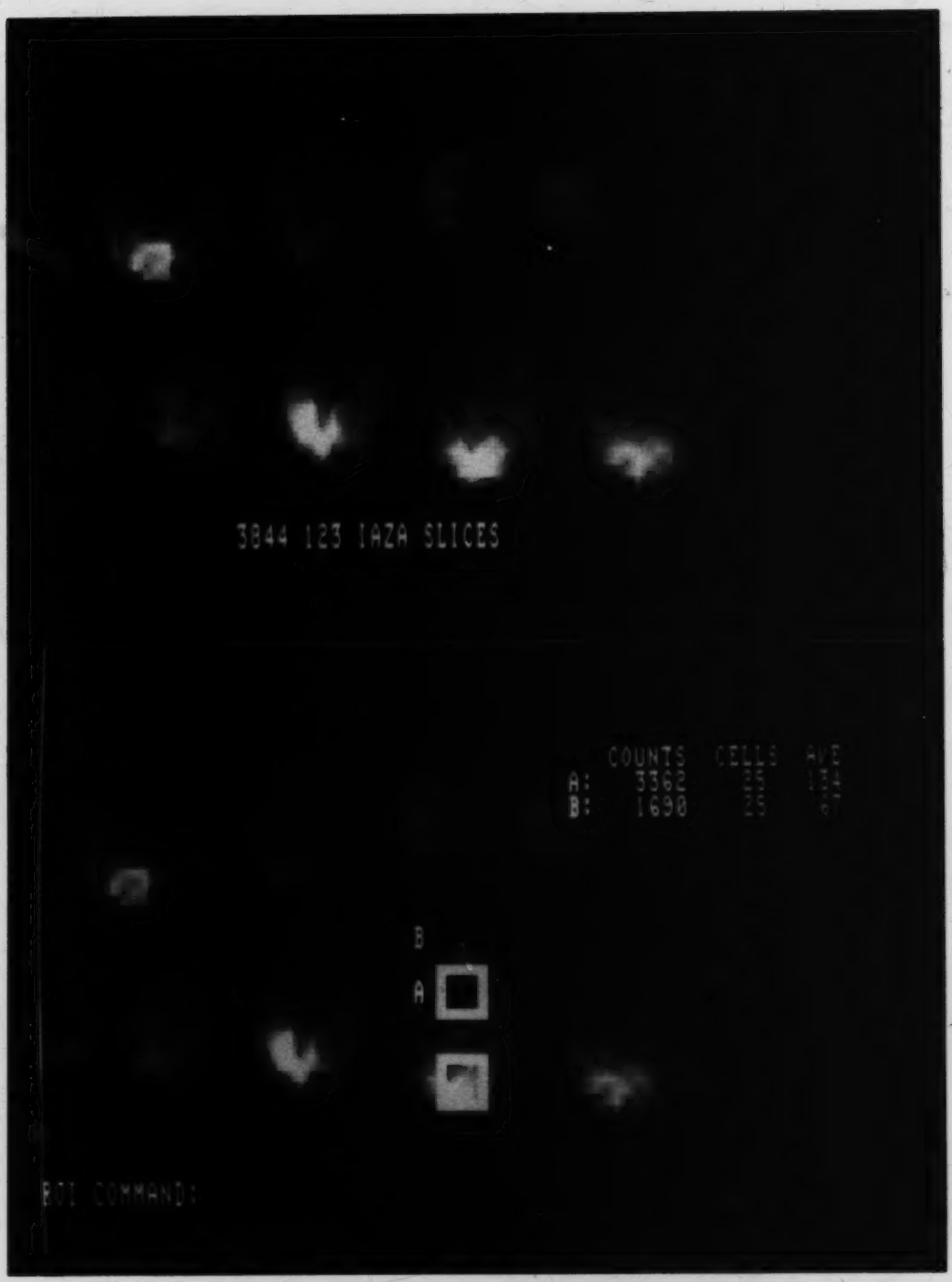


Figure 2.12: Tomographic scintigrams of the tumor removed from the rat in Figure 2.11 demonstrating selective intra-tumor retention of $^{123}$I-IAZA. ROIs with the sections reveal a 2:1 ratio of treated/non-treated tumor.

$^{99m}$TcHMPAO. Nevertheless $^{123}$I-IAZA retention, on average was 1.9 X greater in the treated tumors compared with non-treated tumors. Tumor/brain ratios of $^{123}$I-IAZA and $^{99m}$TcHMPAO, in the same animals show an inverse correlation (R=-0.783) of tumor perfusion to $^{123}$I-IAZA retention (Figure 2.13).

## 2.4 DISCUSSION

### 2.4.1 PERFUSION STUDIES

The two extremes of tumor differentiation were chosen for these experiments because of their difference in proliferation kinetics and perfusion which might influence PDT outcome. Previous experiments performed in this laboratory had shown the R3327-AT tumor to be more resistant to ionizing radiation than its well differentiated counterpart the R3327-H tumor (Mador *et al.*, 1982; Thorndyke *et al.*, 1985). This increased radioresistance was attributed to a 15-25% hypoxic fraction, demonstrated by $^{14}$C-misonidazole labelling, which was not demonstrable in well differentiated tumors of similar size. In this current study comparison of tumor/brain ratios of $^{99m}$Tc HMPAO revealed that the well differentiated tumor, on average, is 1.75 X better perfused than the anaplastic tumor (Table 2.1). Since PDT is also dependent on oxygen for cell killing (Moan and Sommer, 1985; Mitchell *et al.*, 1985) it might be hypothesized that the anaplastic tumor would also be more resistant to PDT. In fact previous studies by Hirsch *et al.*

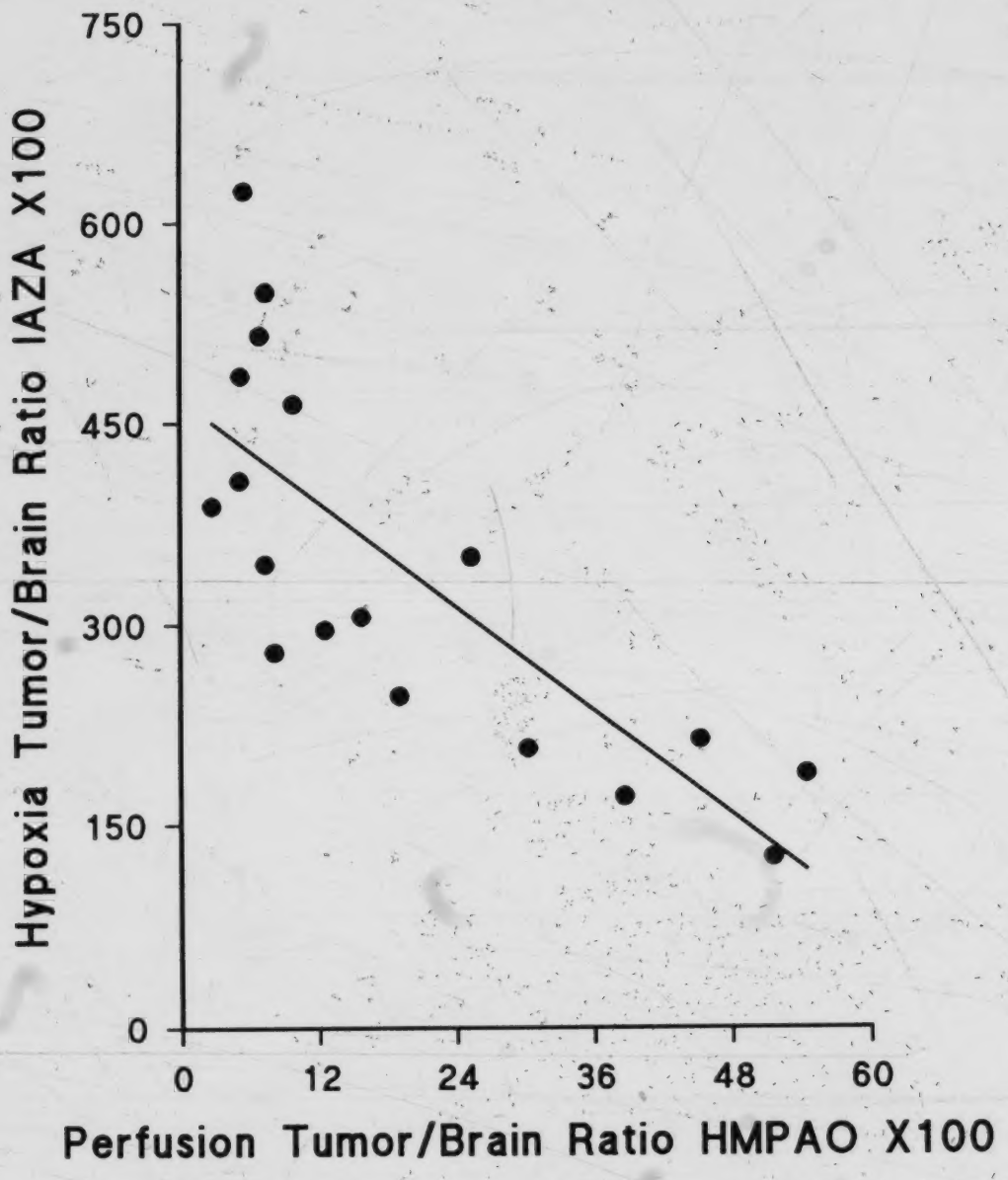


Figure 2.13: Correlation of hypoxic marker retention and perfusion. Each point represents a single tumor. The line was generated by linear regression analysis, with a correlation coefficient (r) = -0.783.

(1987) had shown R3327-H tumors to have a better response to PDT than did R3327-AT tumors. Investigation of perfusion shutdown in this study, however, failed to demonstrate any marked difference in tumor response to PDT (Figure 2.7). In relative terms both tumor sublines show similar responses in light dose- and time-dependence of perfusion shutdown. However, in absolute terms there is less perfusion in the AT tumor at all times. The difference in tumor response to PDT reported by Hirsch *et al.* (1987) could possibly be attributed to the more "hardy" R3327-AT cells surviving the induced ischemia if they were able to find limited perfusion or imbibe as a graft from surrounding normal tissue.

The tomographic studies revealed that the penetration of "effective" light to produce acute vascular shutdown (at a total dose of 2400 Joules) is limited to less than 3 mm in this experimental setup at 1 hr post-treatment. When compared with *in-vivo* light dosimetry this corresponds to a threshold dose of ~ 35 Joules/$cm^2$. However, the light dose delivered to the boundary of the remaining perfused tissue ranged from 35-100 Joules/$cm^2$. This variance results from the rapid attenuation of 630 nm light in this tissue and the limited resolution of the tomographic assay. Other potential factors producing this heterogeneity are non-uniform $P_{II}$ distribution and variable tissue oxygenation as a result of regional differences in tumor perfusion. The observed fluence values however, coincide with those reported by

other investigators. Tromberg *et al.* (1990) used transcutaneous oxygen electrodes to monitor $O_2$ consumption and depletion and reported a minimal fluence of 20-25 Joules/cm$^2$ to produce permanent vascular collapse with a $P_{II}$ dose of 10 mg/kg. Weinman *et al.* (1988) studied blood flow with laser doppler and dye exclusion techniques and reported a minimal light dose of 22.5 Joules/cm$^2$ to produce permanent vascular collapse with a $P_{II}$ dose of 10 mg/kg. Hilf *et al.* (1987) by $^{31}P$ NMR spectroscopy and Star *et al.* (1986) by sandwich observation chambers have reported higher values of 54 Joules/cm$^2$ and 72 Joules/cm$^2$ respectively, to produce permanent vascular changes.

Although near complete vascular shutdown at 1 hr post-PDT (2400 Joules total dose) was limited to a light penetration of less than 3 mm a marked decrease in perfusion was noted beyond this distance. This could result from the lower light fluence or the diffusion of vasoactive substances released by PDT (Fingar *et al.*, 1990; Henderson and Donovan, 1989) to this region of the tumor. Whatever the cause, this "moderate" hypoxia might be targeted with BRAAs, thereby potentiating PDT (Gonzalez *et al.*, 1986; Henry and Isaacs, 1989).

The time dependence of vascular shutdown in this study reveals that the maximal effect occurs - 8 hr post-PDT. An interval of this duration would allow for the delivery of

adjuvant chemotherapy post-PDT and prior to maximal shutdown. Post-PDT delivery of some BRAAs could be important to avoid interaction with the photo-oxidation processes of PDT (Santus *et al.*, 1991). This observed time prior to the perfusion nadir differs from the studies of Weinman *et al.* (1988) and Tromberg *et al.* (1990) who report maximal shutdown within 5 min. Star *et al.* (1986) however report a nadir occurring several hours and up to a day post-PDT at a fluence of 70 Joules/$cm^2$. The delayed nadir is probably more realistic with cell swelling and interstitial edema resulting in extension of perfusion shutdown.

### 2.4.2 HYPOXIA STUDIES

To assay the correlation of perfusion shutdown and induction of tumor hypoxia, covalent addition of $^{123}$I-IAZA to hypoxic cells was investigated in the R3327-AT tumor. Proof of such a correlation would demonstrate the utility of $^{123}$I-IAZA as a hypoxic marker and the ability to selectively target BRAAs as adjuvant therapy to enhance PDT.

Most BRAAs are electron affinic compounds and can mimic the radiobiological effects of oxygen by virtue of this chemical property. Misonidazole (MISO), the prototype BRAA, is selectively cytotoxic to hypoxic cells (Sutherland, 1974) and forms covalently linked adducts to cellular biomolecules at rates inversely proportional to oxygen concentration (Chapman *et al.*, 1983a). Within mammalian cells these

nitroaromatic compounds can undergo enzyme mediated reduction resulting in formation of radical anions, nitroso, hydroxylamine and amine derivatives (Biaglow *et al.*, 1986; Whitmore and Varghese, 1986). Both the nitroso (Rauth *et al.*, 1989) and the hydroxylamine (Biaglow *et al.*, 1986) products have been implicated as the toxic and adduct forming species. The possible exploitation of the above process for measuring tissue oxygenation status was proposed by Chapman, 1979; Chapman *et al.*, 1981) and has lead to the development of $^{123}$I-IAZA (Mannan *et al.*, 1991), a novel radiopharmaceutical for the detection of hypoxia.

In these studies $^{123}$I-IAZA was retained in treated tumors at an average of 1.9 X greater than that of non-treated control tumors of similar size. Unlike the perfusion studies however, scintigraphy did not reveal a light dose-dependent response to PDT with this probe. Several experimental factors could account for this.

One such factor is the cell swelling and interstitial edema that develops post-PDT even at the lower light doses. This may have precluded the required clearance of unbound drug by a trapping phenomena. Following marker binding to hypoxic tissue, a minimum of 3 pharmacological half-lives of clearance is required to demonstrate selective retention. Figures 2.14A and B are scintigrams of the same animal demonstrating this phenomenon. Figure 2.14A is an early (2

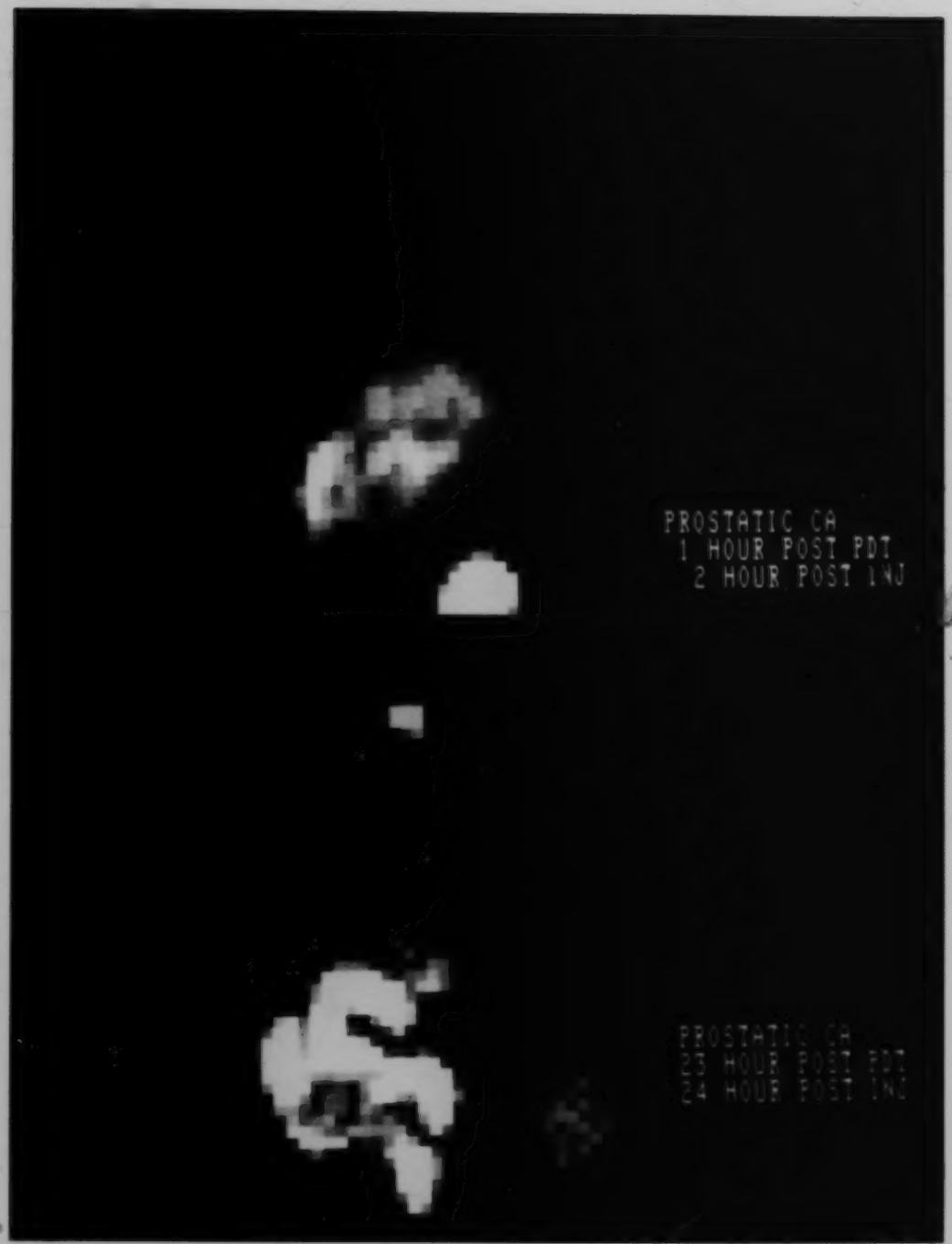


**Figure 2.14:** $^{123}$**I-IAZA scintigrams demonstrating the time dependency of biodistribution and hypoxia labelling. At 2 hr post-injection the drug is largely in the liver and urinary tract. At 24 hr post-injection there is more activity in the thyroid, activity from the liver has shifted to the bowels and there is selective retention in the treated tumor.**

hr) biodistribution image revealing most of the activity in the liver. However, after 24 hr of the activity in the liver has been cleared to the intestines and the tumor demonstrates selective retention (Figure 2.14B). A theoretical graph of this phenomena is shown in Figure 2.15. Both normal and hypoxic tissue covalently bind IAZA, but oxygenated tissue at a lower rate. Maximal binding takes place during peak serum concentrations. Imaging of this differential retention is dependent on clearance of unbound drug. Thus the proportional difference observed is dependent on the pharmacologic half-life and the radioisotopic half-life (Parliament *et al.*, 1991).

Another possible factor is that synchronous cohort tumors were used as controls rather than the same tumors. Thus, intertumor biological heterogeneity may have precluded us from demonstrating a light dose dependent effect with the small populations studied. The oxygenation status of both untreated and PDT-treated R3327-AT tumors has been shown to be extremely heterogeneous by both $^{31}P$ NMR spectroscopy and the $^{3}H$-Miso adduct procedure (Chapman *et al.*, 1991a). Tumor perfusion ($^{99m}$TcHMPAO) heterogeneity in 9 contralateral control tumors showed a mean value with ±42% standard deviation. Likewise the standard deviation of $^{123}$I-IAZA uptake into control tumors was also large at ±25%. A major limitation of $^{123}$I-IAZA imaging is the drug's hepatobiliary

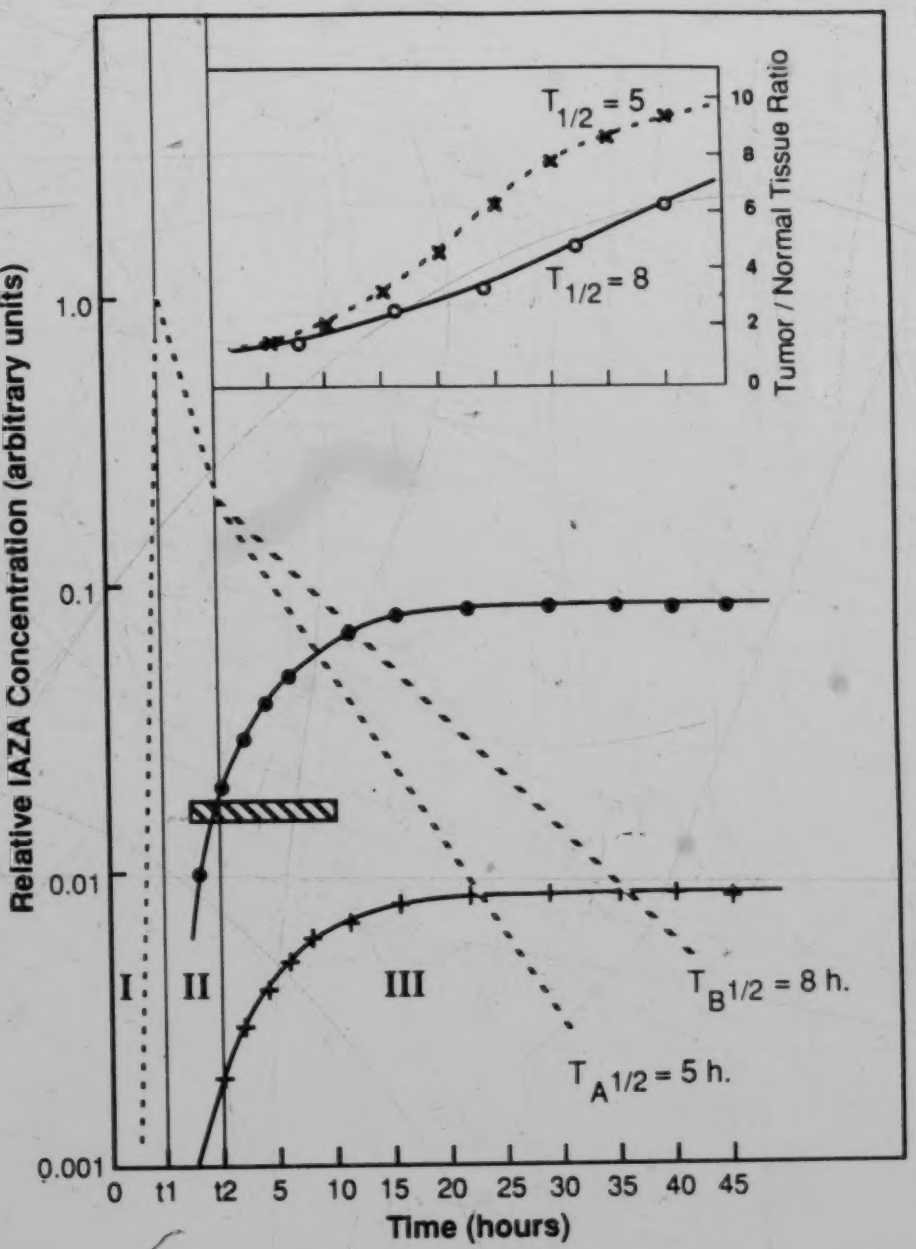


**Figure 2.15:** A log plot of IAZA binding to normal and hypoxic tissue and the pharmacological clearance of unbound drug. The inset is a plot of the observed differential as function of unbound drug clearance. The resolution of scintigraphy is dependent on the activity of the radioisotope. Thus with a very short isotope $t_{\frac{1}{2}}$ the pharmacologic clearance would limit the observation of differential binding. Legend: t1 = time of administration, t2 = time of biodistribution, ●●●● = bound IAZA in hypoxic tissue, +++ = bound IAZA in aerobic tissue, - - - = unbound IAZA in ECF. ▨▨▨▨▨ = time of maximal binding. Figure used with permission from Parliament *et al.* 1991

excretion, precluding imaging of intra-abdominal tumors. Gamma well counting of intestinal lumen tissue and its contents indicated that the majority of radioactivity was in the feces. Therefore catharsis may be effective in the elimination of this undesired signal.

The average ratios of $^{123}$I-IAZA in treated tumor/control tumor and treatment tumor/flank muscle was 1.9 and 2.9, respectively. These ratios could possibly be increased if the marker had a shorter pharmacological half-life or if a radionuclide which allowed for a greater number of pharmacologic half-lives prior to imaging could be utilized (Figure 2.15).

In this study $^{99m}$TcHMPAO had a control tumor/treated tumor ratio of 4.9. This control/treated tumor ratio is 2.5 X greater than that obtained with $^{123}$I-IAZA which had an average treated/control tumor ratio of 1.9. These data suggest that $^{99m}$TcHMPAO is the more sensitive nuclear medicine probe of PDT-induced vascular damage.

## 2.5 CONCLUSION

The studies reported here are consistent with other studies investigating vascular effects of PDT using other techniques such as: radiolabelled microspheres (Selman *et al.*, 1984), sandwich observation chambers (Star *et al.*, 1986), NMR spectroscopy (Hilf *et al.*, 1987) and dye exclusion (Fingar

*et al.*, 1987). They demonstrate that infarction is an early dose-dependent phenomenon that occurs in both well and poorly differentiated tumors, as well as in normal tissue and could account for the majority of cell kill observed following *in-vivo* PDT. Unlike other studies however this study has utilized 2 non-invasive nuclear medicine assays that provide both morphological and functional information.

Two main conclusions can be drawn from this investigation. First $^{99m}$TcHMPAO and $^{123}$I-IAZA can both be used to monitor the effects of PDT. However, $^{99m}$TcHMPAO is more sensitive than $^{123}$I-IAZA. SPECT imaging of $^{99m}$TcHMPAO would be especially useful for monitoring the degree and volume of solid tumor infarction in humans should photosensitizers and light delivery systems be developed that would permit the treatment of solid tumors greater than 3 $cm^3$. A second conclusion from these studies is that BRAAs can be targeted at PDT-induced hypoxia as adjuvant chemotherapy and might effect improved tumor response.

# CHAPTER III

## POTENTIATION OF PDT WITH BIOREDUCTIVE ALKYLATING AGENTS

### 3.1 INTRODUCTION

Bioreductive alkylating agents (BRAAs) have been shown to potentiate PDT (Gonzalez *et al.*, 1986;, Henry and Isaacs, 1989). These compounds in anaerobic mammalian cells undergo enzyme mediated reduction resulting in activated alkylating species. Misonidazole (MISO), the prototype radiosensitizer and BRAA, was shown to be selectively toxic to hypoxic cells in multicellular spheroids (Sutherland, 1974). As a result of their electron affinity nitroaromatic compounds within mammalian cells can undergo enzyme mediated reduction resulting in the formation of various radical forms (Whitmore and Varghese, 1986; Biaglow *et al.*, 1986), some of which can form covalently linked adducts to cellular biomolecules (Chapman *et al.*, 1983a; 1983b). MISO however, was found in Phase I Clinical Trials to cause dose-limiting peripheral neuropathies (Urtasun *et al.*, 1978; 1984). Following studies with MISO, several new compounds were developed to improve upon its radiosensitizing and alkylating capabilities. Etanidazole (ETAN) is a 2-nitroimidazole amide with similar chemical properties to MISO, except that it has a more hydrophilic side chain resulting in less neurotoxicity (Brown *et al.*, 1981). RSU-1069 [1-(2-nitro-1-imadazolyl)-3-(1-aziridinyl-2-propanol)] is a monofunctional alkylating agent which can be activated in cells to a bifunctional agent (Adams *et al.*, 1984). SR-

4233 (3-amino-1,2,4-benzotriazine 1,2,4-dioxide) is a BRAA that undergoes one electron reduction in hypoxic conditions resulting in free radical intermediates that produce DNA single- and double- strand breaks (Zeman *et al.*, 1986).

A study was undertaken to evaluate these compounds for potentiation of PDT using an *in-vivo/in-vitro* clonogenic assay.

## 3.2 MATERIALS AND METHODS

### 3.2.1 TUMOR MODEL

Experimental mammary tumor (EMT-6), initially obtained from Dr. R.F. Kallman of Stanford University (Stanford, CA) was used in these experiments. This tumor has been propagated both *in-vitro* and *in-vivo* in the laboratory of Dr. Chapman for several years. The tumor cells are anaplastic and aneuploid with a generation time of approximately 12 hr *in-vitro*. In tissue culture these cells are maintained as monolayers in plastic tissue culture flasks with Waymouth's media (Gibco) supplemented with 12.5% serum (10% NU-serum + 2.5% fetal calf serum) and antibiotics (50 units/ml Penicillin and 50 μg/ml Streptomycin). Stock cultures are transferred twice weekly. From these cultures single cell suspensions were prepared ($1 \times 10^6$ cells/ml in Hanks Balanced Salt Solution {HBSS}) and inoculated subcutaneously (0.1 ml) into the left flanks of BALB/c mice using a 25 gauge Tuberculin$^{Tm}$ needle. This procedure would produce an

ellipsoid tumor, 400-600 $mm^3$ in volume, in - 18-21 days time.

The BALB/c mice were obtained from the University of Alberta Health Sciences Laboratory Animal Services and cared for in accordance with the Guidelines of the Canadian Council on Animal Care. Animals were housed in shoe box cages (6 per cage) and fed Purina$^{Tm}$ rodent chow and water *ad lib*. Animals were implanted with tumor cells when they were greater than 6 weeks of age. Ethic approval for all experimentation was obtained through the local animal care committee.

### 3.2.2 ANAESTHETICS

For short-term duration anaesthesia (i.e. tumor inoculation) inhalation Metafane$^{Tm}$ (methoxyflurane) was employed. For long duration anaesthesia (i.e. phototherapy) ketamine (100 mg/kg) and xylazine (10 mg/kg) were administered interperitoneally. During anaesthesia with ketamine the animal's eyes were coated with Lacralube$^{Tm}$ to prevent desiccation.

### 3.2.3 PHOTOSENSITIZER

The photosensitizer Photofrin$^{Tm}$ ($P_{II}$) was obtained from Quadralogic Technologies (Vancouver, Canada). This lyophilized drug (lot #P89-0089) was dissolved in 30 ml of sterile 5% dextrose and water to a final concentration of 2.5 mg/ml. It was then stored frozen in aliquots, protected

from light and administered at 5 mg/kg IV by tail vein injection 2 hr prior to phototherapy.

### 3.2.4 BIOREDUCTIVE ALKYLATING AGENTS

All BRAAs were administered intraperitoneally at the time of phototherapy at approximately equitoxic doses (1/3 the reported $LD_{50}$). The bioreductive alkylating drugs were obtained in a pure powder form without carrier. All drugs were prepared in suspension immediately prior to each experiment. MISQ obtained from Hoffman La Roche (Vaudreville, Quebec) was suspended in 0.9% saline to 25 mg/ml and administered at 0.5 mg/gm. ETAN (SR-2508) was obtained from Roberts Pharmaceutical Corporation (Eaton Town, NJ) and suspended in 0.9% saline to a concentration of 75 mg/ml and administered at 1.5 mg/gm. SR-4233 and RSU-1069 were obtained from the National Institutes of Health, Division of Cancer Treatment (Bethesda, MD) and suspended in 10% DMSO (volume per volume) in 0.9% normal saline to a final concentration of 2 mg/ml and administered at 20 μg/gm.

### 3.2.5 INTERSTITIAL PHOTOTHERAPY

The light source and optical delivery system used in these experiments were the same as described in Chapter 2. Interstitial phototherapy, however, was carried out using a single fiber inserted into an acetal plastic needle which was implanted axially into the ellipsoid tumor. The ellipsoid shape of the tumors, which resulted from the lines

of tension in the skin, had an axial length that ranged between 10 and 15 mm. The width and depth of these tumors ranged between 8 and 10 mm. This experimental setup allowed the treatment of up to 7 animals at one time. However, on average, only 5 animals were treated at any one time (Figure 3.1). A Laserguide$^{Tm}$ power meter was used to determine the power output from each fiber and to confirm the wavelength. A remaining fiber was left in the power meter to continuously monitor the power output. The power output (dose rate) was kept constant at ~ 90 mW per fiber and the time of exposure varied to yield different doses as required.

### 3.2.6 *IN-VITRO* CLONOGENIC ASSAY

Animals were sacrificed, by cervical dislocation, either immediately or 24 hr following PDT and their tumors surgically excised using aseptic technique. Following excision the tumors were protected from direct light exposure. Each tumor was weighed and then transferred to the laminar flow hood, where it was mechanically broken up using a motorized dermatome blade. The minced tumor was placed in a 50 ml Erlenmyer flask containing an enzyme cocktail of collagenase (12.5 mg), DNAse (20 mg) and pronase (25 mg) in 50 ml of phosphate balanced salt solution. The mixture was gently stirred at 37$^{o}$C for 30 min to yield a single cell suspension. This slurry was then pelleted in a centrifuge (100 x g) and resuspended in 20 ml of spinner minimal

Figure 3.1: Experimental setup for treating EMT-6 tumors in mice with PDT. The animals have been anesthetized with ketamine and xylazine and their eyes coated with Lacralube. Four of the animals are receiving PDT. The control is second from the right and receives identical treatment, including acetal needle implantation, but no light exposure.

essential media (MEM) containing 5% fetal calf serum. Cell numbers were determined by Coulter counting and by vital staining with trypan blue using a hemocytometer. A known number of cells were then plated into replicate petri dishes (n=4), at both high and low concentrations in Waymouths media plus 12.5% serum (10% NU-serum + 2.5% fetal calf serum) and antibiotics. Cultures were incubated in the dark at 37$^{o}$C in a humidified atmosphere of 5% $CO_2$ in air for 7 days, at which time they were fixed, stained and the macroscopic colonies per plate counted. From these data plating efficiencies (P.E.) and cell yield (C.Y.) per gram of tissue were calculated for each individual tumor.

### 3.2.7 EXPERIMENTAL PROTOCOL

Tumor was transplanted into 30 mice at a time. Tumor growth was variable, such that 4-5 mice were available for treatment at any one time. Animals were randomly assigned to various treatment groups when their tumors reached volumes of ~ 500 $mm^3$. Initially a dose response curve was determined for PDT without the addition of a BRAA. All animals received $P_{II}$, a general anaesthetic and were implanted with an acetal plastic needle. The control group received no light (0 Joules). The other groups were exposed to 100, 200, 300 and 400 Joules of light. Tumors were excised at 24 hr after phototherapy except for the 300 Joules group where tumors were excised immediately and 24 hr post-PDT to demonstrate both the direct and indirect killing of PDT. A group treated

with light only (i.e. 300 Joules without $P_{II}$) was also included.

A dose response curve was then established for PDT plus the BRAA, ETAN. The control group received $P_{II}$ plus ETAN and no light (0 Joules). The other groups received $P_{II}$ plus ETAN and were exposed to 100, 200 or 300 Joules of light. Tumors were excised at 24 hr in all groups except the 300 Joules group where tumors were removed immediately and at 24 hr post-PDT to demonstrate the indirect killing of PDT. For the remaining bioreductive alkylating drugs (MISO, SR-4233 and RSU-1069) only 200 and 300 Joules light exposures were assayed. Again control group receiving $P_{II}$ and a bioreductive alkylating drug but no light were included to assay for direct toxicity. All tumors were removed at 24 hr post-PDT except for the 300 Joules group where tumors were removed both immediately and at 24 hr post-PDT to demonstrate the indirect cell killing of PDT.

**3.3 RESULTS**

The results of all tumor groups are tabulated in Table 3.1 as P.E. and C.Y. ± standard deviations. For the control group receiving $P_{II}$ and no light this assay produced a C.Y. of 52 x $10^6$ cells/gram and a P.E. of - 37%. PDT alone with increasing light exposure demonstrated a light dose dependent decrease in C.Y. and P.E. If tumors were excised immediately following PDT, with or without the addition of a

## TABLE 3.1

**EMT-6 TUMOR CLONOGENICITY AFTER IN-VIVO PDT WITH OR WITHOUT BIOREDUCTIVE CHEMOTHERAPY**

| LIGHT DOSE (Joules) | BRAAs | INTERVAL TO EXCISION(hr) | (%)PLATING EFFICIENCY | CELL YIELD ($x10^6$/gm) | CLONOGENS/TUMOR ($x10^6$ cells/gm) |
|---|---|---|---|---|---|
| 0 (n=13) | NONE | 0 | 37.0 ± 14.4 | 51.9 ± 24.5 | 19.203 |
| 0 (n=7) | NONE | 24 | 30.4 ± 11.8 | 34.3 ± 10.7 | 10.427 |
| 300 (n=5) | NONE | 0 | 34.6 ± 8.20 | 22.5 ± 9.10 | 7.785 |
| 100 (n=12) | NONE | 24 | 20.1 ± 16.9 | 24.6 ± 18.4 | 4.945 |
| 200 (n=10) | NONE | 24 | 6.68 ± 7.20 | 19.5 ± 19.9 | 1.303 |
| 300 (n=13) | NONE | 24 | 6.40 ± 8.22 | 11.8 ± 14.2 | 0.755 |
| 400 (n=7) | NONE | 24 | 1.35 ± 1.57 | 6.90 ± 4.91 | 0.093 |
| 0 (n=5) | ETAN | 24 | 25.6 ± 12.7 | 29.8 ± 11.1 | 7.629 |
| 100 (n=15) | ETAN | 24 | 11.8 ± 9.23 | 22.6 ± 17.1 | 2.667 |
| 200 (n=11) | ETAN | 24 | 2.52 ± 3.35 | 6.10 ± 4.24 | 0.154 |
| 300 (n=13) | ETAN | 24 | 1.81 ± 2.97 | 3.86 ± 2.05 | 0.070 |
| 0 (n=5) | MISO | 24 | 29.5 ± 9.45 | 24.0 ± 7.54 | 7.080 |
| 200 (n=6) | MISO | 24 | 1.16 ± 1.46 | 4.70 ± 1.12 | 0.055 |
| 300 (n=5) | MISO | 24 | 1.88 ± 1.68 | 6.35 ± 2.73 | 0.112 |
| 300 (n=6) | MISO | 0 | 27.9 ± 4.76 | 19.0 ± 5.10 | 5.301 |
| 0 (n=5) | SR4233 | 24 | 25.6 ± 5.35 | 22.0 ± 5.49 | 5.632 |
| 200 (n=5) | SR4233 | 24 | 1.52 ± 1.16 | 2.95 ± 1.53 | 0.045 |
| 300 (n=10) | SR4233 | 24 | 1.24 ± 1.82 | 3.11 ± 1.38 | 0.038 |
| 300 (n=5) | SR4233 | 0 | 25.6 ± 5.34 | 22.5 ± 7.61 | 5.760 |
| 0 (n=7) | RSU1069 | 24 | 23.8 ± 4.59 | 22.8 ± 6.44 | 5.426 |
| 200 (n=6) | RSU1069 | 24 | 3.01 ± 1.90 | 2.85 ± 0.18 | 0.086 |
| 300 (n=4) | RSU1069 | 24 | 0.92 ± 0.44 | 4.49 ± 1.04 | 0.041 |

BRAA there was virtually no cell kill (the average P.E. = 29.4% and C.Y. 21.3 x $10^6$). If the tumors were left *in-situ* for 24 hr prior to excision there was a light dose dependent decrease in P.E. and C.Y., that was potentiated by all the bioreductive alkylating drugs tested. The decrease in C.Y. for tumors left *in-situ* for 24 hr is demonstrated graphically in Figure 3.2. Only the data from PDT alone and PDT plus ETAN are shown and they demonstrate the further decrease in C.Y. by the addition of a BRAA. The decrease in P.E. is demonstrated graphically in Figure 3.3. If the tumors are removed immediately after PDT there is virtually no decrease in P.E. up to 300 Joules with or without the addition of a bioreductive alkylating drug (dotted line). The 2 solid lines represent linear regression fits to the data from tumors removed 24 hr after treatment and demonstrate the light dose dependent decrease in P.E. and potentiation by the BRAA, ETAN. The limited data obtained with the remaining BRAAs (MISO, RSU-1069 and SR-4233) are plotted as single points on this graph. This *in-vivo/in-vitro* clonogenic assay was unable to demonstrate a significant difference in potentiation of PDT between these BRAAs. However, the data suggests a maximal asymptotic potentiation of tumor cell kill of about 1½ decades (dashed line).

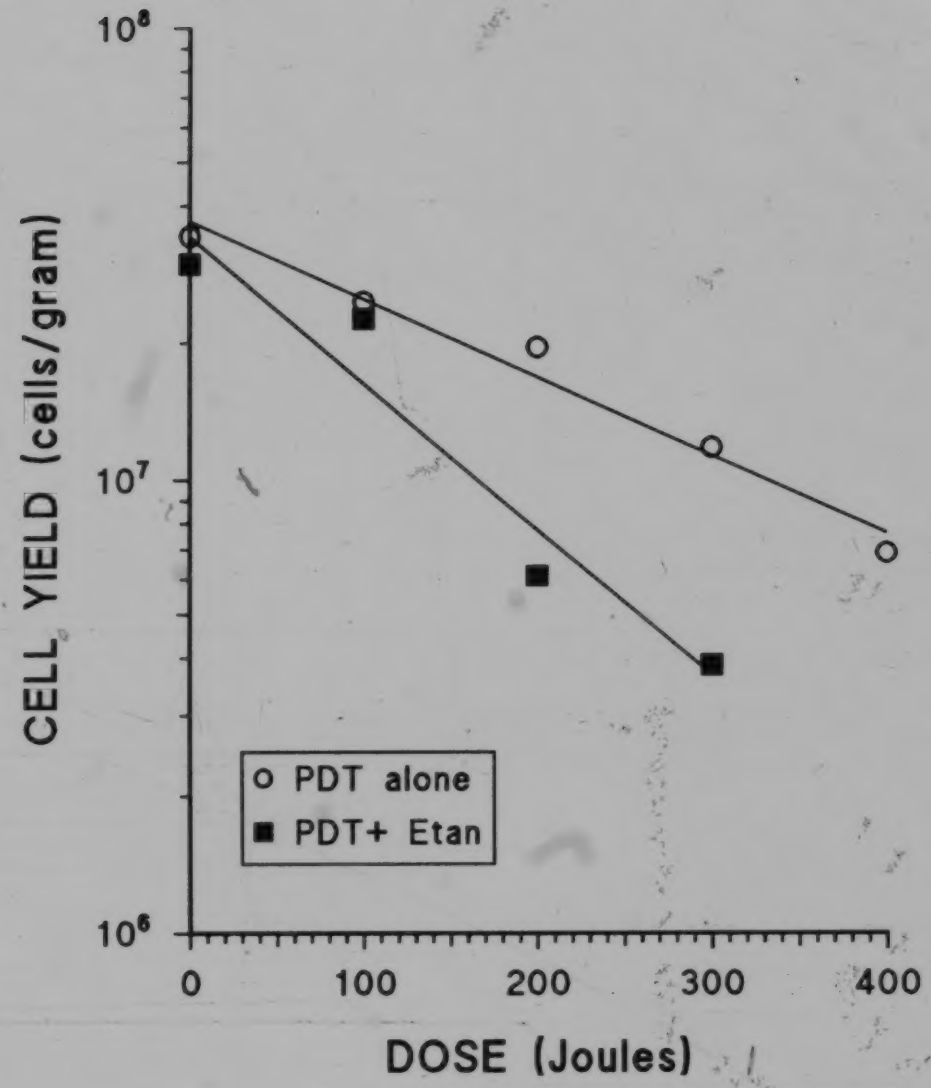


Figure 3.2: Cell yield (C.Y.) following PDT in-vivo, with or without the addition of ETAN demonstrating a decrease in C.Y. with increasing light dose and the addition of BRAAs.

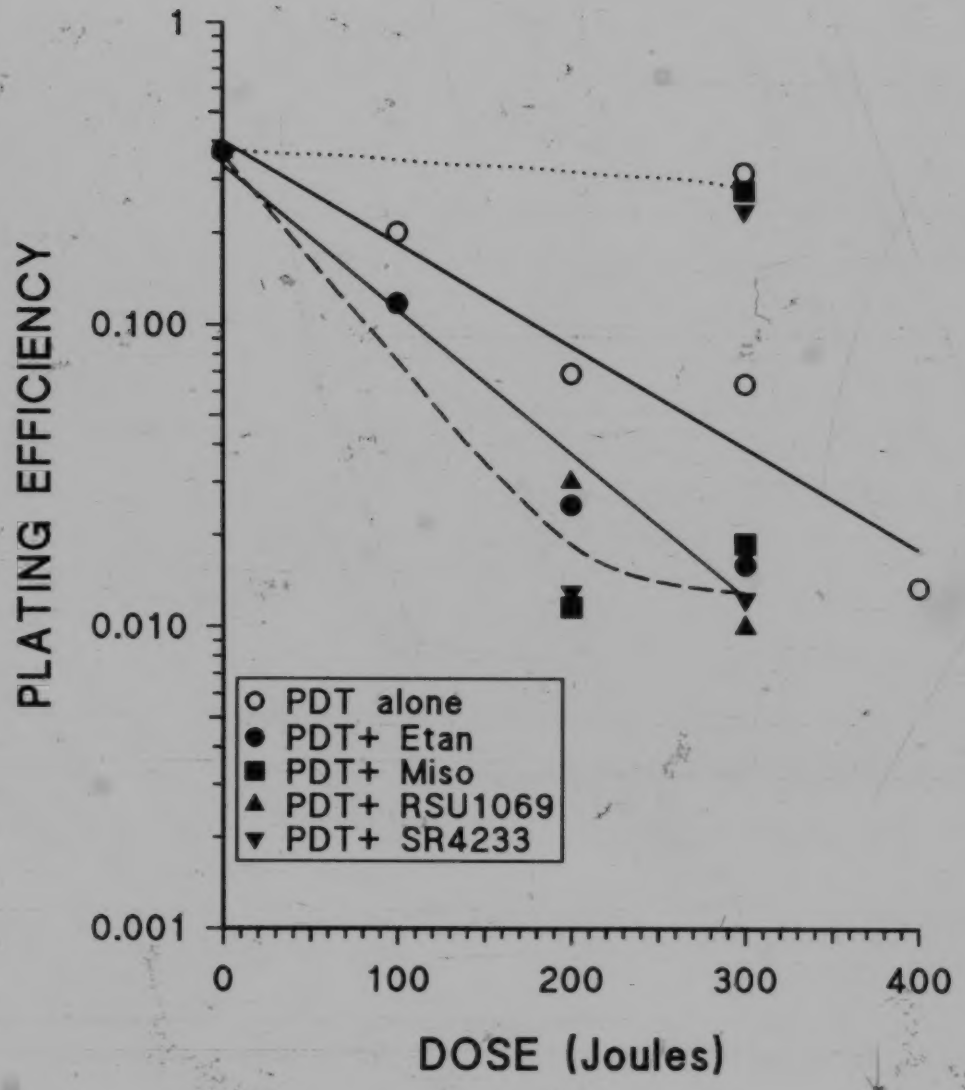


Figure 3.3: Plating efficiencies (P.E.) as a function of light dose, with or without the addition of BRAAs with immediate excision post-PDT there is no decrease in P.E. (dotted line). If the tumor is left in-situ 24 hrs there is a light dependent decrease in P.E., which is enhanced by the addition of BRAAs. However there appears to be a maximal effect (dashed line).

From the P.E. or C.Y. data alone a moderate amount of tumor cell inactivation can be demonstrated. However, the total tumor effect may best be represented by the product of both P.E. x C.Y. (Figure 3.4). This figure depicts the number of clonogenic cells isolated per gram of tumor tissue excised. Again if the tumor cells were isolated immediately following PDT there was a small loss of tumor clonogeniety (dotted line). The maximal loss of tumor clonogeniety at 24 hr post-PDT, including adjuvant bioreductive chemotherapy is - 2.5-3.0 logs. Again taking into account all the data points there appears to be a maximum effect of PDT + BRAA chemotherapy in this tumor system (dashed line).

**3.4 DISCUSSION**

Previous studies have shown that BRAAs can potentiate PDT *in-vivo* in some animal tumor systems (Gonzalez *et al.*, 1986; Henry and Isaacs, 1990) but not in others (Winther *et al.*, 1988). Recent *in-vitro* studies (Santus *et al.*, 1991) have demonstrated protection from the photo-oxidative effects of PDT by BRAAs which was dependent on the photoprotectors lipophilicity. This *in-vivo* study was designed to demonstrate three points; (1) that PDT-induced tumor cell killing *in-vivo* is indirect, (2) that adjuvant bioreductive chemotherapy can potentiate this indirect killing and (3) to determine which of 4 available BRAAs is most efficacious.

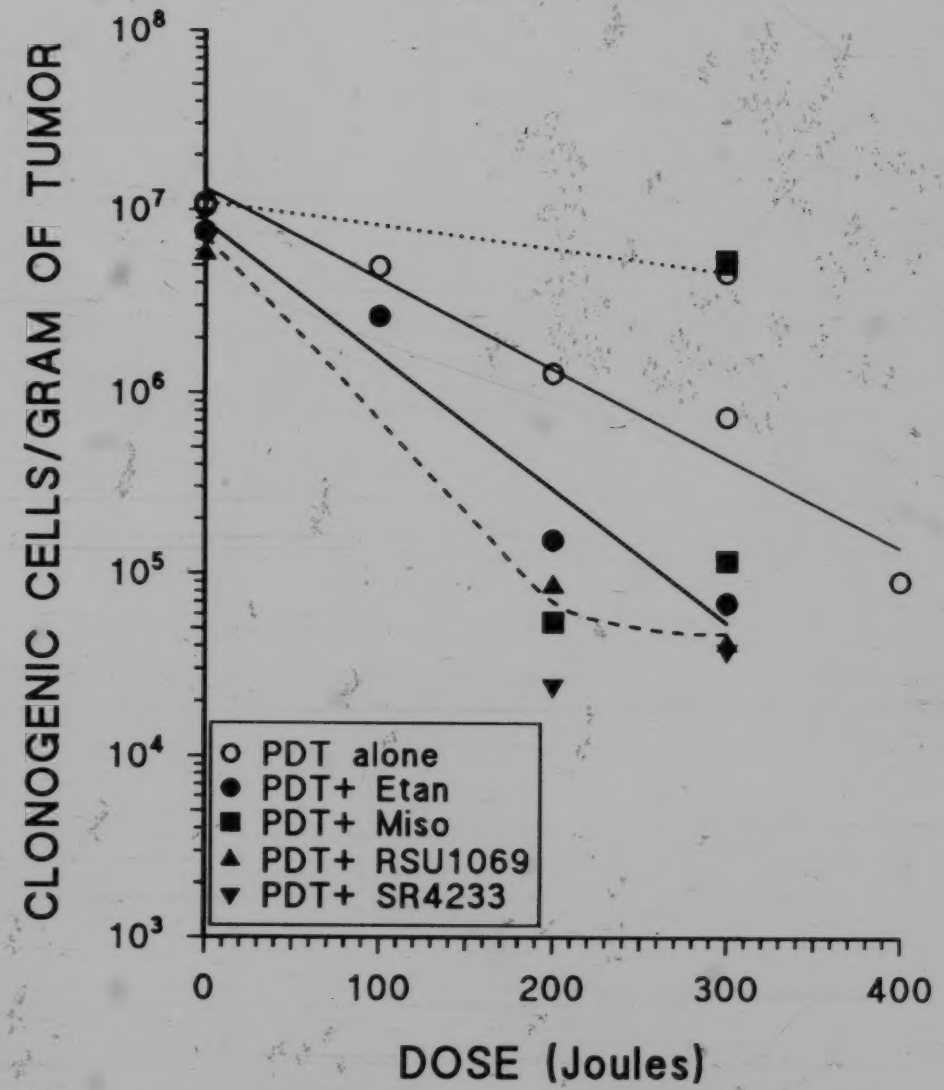


**Figure 3.4:** Number of clonogenic cells isolated per gram of tumor tissue (P.E. x C.Y.). There is minimal loss of clonogens if tumor is removed immediately post-PDT (dotted line). If the tumor is left in-situ for 24 hrs there is a light dose dependent decrease in clonogens potentiated by the addition of BRAAs. This potentiation appears to be asymptotic (dashed line).

The results reported in this study demonstrate and confirm the findings of Henderson *et al.* (1985), that PDT killing *in-vivo* is primarily indirect. If tumors were removed immediately post-PDT there was virtually no cell kill, even in the presence of BRAAs. Therefore within the limit of this assay little or no direct tumor cell kill could be demonstrated by the BRAAs alone. The indirect killing is consistent with the nuclear medicine assays reported in the previous chapter demonstrating perfusion shutdown and the targeting of BRAAs at this induced hypoxia.

If an analogy can be drawn between potentiation of radiotherapy and phototherapy, then BRAAs in combination with PDT can produce an enhancement ratio of ~ 1.6 for ETAN (at the 1% survival level) and a maximum enhancement ratio of ~ 2.3 if one averages the combined response for all 4 BRAAs.

This apparent maximum to cytotoxic cell killing could be due to several factors. First this may represent the limit of cell kill produced with 24 hr of ischemia based upon drug cytotoxic kinetics (concentration X time). Secondly, this could represent a limitation of BRAA drug distribution within the tumor prior to vascular shutdown. And thirdly, the non-uniform shape of the tumors may have resulted in peripheral cells not receiving an adequate light exposure. Cells being outside the effective light diffusion of 3-4 mm

(at 200-300 Joules) from the cylindrical fiber would be mixed with cells receiving adequate exposure and result in the observed cell kill plateau.

Within the limitations of this assay no significant difference in potentiation between the various BRAAs could be demonstrated. In fact, with what were selected to be equally toxic drug doses there was a greater number of animal deaths resulting from the addition of RSU-1069 and SR-4233. Since ETAN potentiates this PDT-induced ischemic cell kill to a similar degree as SR-4233 and RSU-1069 and is currently being used clinically to treat patients, it should not be overlooked as a BRAA for potentiating PDT and other forms of vascular targeted cancer therapies. In fact ETAN, being the least lipophilic of the BRAA's may offer a theoretical advantage in porphyrin PDT, where the lipophilic porphyrins partition into the lipid environments. ETAN could therefore be administered well in advance to PDT, ensuring maximal delivery to the tumor, and by partitioning into different compartments, avoid interaction with the photo-oxidative process (Santus *et al.*, 1991).

**3.5 CONCLUSION**

From the results reported in this chapter several conclusions can be made. The first is that the majority of cell kill observed in PDT-treated tumors is time-dependent and secondary to tumor infarction, which is light dose-

dependent. Secondly, this indirect cell kill can be potentiated by BRAAs with an enhancement ratio of ~ 2 for doses studied. The extent of PDT enhancement is probably limited by BRAA delivery to the tumor, as a result of acute infarction. Since perfusion shutdown is rapid and complete to a major portion of the tumor this represents a major limitation in the timing of drug delivery, in that bioreductive alkylating drugs present at the time of photo-irradiation can interfere with the photo-oxidative process. And finally, the bifunctional alkylating agent, RSU-1069 and the DNA target specific BRAA SR-4233 demonstrated no significant therapeutic advantage over ETAN (SR-2508) in this PDT-induced hypoxia.

# CHAPTER IV

# IN-VITRO PHOTOBIOLOGY

## 4.1. INTRODUCTION

PDT cell killing is a complex process, requiring an adequate amount of photosensitizer, oxygen and activating light within cellular target structures. These parameters are very difficult to precisely define *in-vivo*, if not impossible to control. Photosensitizer distribution (both intra- and extra-cellular) can be very heterogeneous, dependent upon the time and mode of administration, especially for drugs like $P_{II}$ which is a mixture of monomer and oligomer porphyrins (Dougherty *et al.*, 1984b; Dougherty, 1987; Moan, 1986). Intratumor oxygenation can also be heterogeneous as demonstrated by autoradiography using radiolabelled misonidazole (Chapman *et al.*, 1981). Even light delivery with interstitial delivery systems can produce marked heterogeneity in tissue light distribution (Arnfield *et al.*, 1990). Therefore in order to gain an better understanding of cellular PDT mechanisms, *in-vitro* assays are required where the above factors can be better controlled.

The previous 2 chapters have demonstrated and discussed the importance of the vasculature in tumor response to PDT. There is increasing evidence that vascular stasis caused by either platelet plugging or vasoactive compound release is important in PDT outcome (Ferrario and Gomer, 1990; Fingar *et al.*, 1990). Berenbaum *et al.* (1986), studying PDT-induced

cerebral damage, suggested selective initial damage to the endothelium. Two recent *in-vitro* photobiology studies have examined the photosensitivity of endothelial cells. West *et al.* (1990), using $^{3}$H-thymidne uptake and clonogenic assays demonstrated a 3.9 X greater sensitivity of endothelial cells versus tumor cells in part explained by 2.6 X greater uptake of the photosensitizer into the endothelial cells. Gomer *et al.* (1988a), using a clonogenic assay, demonstrated that endothelial cells were more photosensitive than smooth muscle and fibroblast cells, but could not demonstrate a preferential uptake of $P_{II}$ to account for this. Both of these studies however, have utilized bovine endothelial cells which might not be directly comparable with murine or human tumor cells.

Previous studies in this laboratory have established an *in-vitro* assay system in which oxygen concentration, photosensitizer concentration, and light exposure can be rigorously controlled (Chapman *et al.*, 1991b; 1991c). Using this system, experiments were designed to characterize the photosensitivities of various elements of 2 murine tumors (EMT-6 and R3327-AT) and to measure the inherent photosensitivity of murine endothelial and tumor cells. Knowing the inherent photosensitivity and oxygen response of these cells could be useful in predicting and understanding PDT response *in-vivo*. For example, determination of *in-vivo* cellular $P_{II}$ concentration and intra-tumor light

distribution would allow a prediction to be made as to which elements of the tumor could be directly killed by PDT.

## 4.2. MATERIALS AND METHODS

### 4.2.1 CELL CULTURE

The Dunning R3327-AT tumor cells were isolated from a male rat (Copenhagen 2331 x Fischer 344 F1 Hybrid) bearing the tumor subcutaneously in its flank. This tumor was initially obtained from Dr. D. Coffey of John Hopkins University (Baltimore, MD, USA) and was serially passaged as described in Chapter 2. Following cervical dislocation a 500 $mm^3$ tumor was surgically removed using aseptic technique and placed in a sterile petri dish. In a laminar flow hood the tumor was minced with iris scissors, and placed in a 50 ml Erlenmeyer flask containing collagenase (12.5 mg), DNAse (20 mg) and pronase (25 mg) in 50 ml phosphate buffered salt solution (PBS). The mixture was slowly stirred at 37$^{o}$C for 30 min using a magnetic stir bar. The resulting mixture was then filtered through a fine wire mesh screen to remove large debris. The resulting single cell suspension was centrifuged at 100 X G, the supernatant discarded and the pellet resuspended in spinner minimal essential media (Gibco$^{Tm}$) supplemented with 5% fetal calf serum (FCS) and antibiotics (50 units/ml penicillin and 50 µg/ml streptomycin). The viable cell number was determined using a hemocytometer and trypan blue. 1 x $10^6$ cells were seeded into a spinner culture flask containing ~ 60 ml of Eagles

basal media (Gibco$^{Tm}$) supplemented with 12.5% FCS and antibiotics. The culture was incubated at 37$^{o}$C while being slowly stirred in the sealed flask with intermittent gassing with 5% $CO_2$. Tumor cells were isolated from stromal cells by their propensity to grow as multicellular colonies (spheroids) in suspension culture (Figure 4.1). After 21 days of incubation with intermittent feeding and thinning of the colonies, the spheroids were removed and trypsinized (0.5% trypsin, Gibco$^{Tm}$) in petri dishes on an oscillating platform. The single cell suspension was then pelleted (100 X G), resuspended in Eagle's basal media containing 12.5% FCS and antibiotics (BME) and cell number determined using a Coulter$^{Tm}$ counter. 1 x $10^5$ cells were then seeded into Corning$^{Tm}$ T-25 plastic flasks, incubated at 37$^{o}$C in $H_2O$ saturated 5% $CO_2$/air and passaged every 7 days thereafter. These cells in exponential growth had a doubling time of -24 hr.

Mouse endothelial cells were obtained from Dr. Una Ryan (Monsanto Corp., St. Louis, Mo). These cells were isolated by Linda White using techniques developed in Dr. Ryan's lab which characterized the cells by assaying for Factor VIII R:Ag and angiotensin factor [kinase II] (Ryan *et al.*, 1982; Ryan, 1988). Cells were cultured as monolayers in plastic tissue culture flasks containing M199 media (Gibco$^{Tm}$) supplemented with 12.5% FCS, thymidine (50 $\mu$g/ml), penicillin (100 units/ml), streptomycin (100 $\mu$g/ml) and

Figure 4.1: Scanning electron micrograph of Dunning R3327-AT multicellular spheroid. (Magnification: X 312).

gentamycin (8 μg/ml) at 37°C in humidified 5% $CO_2$/air. From the initial culture received, cells that formed colonies were selected. This was accomplished by repeatedly selecting and expanding discrete colonies with a cobblestone morphology. The selected cells were designated UNA-ME. These cells were passaged every 7 days by plating 1 x $10^5$ cells, as determined by Coulter$^{Tm}$ counting, into Corning$^{Tm}$ T-25 flasks. Under these conditions the exponentially growing cells had a doubling time of -24 hr.

The EMT-6 tumor cells used in these experiments are from the same source as described in Chapter 3. Cells were passaged twice a week by plating 1 x $10^5$ cells in Corning$^{Tm}$ T-25 flasks containing Waymouth's media supplemented with 12.5% serum (10% NU-serum +2.5% FCS) + antibiotics and incubating them at 37°C in humidified 5% $CO_2$/air. Under these conditions the exponentially growing cells had a doubling time of ~ 12 hr.

4.2.2 CELL CHARACTERIZATION

Cell ploidy analysis was carried out using a Becton Dickinson FACScan$^{Tm}$ flow cytometer. Exponentially growing cells were harvested with trypsin (0.25%), washed with PBS and resuspended (1 x $10^6$ cells/ml) in 5% DMSO, sucrose (250mM) and trisodium citrate (40mM) buffer. Nuclei were prepared for DNA analysis using a detergent-trypsin technique [modified NP-40 method] (Vindelov *et al.*, 1983).

Briefly 200 µl of the cell suspension was lyzed in 0.003% trypsin in 1800 µl stock solution [Nonidet P 40 (0.1%), Spermine tetrahydrochloride (1.5mM) and Tris (hydroxymethyl) aminomethane (0.5mM), pH 7.6 ] for 10 min. An equal volume of trypsin inhibitor (0.05%) and Ribonuclease A (0.01%) in stock solution was added and mixed for another 10 min. Then propidium iodide (0.042%) and spermine tetrahydrochloride (0.12%) in 1800 µl stock solution was added and the resulting suspension mixed for a further 15 min in an ice bath protected from light. The sample was then filtered through a 30 µm nylon mesh prior to analysis.

Cell volumes were determined using the Coulter$^{Tm}$ counter system. The median cell volume of a cell population was determined from the median channel number of the volume distribution using a constant derived from calibration curves constructed with latex spheres of uniform size.

The UNA-ME cells were locally tested for von Willebrand's factor (Factor VIII R:Ag) using an immunocytochemistry assay (Giddings *et al.*, 1983; Wu *et al.*, 1987). Exponentially growing cells were harvested with trypsin, washed and resuspended in 5% FCS + PBS. The cells were cytospun onto glass slides and air dried overnight prior to fixation with acetone. Mouse monoclonal antihuman Factor VIII R:Ag $IgG_1$ (American Diagnostic$^{Tm}$, Catalog # E6VF7, Lot # 603068 ) was applied in various dilutions for 30 min. The slides were

washed in PBS and Goat antimouse antibody added for 15 min followed by a repeat PBS washing. Avidin Biotin Complex was applied at room temperature for 20 min and the slides washed with PBS. The slides were developed in Diaminobenzidine for 5 min and washed. Harris hematoxylin was used as a counter stain. The cells were dehydrated in a series of graded ethanol steps, placed in xylene and cover slip applied. The slides were examined at various magnifications using a light microscope. A confirmatory test was also carried out in a similar fashion using Rabbit polyclonal antihuman F VIII R:Ag (Behring Diagnostics$^{Tm}$, Catalog # 0T0M05, Lot # 105717B).

The glutathione content of the 3 cells lines was analyzed using the Tietze assay (Tietze, 1969). Briefly exponentially growing cells were removed from tissue culture flasks and resuspended at 1 x $10^6$ cells/ml in 2 ml trichloroacetic acid (TCA) to release the endogenous thiols. TCA was extracted from the solution with repeated washes of ether so that enzymatic colormetric rate reactions could be performed using a Beckman spectrophotometer (DU-7). Samples containing thiols from known cell numbers and standards containing known concentrations of GSH (Sigma$^{Tm}$) were enzymatically reduced with GSH reductase (Sigma$^{Tm}$) and NADPH (Sigma$^{Tm}$) in the presence of DTNB (Sigma$^{Tm}$) for each experiment. Rates of enzymatic reduction were plotted against standard GSH concentration and cellular GSH content determined.

4.2.3 PHOTOSENSITIZER

The photosensitizer used in these studies was $P_{II}$ (75 mg/vial P89-0089) obtained from Quadralogic Technologies (Vancouver, BC). The lyophilized compound was dissolved in 30 ml of 5% dextrose and water to a final concentration of 2.5 mg/ml. The compound was then aliquoted into 0.5 ml quantities, frozen and stored, protected from light. For each experiment a new aliquot was thawed immediately prior to use. Cells were incubated in $P_{II}$ for 1 hr or 24 hr prior to light exposure. For short-term exposure (1 hr) single cell suspensions ($1 \times 10^5$ cells/ml) were incubated at room temperature (23°C) in spinner MEM at final concentrations of 5 μg/ml, 20 μg/ml, and 100 μg/ml (80 μg/ml for EMT-6). Cells were slowly stirred in this media throughout incubation and light exposure. Single cell suspensions were produced by harvesting exponentially growing monolayer cultures with trypsin (0.5%) immediately prior to drug exposure. For long-term exposure (24 hr) $P_{II}$ was added directly to exponentially growing cells in monolayer culture and incubated at 37°C in their respective media at final concentrations of 2 μg/ml, 5 μg/ml and 10 μg/ml. Immediately prior to light exposure the cells were harvested with trypsin (0.5%), pelleted by centrifugation (100 X G) and resuspended at $1 \times 10^5$ cells/ml.

4.2.4 PHOTOSENSITIZER UPTAKE

Cellular $P_{II}$ content was measured by a spectofluorometric assay (Boegheim *et al.*, 1987). Suspensions were pelleted by centrifugation (100 X G) and the supernatant discarded. The resulting pellet was washed by resuspending the cells in PBS, vortexing and repeating the centrifugation. The cells were then lysed in 2 ml of nanopure filtered distilled water ($dH_2O$) and stored in the fridge until assayed for fluorescence. Prior to fluorescence assay 2 ml of 2% sodium dodecyl sulphate (SDS) and 0.1 N NaOH were added and the suspension heated for 5 minutes at 100°C in boiling water to yield soluble monomeric products. The resulting suspension was cooled to room temperature and fluorescence measured using a Perkin Elmer$^{Tm}$ spectrofluorometer (LS-5). Using a glass cuvette, the suspensions were excited with 403 nm light and emissions at 625 nm recorded. Fluorescence intensities were converted to absolute $P_{II}$ concentrations from standard curves generated with each assay, from known concentrations of drug.

The rate of $P_{II}$ uptake into single cells was assayed in suspension culture. Single cell suspensions ($1 \times 10^5$ cells/ml) were prepared in spinner MEM + 5% FCS and slowly stirred at 37°C. Immediately following preparation $P_{II}$ was added to a final concentration of 20 µg/ml. Five ml aliquots of the suspension were removed at 0.25, 0.5, 1, 2, 3, 4, 6, 8 and 24-hr intervals and assayed for $P_{II}$ content.

Cellular $P_{II}$ content was analyzed for each survival curve generated. Following 1 hr or 24 hr incubation with the drug plus exposure to 630 nm light, 4 ml of the irradiated suspension was removed and assayed for $P_{II}$.

*In-vivo* cellular $P_{II}$ content was also analyzed for comparison to *in-vitro* studies. Rats bearing R3327-AT tumors ~ 1 $cm^3$ in volume were administered $P_{II}$ (7.5 mg/kg IV). Two or 24 hr post-administration the animals were sacrificed and the tumors surgically removed. The tumor tissue was weighted and processed in two different ways as follows; (1) Tumor tissue was diced and a single cell suspension generated using the enzymatic cocktail described above. Tumor cells were selectively isolated in a ficol gradient. Known cell numbers were then assayed for $P_{II}$ content. (2) Diced tumor was made into a single cell suspension by mechanically passing pieces of tumor through 2 screens of progressively smaller grid size (80/in & 100/in). Again tumor cells were selectively isolated using a ficol gradient and known numbers assayed for $P_{II}$ content.

4.2.5 PHOTODYNAMIC TREATMENT

The same laser as described in Chapters 2 and 3 was used to generate 630 nm light for these experiments. The monochromatic beam was attenuated with a Kodak$^{Tm}$ filter and split into 4 separate beams. A single beam was coupled to a

quartz fiber and transported to an optical bench where it was focused with a micro-lens to a spot size of 3 cm in diameter. Power output was assessed with a Coherent$^{Tm}$ 210 power meter and adjusted to 107 mW, yielding a fluence of 0.8 J/cm$^2$/min. The light beam was projected upon the flat face of a cylindrical glass irradiation chamber whose dimensions were 3 cm in diameter and 1.5 cm deep. This glass irradiation chamber was initially designed for charged-particle studies and has a stoppered sample port as well as both a gas inlet and outlet port (Chapman *et al.*, 1977). The total chamber volume is ~ 12 cm$^3$ and holds a maximum of ~9.5 ml of fluid (Figure 4.2). Nine ml of $P_{II}$ exposed cell suspension (1 x 10$^5$ cells/ml) was added to the chamber and slowly stirred with a magnetic stir bar. The chamber was gassed at 1 L/min with 5% $CO_2$ and various concentrations of oxygen 45 min prior and during irradiation. Cylinders of ultrapure $N_2$ which contained 5% $CO_2$ and specific quantities of oxygen (<0.03, 0.3, 1, 3 and 20%) were purchased from Linde Special Gases (Union Carbide$^{Tm}$). For photosensitizer dependent studies (both short- and long-term exposure) the cells were irradiated in 20% $O_2$. For the $O_2$ dependent studies, cells were irradiated following 1 hr exposure to $P_{II}$ at 20 μg/ml.

### 4.2.6 CLONOGENIC CELL SURVIVAL

All irradiation and cell platings were performed in diminished light. Prior to and following specific increments

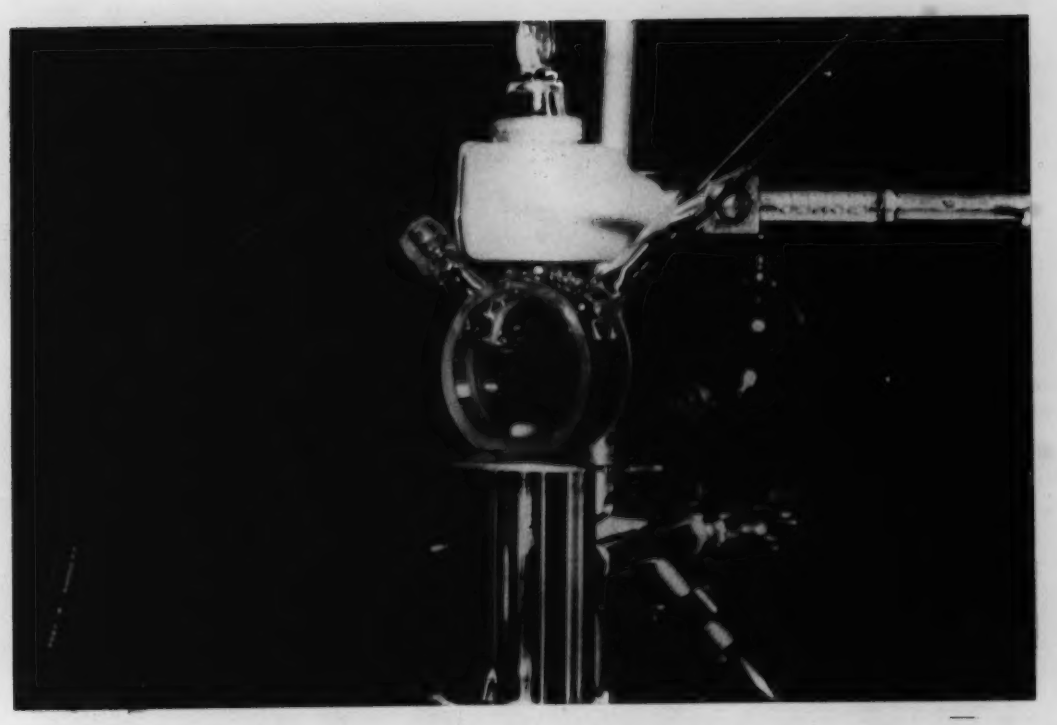

Figure 4.2: In-vitro photobiology irradiation setup. A stir bar is used to contiuously agitate the cell suspension. The chamber is gassed with humidified 5% $CO_2$ and various $[O_2]$ via the tygon tubing. Gas is vented and samples removed via the long arm on the opposite side of the chamber. A focused beam of light (3 cm in dia) is made to impinge on the flat circular face, of equal diameter.

of light exposure, appropriate aliquots of cell suspension were removed through the sampling arm of the chamber and placed in their respective dilution tube. Once all samplepoints were removed 0.5 ml was removed for post-PDT cell count and cell size determinations, and 4 ml was removed for $P_{II}$ uptake analysis. Appropriate cell numbers for each survival determination were plated in Falcon$^{Tm}$ petri dishes (60 x 15 mm) in replicates of 6 in their respective media. Each experiment was repeated 3 times. Endothelial growth factor (25 ng/ml, Sigma$^{Tm}$) was added to M199 for clonogenic assay only. The dishes were incubated at 37$^{o}$C in $H_2O$ saturated 5% $CO_2$/air. After 12 days (R3327 and UNA-ME) or 7 days (EMT-6), colonies were fixed, stained with methylene blue and macroscopic colonies counted. Surviving fractions (S/So) were computed by dividing the plating efficiencies of treated cells by the plating efficiencies of untreated cells.

## 4.3. RESULTS

### 4.3.1 CELL CHARACTERIZATION

Cell characterization is tabulated in Table 4.1. The mean cell volumes of EMT-6, R3327-AT and UNA-ME were 1.5, 3.0 and 1.3 picoliters respectively. The cellular GSH content of exponentially growing EMT-6, R3327-AT and UNA-ME cells was 0.808, 1.4 and 0.223 nm/$10^6$ cells respectively. When GSH is corrected for cell volume the tumor cells have a similar concentration at ~ 0.5 mM. The endothelial cells had a lower

**TABLE 4.1**

**CELL CHARACTERIZATION**

| CHARACTERISTIC | EMT-6 | R3327-AT | UNA-ME |
|---|---|---|---|
| CELL VOL picoliters | 1.5 ± 0.2 | 3.0 ± 0.4 | 1.3 ± 0.2 |
| GSH $nm/10^6$cells | 0.808 | 1.400 | 0.223 |
| [GSH] nm/mcl | 0.538 | 0.467 | 0.179 |
| PLOIDY n | 2n+ | 2n+ | 2n |
| $D_{10}$ Short term P 20 µg/ml | 1.01 | 1.6 | 1.0 |
| $D_{10}$ Long term P 10 µg/ml | 0.6 | 1.0 | 0.8 |
| Km $\%O_2$ | 0.5 * | 0.7 | 1.0 |
| % Plating Efficiency | 70-80 | 40-50 | 40-50 |

* EMT-6 $O_2$ Km taken from published work of Chapman et al., 1991b.

GSH concentration at ~ 0.2 mM. Ploidy analysis revealed the tumor cells to be aneuploid and the endothelial cells to be diploid. The purified endothelial cells were positive for von Willebrand's factor (Factor VIII R:Ag) by both antisera tests.

### 4.3.2 PHOTOFRIN UPTAKE

The mean $P_{II}$ uptake of all 3 cell lines to different drug concentrations at various times is recorded in Table 4.2. Short-term exposure is not dependent upon cell type nor volume, only the drug concentration. Long-term exposure however, is dependent upon cell volume (surface area) and drug concentration as suggested by the larger uptake into R3327-AT cells. There is no difference in uptake between the mouse endothelial and tumor cells. Cellular uptake is curvilinear and does not plateau in the 24 hr time span studied. Initial cell uptake is rapid doubling in 4-5 hr, whereas the next doubling of drug uptake requires almost 16 hr (Figure 4.3).

Fluorescence analysis of cellular $P_{II}$ uptake *in-vivo* was dependent upon the method of cell isolation and time post-administration (Figure 4.4). Enzymatic processing resulted in a lower cellular recovery of fluorescence at both 2 and 24 hr post-administration. However both methods showed greater retention at 24 hr. The enzymatic method was 4.5 X greater and the mechanical method 4.0 X greater at 24 hr.

**TABLE 4.2**

| $P_{II}$ Exposure μg/ml | $P_{II}$ Uptake μg/$10^6$ cells | $D_{50}$ J/cm$^2$ | $1/D_{50}$ cm$^2$/J | $D_{10}$ J/cm$^2$ | $1/D_{10}$ cm$^2$/J |
|---|---|---|---|---|---|
| | EMT-6 SHORT TERM EXPOSURE | | | | |
| 5 | 0.392 | 2.63 | 0.333 | 3.92 | 0.255 |
| 20 | 1.451 | 0.60 | 1.667 | 1.01 | 0.990 |
| 80 | 6.00 | 0.18 | 5.555 | 0.35 | 3.045 |
| | EMT-6 LONG TERM EXPOSURE | | | | |
| 2 | 0.025 | 5.3 | 0.189 | 8.0 | 0.125 |
| 5 | 0.057 | 1.8 | 0.555 | 2.8 | 0.357 |
| 10 | 0.176 | 0.4 | 2.500 | 0.6 | 1.670 |
| | UNA-ME SHORT TERM EXPOSURE | | | | |
| 5 | 0.448 | 2.4 | 0.420 | 3.5 | 0.286 |
| 20 | 2.000 | 0.7 | 1.430 | 1.0 | 1.000 |
| 100 | 7.600 | 0.1 | 10.000 | 0.2 | 5.000 |
| | UNA-ME LONG TERM EXPOSURE | | | | |
| 2 | 0.030 | 4.5 | 0.222 | 7.1 | 0.141 |
| 5 | 0.063 | 1.6 | 0.625 | 2.6 | 0.380 |
| 10 | 0.231 | 0.5 | 2.000 | 0.8 | 1.250 |
| | R3327-AT SHORT TERM EXPOSURE | | | | |
| 5 | 0.453 | 4.1 | 0.244 | 6.8 | 0.147 |
| 20 | 1.690 | 1.0 | 1.000 | 1.6 | 0.625 |
| 100 | 6.000 | 0.2 | 5.000 | 0.4 | 2.500 |
| | R3327-AT LONG TERM EXPOSURE | | | | |
| 2 | 0.130 | 4.5 | 0.224 | 8.3 | 0.120 |
| 5 | 0.307 | 1.7 | 0.588 | 2.9 | 0.345 |
| 10 | 0.796 | 0.6 | 1.667 | 1.0 | 1.000 |

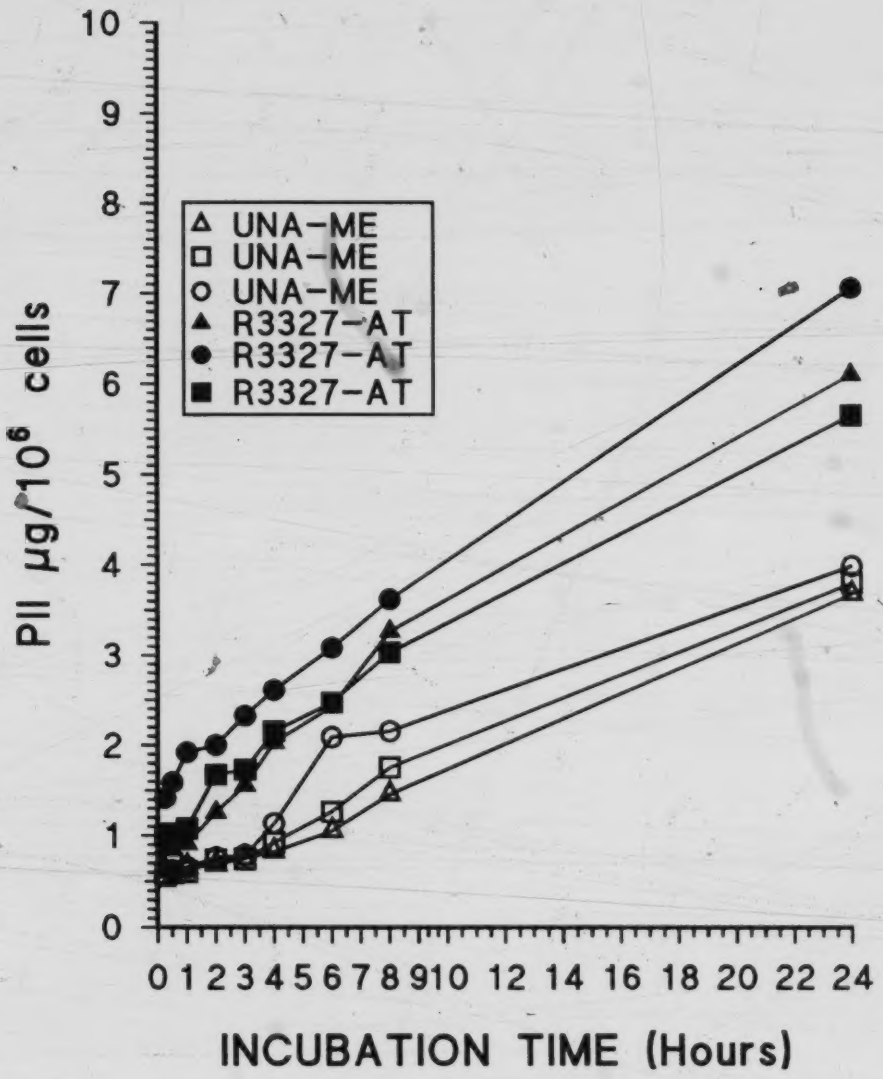


**Figure 4.3:** In-vitro cellular uptake of $P_{II}$ as a function of time for UNA-ME and R3327-AT cells. With prolonged exposure there is greater drug uptake in the larger R3327-AT cells as evident by the steeper slope. Cellular uptake for both cell lines is curvilinear and does not plateau in 24 hrs of $P_{II}$ (µg/ml) exposure. The different symbols represent repeat determinations to demonstrate reproducibility.

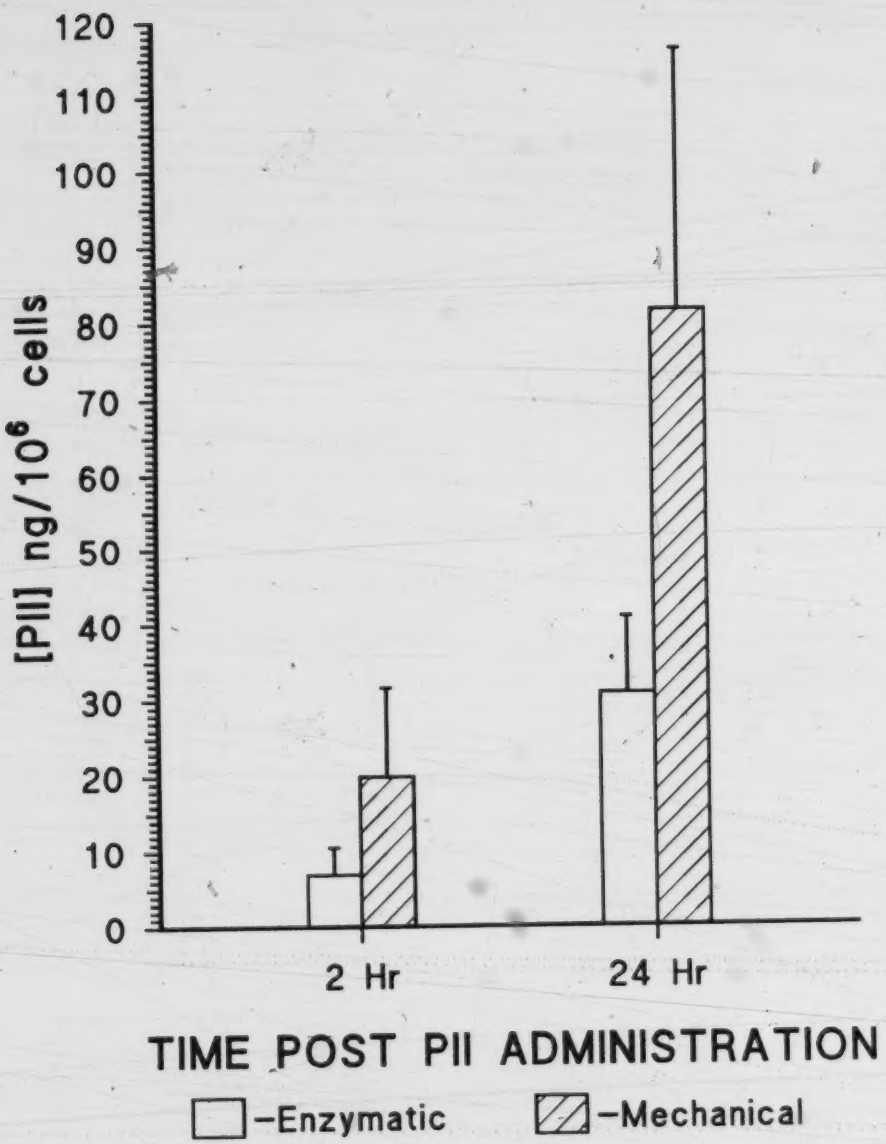


Figure 4.4: Histogram of in-vivo cellular uptake of $P_{II}$, comparing the enzymatic and mechanical cell isolation techniques. With mechanical isolation there is probably an over estimation because of $P_{II}$ release. With enzymatic isolation there is probably an underestimation as a result of washing out $P_{II}$.

Both methods were performed because neither is ideal for this assay. Chapman *et al.* (1991c), have shown that following short-term exposure of EMT-6 cells to $P_{II}$ some drug could readily be washed out, they termed this drug "unbound". After long-term exposure the drug could not be readily washed out. The enzymatic assay would have a tendency to wash out the drug and therefore under estimate levels within tumor cells at time of illumination particularly after short-term drug exposures. The mechanical assay would have the tendency to release drug from other cells in solid tumors and produce an over estimation. The mean uptake by the enzymatic method at 2 and 24 hr was 6.7 and 31 ng/$10^6$ cells respectively. For the mechanical method the mean uptake at 2 and 24 hr was 20 and 80 ng/$10^6$ cells respectively.

4.3.3 CLONOGENIC CELL SURVIVAL (PHOTOFRIN DEPENDENCY)

Survival curves were generated with EMT-6, UNA-ME and R3327-AT cells exposed to incremental doses of 630 nm light at different concentrations of $P_{II}$, following both short- or long-term exposures. Typical survival curve for R3327-AT cells are depicted in Figure 4.5. Similar curves were obtained for the other cell lines studied. Cell inactivation is characterized by a shoulder or threshold light dose beyond which exponential cell killing occurs. The shoulder is almost non-existent for high concentrations of unbound $P_{II}$ and short-term exposures. This most likely results from

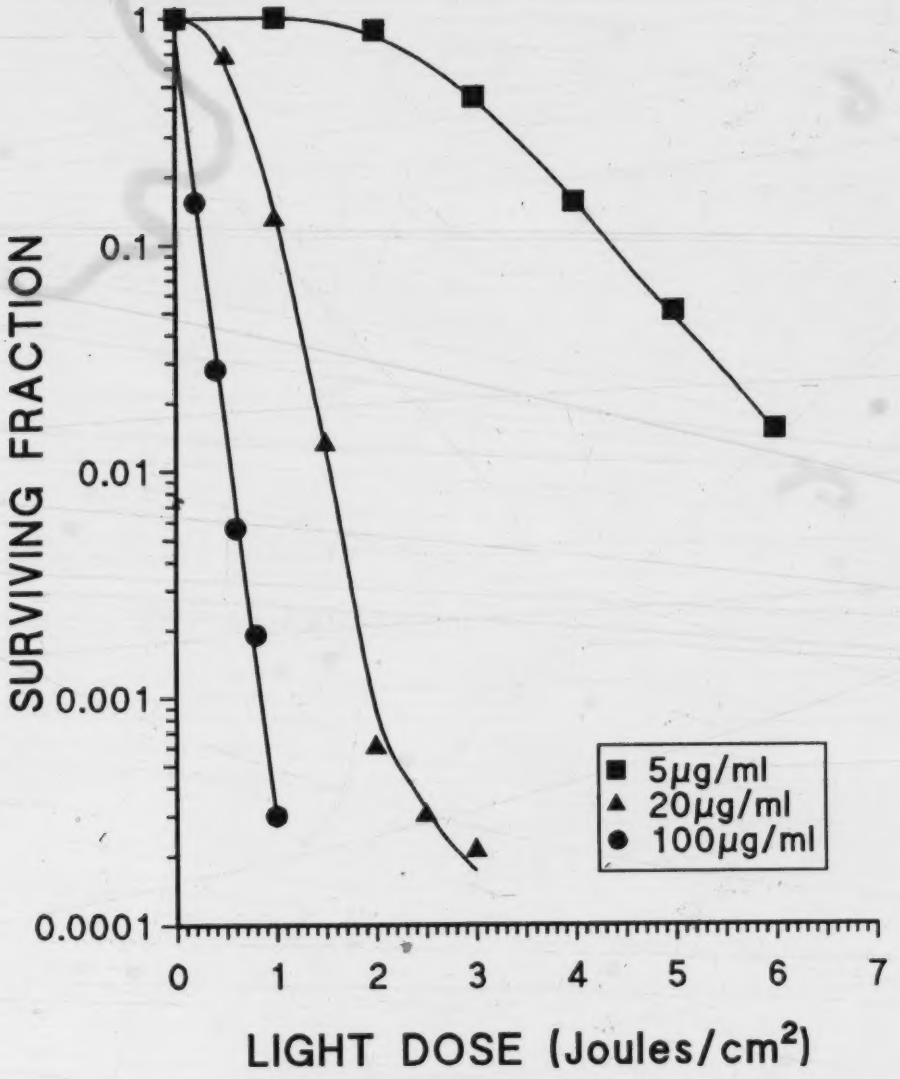


Figure 4.5: In-vitro PDT survival curves for R3327-AT tumor cells following 1 hr incubation in various concentrations of $P_{II}$ prior and during light exposure. With abundant $P_{II}$ cell kill is exponential. With decreasing amounts of $P_{II}$ the initial shoulder becomes wider and the exponential cell kill less steep.

an over whelming abundance of diffusible drug available for the photo-oxidative processes. Greater than 3 logs of exponential cell kill was observed in both the short-term and long-term exposure studies. However short-term exposures were more consistent at producing a greater magnitude of cell kill. Resistant tails were sometimes observed, especially at lower photosensitizer concentrations. This observed resistance could be due to inter-cellular heterogeneity or limitations in drug uptake since expanded populations of cells surviving 3 decades of cell kill do not demonstrate photoresistance (Chapman *et al.*, 1991c).

The exponential slope was also dependent on photosensitizer concentration after both long- and short-term exposures. Since there is no mathematical model for cell photo-inactivation, as for ionizing radiation, photokilling effectiveness is reported as $1/D_{50}$ and $1/D_{10}$. The inactivation "rates" of all 3 cell types as a function of concentration and time of $P_{II}$ exposure are given in Table 4.2. Following short-term exposure the R3327-AT cells were the least sensitive. The endothelial cells were slightly more sensitive than EMT-6 cells, but not significantly. Inactivation rates after long-term exposure were similar with EMT-6 being slightly more sensitive. When inactivation rates are plotted against the amount of $P_{II}$ measured in the cells ($\mu g/10^6$ cells), a large difference in sensitivity between short- and long-term exposure can demonstrated

(Figure 4.6). There is a 3 fold increase in sensitivity for the R3327-AT cells and a 10 fold increase for the UNA-ME and EMT-6 cells. Had these data been corrected for cell volume the amount of $P_{II}$ in the long-term exposure of R3327-AT cells would have been less by a factor of 2 and an increase in sensitivity similar to the UNA-ME and EMT-6 cells demonstrated. This 10 fold increase is similar to that reported by Chapman *et al.* (1991c) for EMT-6 cells.

### 4.3.4 CLONOGENIC CELL SURVIVAL ($O_2$ DEPENDENCY)

Survival curves were also generated with EMT-6, UNA-ME and R3327-AT exposed to incremental doses of light under defined levels of oxygenation. An example of such a survival curve for UNA-ME cells is shown in Figure 4.7. Again the survival curves had shoulders followed by exponential cell kill. The $O_2$ concentration affected both the shoulder width and the slope of the survival curves. In $N_2$ there was no cell killing up to exposures of 21 J/cm$^2$. With incremental increases in $O_2$ there was a graded increase in the rate of inactivation up to a maximum photosensitivity observed at 3% $O_2$ and greater. The effectiveness of photo-inactivation was measured as $1/D_{50}$ and plotted against the log of percent $O_2$ concentration, as depicted for UNA-ME cells in Figure 4.8. Half maximal rates (Km) for each cell line are tabulated in Table 4.1. The Km for R3327-AT and EMT-6 are very similar at 0.7 and 0.5 respectively. The endothelial cells were slightly more resistant to oxidative damage with a Km of

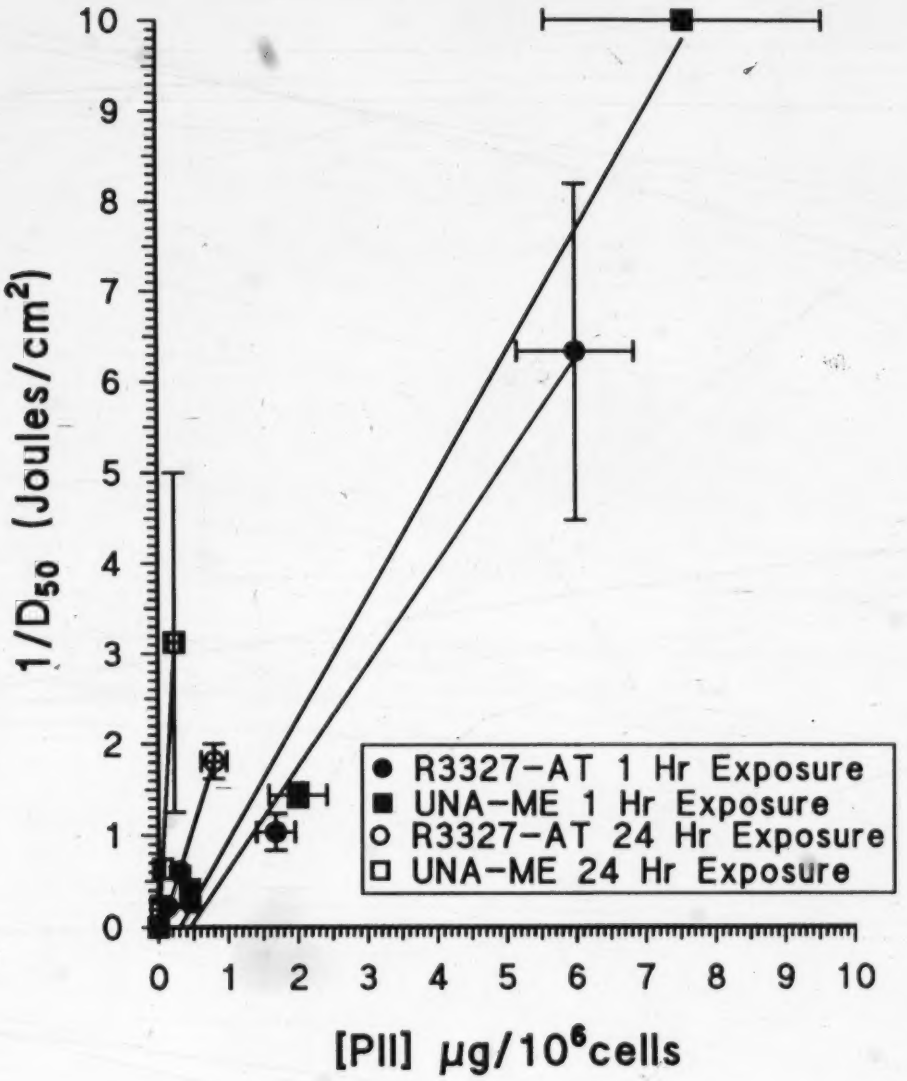


**Figure 4.6:** Inactivation rate ($1/D_{50}$) for UNA-ME and R3327-AT cells following 2 hr or 24 hr incubation in various concentrations of $P_{II}$. Following long-term incubation cell killing is more efficient per microgram of cellular $P_{II}$.

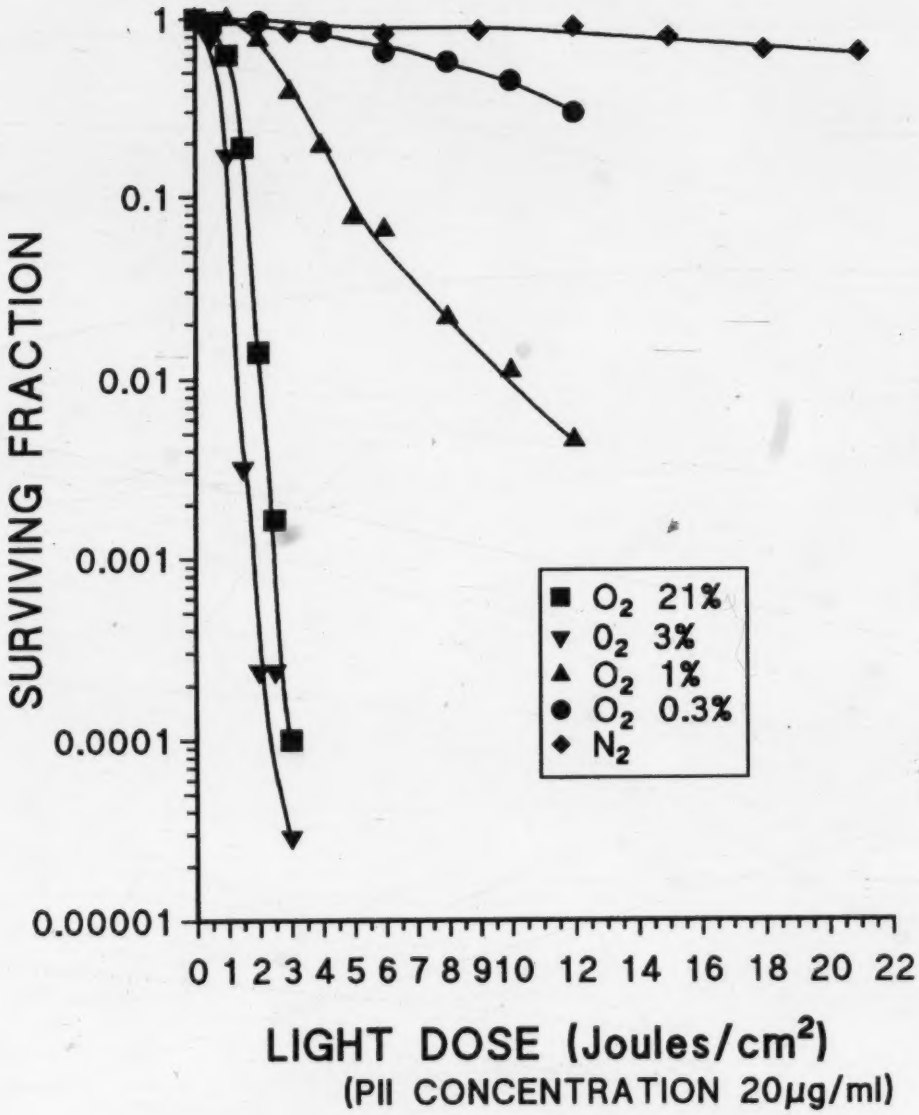


Figure 4.7: In-vitro PDT survival curve for UNA-ME cells as a function of $O_2$ concentration. In the absence of $O_2$ there is virtually no cell killing demonstrating the absolute requirement of $O_2$ in PDT. With increasing $pO_2$ the shoulder becomes narrower and the exponential cell kill steeper up to a $pO_2$ of 3%, beyond which there is no further increase.

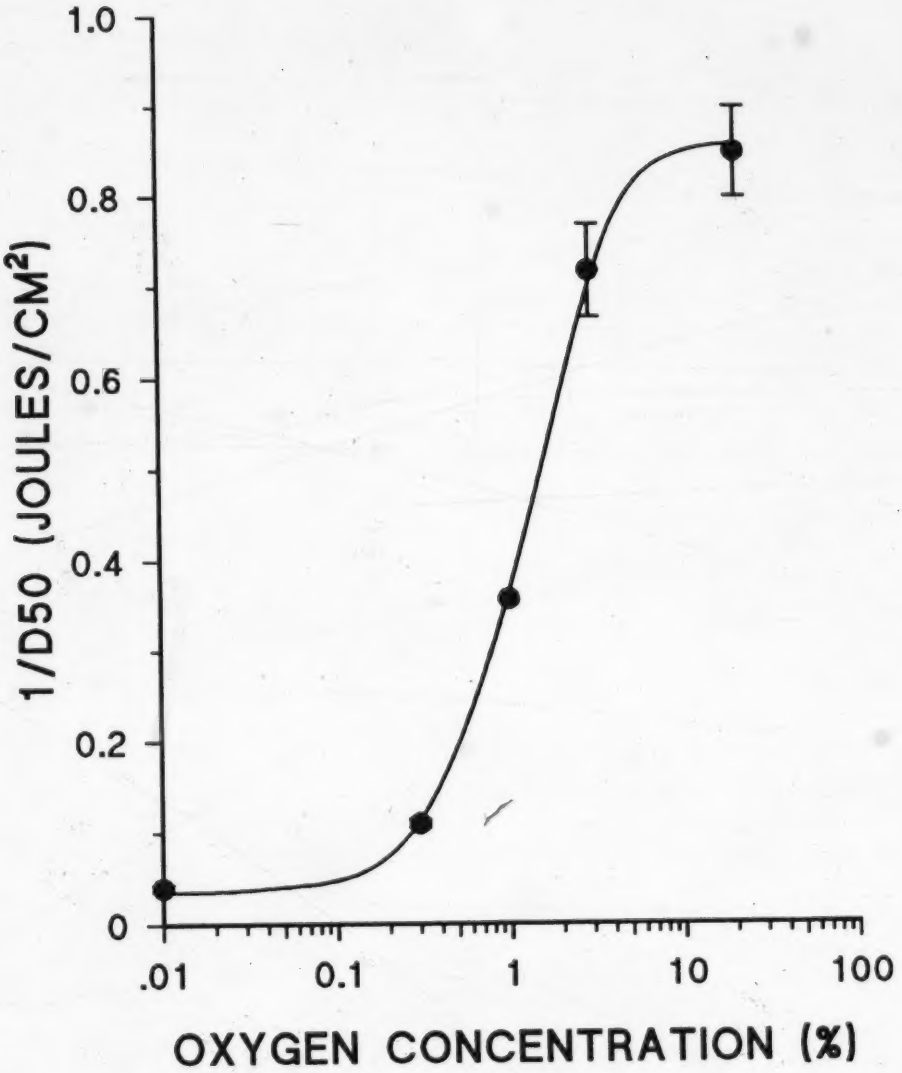


Figure 4.8: Inactivation rate ($1/D_{50}$) as a function of $O_2$ concentration for UNA-ME cells. The $pO_2$ required for half maximal rate (km) of cell inactivation is 1%.

1.0. Physiologically this makes sense in that endothelial cells are exposed to higher concentrations of $O_2$ and may have adapted mechanisms to deal with oxygen radicals.

## 4.4 DISCUSSION

The measurements of cellular uptake, retention and biological effectiveness of $P_{II}$ (DHE) described in this chapter of the thesis are quite similar to previous *in-vitro* studies performed with hematoporphyrin derivative (HPD) by Henderson *et al.* (1983). The experimental setup is the same as that used by Chapman *et al.* (1991b; 1991c) to study EMT-6 cells and confirms their findings using 2 other cell lines compared under similar conditions. These studies demonstrate the interdependency of the 3 main requirements for PDT; namely oxygen, photosensitizer and activating light. Strict control of these variables and cell characterization allow further interpretation of *in-vitro* cell killing which may shed light on the mechanism of cell kill *in-vivo*.

Differences in photosensitivity between normal and neoplastic cells to *in-vitro* PDT has been the subject of numerous papers yielding contrasting results. In certain studies malignant cells have been shown to accumulate higher levels of porphyrins and to be more sensitive to PDT than normal cells (Mossman *et al.*, 1974; Shulok *et al.*, 1986; Sprik *et al.*, 1988). Other studies suggest that malignant and normal cells accumulate similar levels of porphyrins and

have similar sensitivity to PDT (Moan *et al.*, 1981; Chang and Dougherty, 1978). Gomer *et al.* (1988a) studying bovine endothelial, smooth muscle and fibroblast cells showed the endothelial cells to be more sensitive despite equal $P_{II}$ uptake by fluorescence assay. However they did not report on cell size. West *et al.* (1990) compared endothelial cells of bovine origin with human adenocarcinoma cells of equal size and demonstrated the endothelial cells to be more sensitive primarily as a result of greater HPD uptake, as demonstrated by fluorescence assay. The studies reported in this chapter compared murine tumor to murine endothelial cells and could not demonstrate a significant difference in intrinsic photosensitivity between mouse endothelial cells and mouse tumor cells of equal size. There was no significant difference in $P_{II}$ uptake between the mouse cells which were of equal size. Differences in $P_{II}$ uptake were noted at 24 hr between R3327-AT cells and the other cells but could be accounted for by cell size (membrane surface area). This is consistent with this lipophylic drug partitioning to membranes (Brault, 1990). Gomer *et al.* (1988a) hypothesized that endothelial cells could be more sensitive to PDT as result of LDL receptor mediated uptake, however tumor cells also have acetylated LDL receptors (Barel *et al.*, 1986). Future studies should measure LDL levels under vigorously controlled conditions to determine the role of LDL receptors on $P_{II}$ uptake in normal and neoplastic cells. Partitioning of the drug with time into membrane appears to play a

significant role in the mechanism of cell kill as postulated by Ricchelli and Jori (1990). At low doses of light, the major effects occur on plasma and mitochondrial membranes; at high light doses or long incubation times with the sensitizer, lysosomal, microsomal and nuclear membranes are also affected (Spikes and Jori, 1986). When the drug has partitioned into different compartments, the physical properties of that environment can affect the cellular photochemistry (Chapman *et al.*, 1991b; 1991c).

A previous study of R3327-AT cell photobiology *in-vitro* was reported by Camps *et al.* (1985). They followed uptake of HPD as a function of time using a fluorescence assay and reported that with varying concentrations of HPD, uptake was maximal at 2 hr. This was not observed in the studies reported herein; $P_{II}$ uptake did not peak even after 24 hr of incubation. In fact incubation was carried out at a maximum concentration (20 μg/ml), beyond which dark toxicity killed the majority of the cells with 24 hr of incubation. Saturation, if it were to occur, should have done so under these conditions.

The oxygen dependency of PDT was demonstrated for 3 different cell lines under identical conditions and the Kms determined (Table 4.1). These values are very similar to the Km of 1 KPa (1%) $O_2$ reported by Moan and Sommer (1985) and Henderson *et al.* (1987) for $P_{II}$ mediated PDT. The values are

also close to the Km of 0.33 KPa reported for phthalocyanine PDT (Rosenthal *et al.*, 1986). The tumor cells had similar Kms and were slightly more sensitive than endothelial cells. This intrinsic difference did not result from elevated GSH which has been shown to protect cells from lipid peroxidation (Thomas and Girotti, 1989; Miller and Henderson, 1986). However, it could result from other scavenging mechanisms like superoxide dismutase (SOD) that can quench singlet $O_2$ (Matheson *et al.*, 1975).

Can this *in-vitro* data on cellular photosensitivity be directly related to *in-vivo* tumor response? In regards to $O_2$, if blood vessels are the target, the arterioles should be exposed to a $pO_2$ of at least 3%. Therefore $O_2$ should not pose a limitation. However if tumor response required direct inactivation of individual tumor cells, hypoxic cells which have been demonstrated in most rapidly-growing rodent tumors would not be readily inactivated by PDT. In regards to $P_{II}$ concentration; if we average the data from *in-vivo* uptake measurements (mechanical and enzymatic cellular isolation), at 2 hr there is 13.5 ng/$10^6$ cells and at 24 hr there is 55.5 ng/$10^6$ cells. Taking these numbers and fitting them into a linear regression equation (forced through zero) of $1/D_{10}$ versus drug concentration ($P_{II}$ $\mu$g/$10^6$ cells) the fluence required to inactivate 90% of the cells can be determined. For short-term exposure (13.5 ng/$10^6$) the light fluence required would be 179.5 J/cm$^2$. For long-term (55.5

ng/$10^6$) the light dose required would be 14.6 J/$cm^2$. Thus after short-term exposures to the drug, tumor cell killing by direct means is not likely to occur with the isodose plots obtained for the Dunning R3327-AT tumor (Figure 2.8B). However most of the $P_{II}$ is still in the blood pool 2 hr post-administration (Van Leengoed *et al.*, 1990) at a concentration of ~ 36 μg/ml requiring a $D_{10}$ of only 4 J/$cm^2$. Therefore the most sensitive tumor target would be the vascular cells, producing the indirect effects observed by the HMPAO perfusion studies and the *in-vivo/in-vitro* clonogenic assay. Following long-term exposure to $P_{II}$ the required fluence (14.6 J/$cm^2$) for direct cell killing can be obtained throughout the treated volume (2-3 $cm^3$), assuming uniform light distribution. However following $P_{II}$ redistribution, the endothelial cells would be exposed to a lower drug concentration. Taking into consideration the reciprocity and partitioning demonstrated above, the endothelial cells would be less sensitive at 24 hr post-drug administration, but still a critical target as demonstrated in Chapter 2, where there was a lesser magnitude of perfusion shutdown at 24 hr following drug administration as shown in Table 2.3. Rapid vascular impairment may limit direct cell killing by restricting the amount of $O_2$ available for the photo-oxidative process.

The predictability of these *in-vitro* assays is limited by the photosensitizer $P_{II}$ (DHE) which is a complex mixture of

compounds each with its own pharmacokenetics, photo-oxidative properties and optical parameters. *In-vitro* cell assays may be more predictive with a new pure single component photosensitizer that will allow accurate biodistribution studies and consistent photo-oxidative quantum yields.

## 4.5 CONCLUSIONS

These results reflect the multiplicity of factors which influence photosensitizer-cell interaction. The $O_2$ and photosensitizer dependency studies confirm previous studies on their requirements for PDT with 2 other cell lines. In particular the $O_2$ dependency studies show that the $O_2$ Km of PDT is similar to that for ionizing radiation and would result in the same limitations of cell kill *in-vivo* if it were not for different sites of action, namely the vasculature. The time dependency studies demonstrate the complexity of drug partitioning into microenvironments with different physicochemical properties. Comparison of mouse endothelial to tumor cells revealed slight differences in intrinsic photosensitivity, but these were not significant. The *in-vivo/in-vitro* comparisons suggest that endothelial cells are the *in-situ* target and demonstrate the need for a pure monomeric photosensitizer for experimental and clinical PDT.

# CHAPTER V

## GROSS AND MICROSCOPIC PATHOLOGY OF CELLULAR DAMAGE BY PDT

### 5.1 INTRODUCTION

Recently it has become apparent that PDT tumor destruction involves alteration in the microcirculation of both tumor and normal tissue (Selman *et al.*, 1984, 1985; Star *et al.*, 1986; Reed *et al.*, 1987, 1988). Following both *in-vivo* and *in-vitro* PDT, cytoxic effects have been described with damage noted to cell membranes, mitochondria, and nuclear components. These observed effects however, may be reversible and not necessarily result in cellular death (Gomer *et al.*, 1986). Recent studies by Henderson *et al.* (1985) and those presented in Chapter 3 of this thesis show that cells explanted immediately following *in-vivo* PDT retain their viability, while those remaining *in-situ* demonstrate a dose-dependent cell kill. A morphological pattern of coagulative necrosis has been described following *in-vivo* PDT associated with vascular stasis, cell swelling, basement membrane damage, vacuolization and swelling of mitochondria (Klaunig *et al.*, 1985; Berenbaum *et al.*, 1986; Chaudhuri *et al.*, 1987; Nelson *et al.*, 1988; Tseng *et al.*, 1988). It has been postulated by Ben-Hur *et al.* (1988) that PDT of endothelial cells results in the release of clotting factors resulting in these secondary changes. A histological study was therefore undertaken to describe the early cellular events causing perfusion shutdown and direct cell killing in the Dunning tumor model in hopes that it would

further shed light on the mechanism of cell kill in this particular tumor.

## 5.2 MATERIALS AND METHODS

### 5.2.1 TUMOR MODEL

The tumor model used in this study was the Dunning R3327-AT described previously in the thesis. The *in-vivo* and *in-vitro* biology conditions for handling this tumor were similar to those in Chapters 2 and 4.

### 5.2.2 PHOTOSENSITIZER

The photosensitizer was Photofrin (DHE) obtained from Quadralogic Technologies (Vancouver, Canada, Lot# P89 0089). It was prepared and handled in the same manner as described in Chapter 2, Materials and Methods.

### 5.2.3 LIGHT MICROSCOPY

Excised *in-vivo* tumor tissue was divided into 4 $mm^3$ pieces excluding the center of the tumor. These pieces were fixed in 5% buffered formalin (pH 7.4) for several days, dehydrated through a series of ascending percent ethyl alcohol to xylene and embedded in wax. The blocks were then serially sectioned into 4-5 micron sections and the sections placed onto glass slides. The tissue was stained with Martius-Scarlet-Blue, to identify fibrin deposits. Cover slips were applied and the tissue studied and recorded on film using a light microscope and camera.

5.2.4 ELECTRON MICROSCOPY

Excised *in-vivo* tumor tissue was immediately divided into small pieces (~1 $mm^3$) excluding the tumor center and fixed in 4% glutaraldehyde in cacodylate buffer (pH 7.4). Likewise *in-vitro* tumor cells were immediately washed in PBS, pelleted, and fixed in 4% glutaraldehyde in cacodylate buffer (pH 7.4). Both specimens were then handled in a similar manner. The tissue was washed in cacodylate buffer, post-fixed in Palade's fixative (1% osmium tetroxide, osmolality balanced with sucrose) for 2 hr at 4°C, and rinsed in cacodylate buffer and distilled water. Dehydration was carried out through a series of graded ethyl alcohol, ending in an intermediary solution of propylene oxide. Samples were embedded in epon 812 in Beam™ capsules. The epon was cured for 48 hr at 60°C, thick sectioned (1 micron), placed on glass sides, stained with toludine blue and examined with a light microscope. Selected areas for EM were further trimmed, then sectioned with an ultramicrotome (Reichert™ UM2) producing sections 80-90 nm in thickness. The sections were placed on copper grids and contrasted with uranyl acetate and lead citrate. The tissue was then studied and recorded on film using a Hitachi™ 600 electron microscope.

### 5.2.5 EXPERIMENTAL PROTOCOL

R3327-AT tumor was treated *in-vivo* with interstitial PDT, as described in Chapter 2 and *in-vitro*, as described in Chapter 4. For the *in-vivo* treated tissue a "control" tumor was treated with light only to a total exposure of 2400 Joules. "Treated" tumor was treated with PDT ($P_{II}$ 7.5 mg/kg IV 2 hr prior to light) to a total exposure of 2400 Joules. The animals were sacrificed by cervical dislocation (while anesthetized) 2 hr following treatment and the tumor immediately excised *in-toto*, divided into appropriate sized portions and fixed excluding the center of the tumor. For *in-vitro* treatment, cells were incubated in 20 μg/ml $P_{II}$ 1 hr before and during graded light exposure while gassed in the irradiation chamber with 5% $CO_2$/air. Aliquots containing $1 \times 10^6$ cells were removed prior and following graded light exposure of 0.5, 1.0, 1.5, 2.5, and 3.0 Joules/$cm^2$. The aliquoted cells were pelleted, washed in PBS and fixed.

## 5.3 RESULTS

### 5.3.1 GROSS MORPHOLOGICAL DESCRIPTION

Throughout the experiments reported in this thesis animals treated with PDT were autopsied for various reasons (eg. unexpected death and tissue for histology) and gross morphological findings noted. At 2 hr post-PDT the most notable change was the color of the tumor. Relative to the color of control tumor, which was reddish-pink, the treated tumor had developed a purplish hue and a small amount of

edema was evident. At 24 hr post-PDT there was marked reddish brown edema, extending into the surrounding subcutaneous tissue (Figure 5.1). At 48-72 hr post-PDT the tumors were grossly necrotic as depicted in Figure 5.2. This particular animal died unexpectedly 3 days post-treatment with 2400 Joules and the new lyophilized Photofrin (15 mg/kg,IV) [Lot #89-0089]. The tumor and a surrounding margin of normal flank tissue is ashen grey. This surrounding margin is larger than that observed with the non-lyophilized drug. In fact ischemic damage was noted intra-abdominally to the bowel, which most likely resulted in the demise of this animal. Subsequently, the dosage of the lyophilized $P_{II}$ was reduced to 7.5 mg/kg as guided by a comparative *in-vitro* potency test (Chapman *et al.*, 1991c).

Several days post-PDT an eschar formed and the necrotic tissue sloughed leaving an ulcer of granulation tissue that eventually healed over. If the tumor was not completely infarcted it would grow back from the periphery, producing a donut shaped tumor.

### 5.3.2 MICROSCOPIC DESCRIPTION

On examination of light microscopy specimens at low power, there was no obvious difference between control and treated tumor tissue. At higher power there were hemorrhagic regions in both control and treated tumor most likely arising from

Figure 5.1: Postmortem photograph of a rat with bilateral flank tumors, sacrificed 24 hr post-PDT. The tumor in the rat's right flank has been treated and exhibits reddish brown discoloration and edema. The tumor in the left flank is of equal size and is untreated.

Figure 5.2: Postmortem photograph of a rat that died 3 days post-PDT. This photograph exhibits a necrotic tumor and a sharply demarcated margin of infarcted flank muscle. The boundaries of PDT effect is greater than expected, secondary to the increased potency of the new lypophilized $P_{II}$.

placement of the interstitial acetal needles. Subjectively there were more RBCs in the vasculature of the treated tumor but no evidence of fibrin deposition to account for this.

On examination of the electron micrographs of tumor tissue lased *in-vivo* the most notable difference was the vacuolization of the cells in the treated specimen (Figure 5.3). This vacuolization was present in both endothelial cells and tumor cells and represents swelling of mitochondria along with an increase in cytoplasmic vacuoles (Figure 5.4). Also noted was cell swelling and vascular plugging with erythrocytes and platelets.

Examination of the electron micrographs of tumor cells lased *in-vitro* revealed a similar finding of vacuolization. Figure 5.5 compares the mitochondrial appearance in control and treated cells. Figure 5.5A shows control cells removed immediately prior to light exposure. Figure 5.5B shows cells exposed to 2.0 $J/cm^2$ of 630 nm light and immediately fixed for examination. There was a light exposure dependent increase in cell vacoulization and mitochondrial damage. Figure 5.6 is a higher magnification of similarly treated cells revealing the matrix swelling of the mitochondria. With increasing light exposure however, the morphological appearance of the mitochondria changed from matrix swelling to matrix photo-coagulation (Figure 5.7).

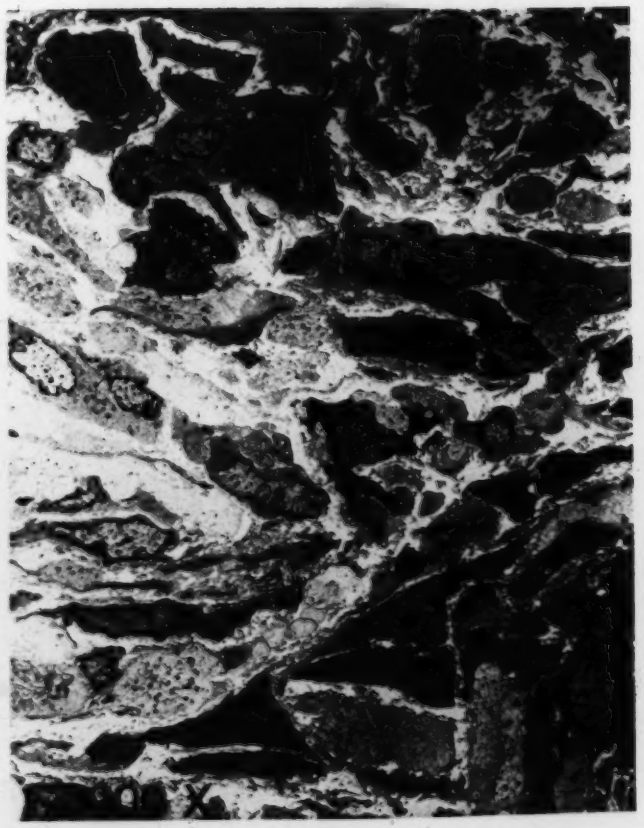

(A)

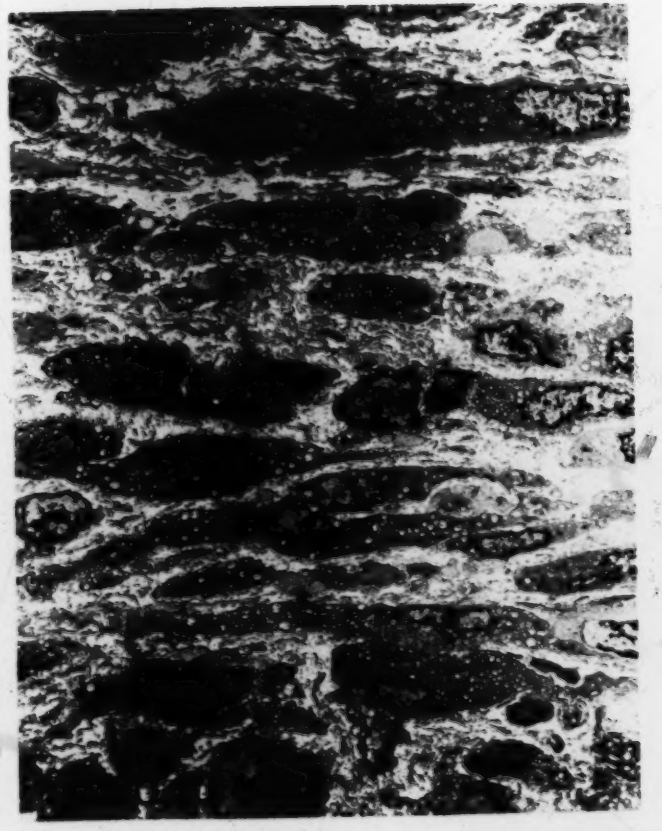

(B)

Figure 5.3: Transmission electron micrographs of the R3327-AT tumor: (A) Control tissue receiving light only. (B) Tissue treated with PDT to 2400 Joules. In comparison to the control tissue, the treated tissue shows extensive vacoulization.

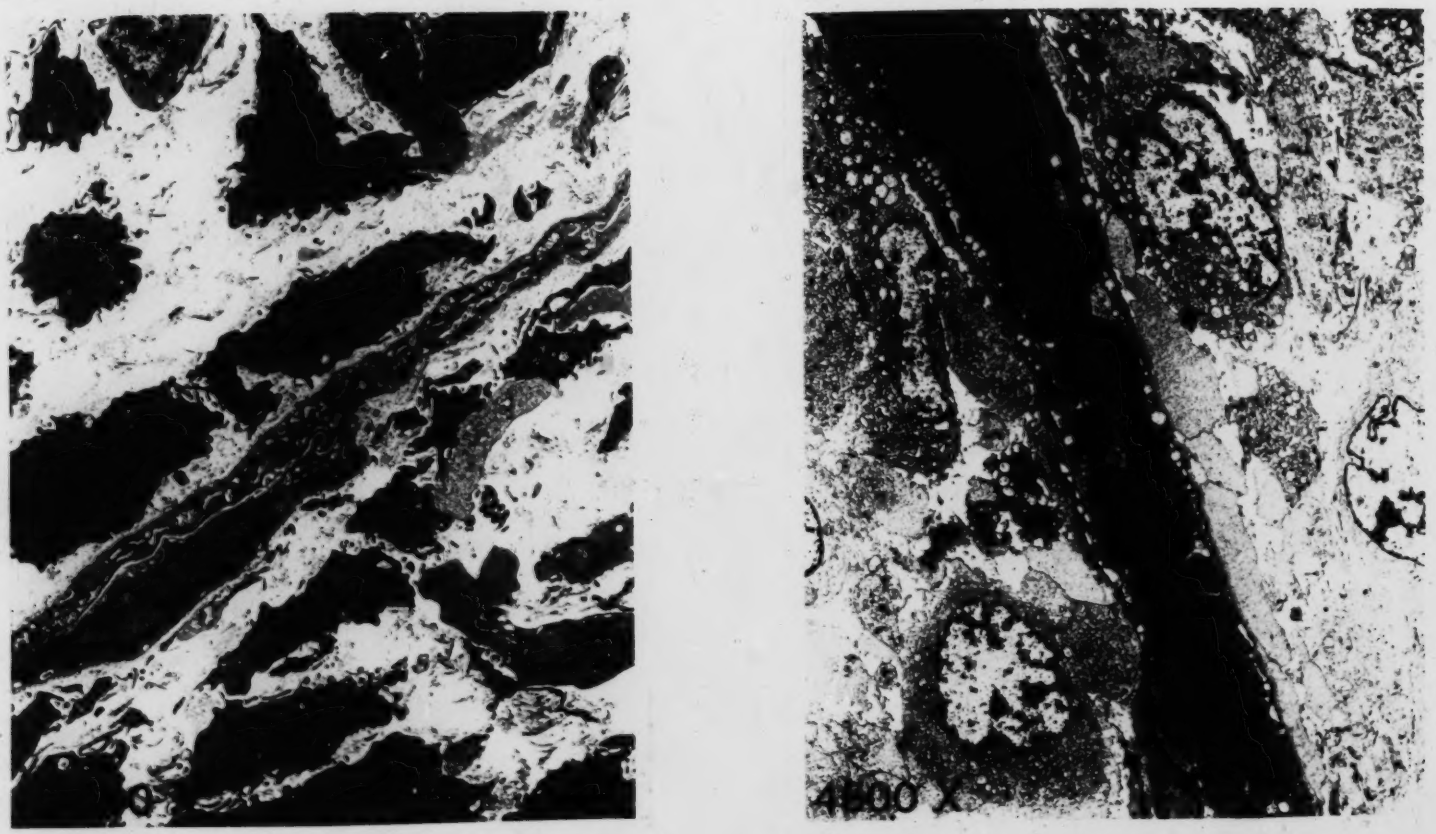


(A) (B)

Figure 5.4: Transmission electron micrographs of (A) non-treated and (B) PDT treated tissue at higher magnification. Both micrographs contain endothelial cells flanked by tumor cells. The treated tissue exhibits vacoulization from mitochondrial swelling in both endothelial and tumor cells. Also evident in the treated tissue is vascular stasis with platelet and RBC plugging.

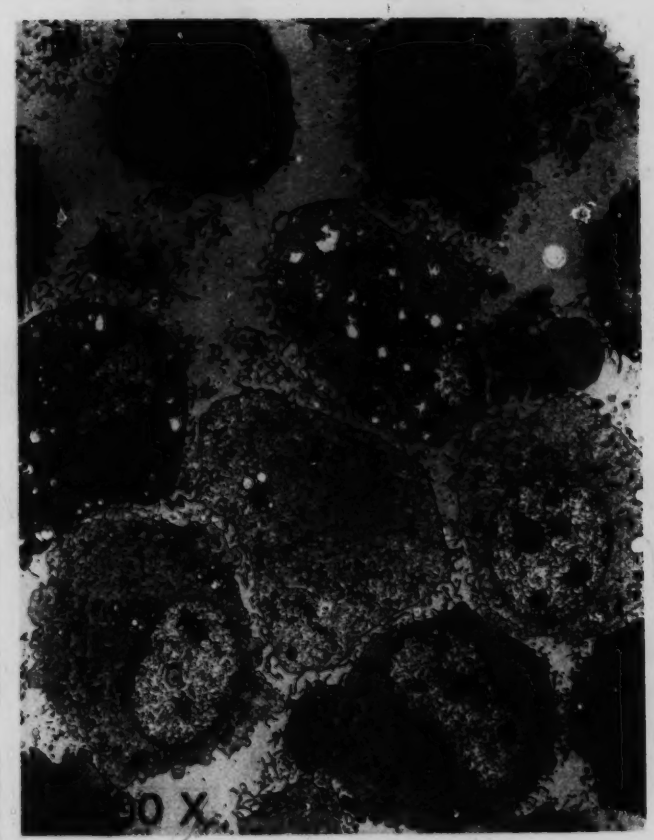


(A)

(B)

Figure 5.5: Transmission electron micrographs of in-vitro R3327-AT tumor cells; (A) non-treated and (B) PDT-treated (2.0 J/cm$^2$). The treated cells exhibit a greater amount of cell vacoulation, and abnormal appearing mitochondria.

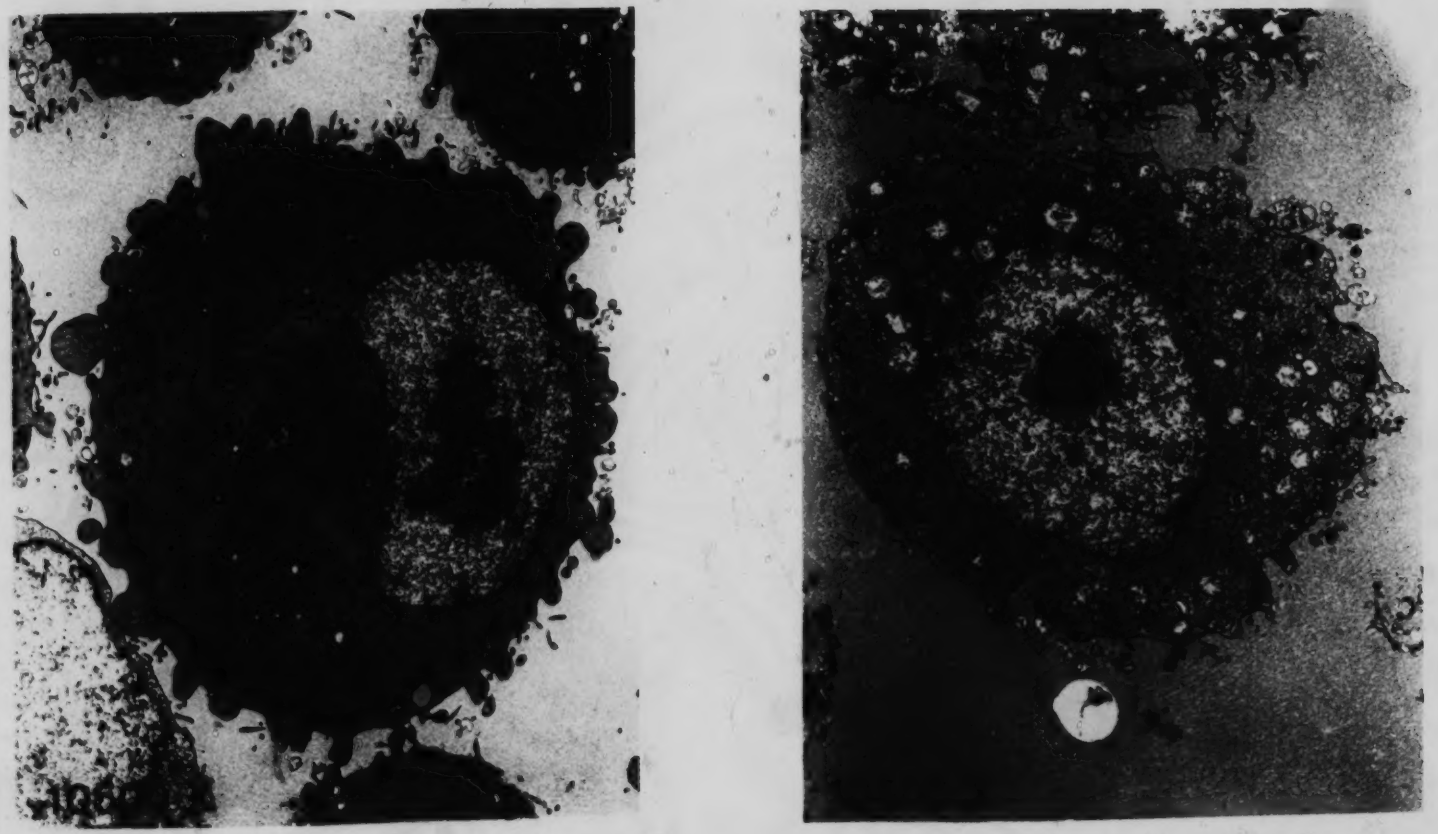

(A) (B)

Figure 5.6: Transmission electron micrographs of the same batch of cells as Figure 5.5, but at higher magnification, revealing the mitochondrial changes. (A) Control cell with normal appearing mitochondrial (B) PDT-treated cell with matrix swelling of mitochondria.

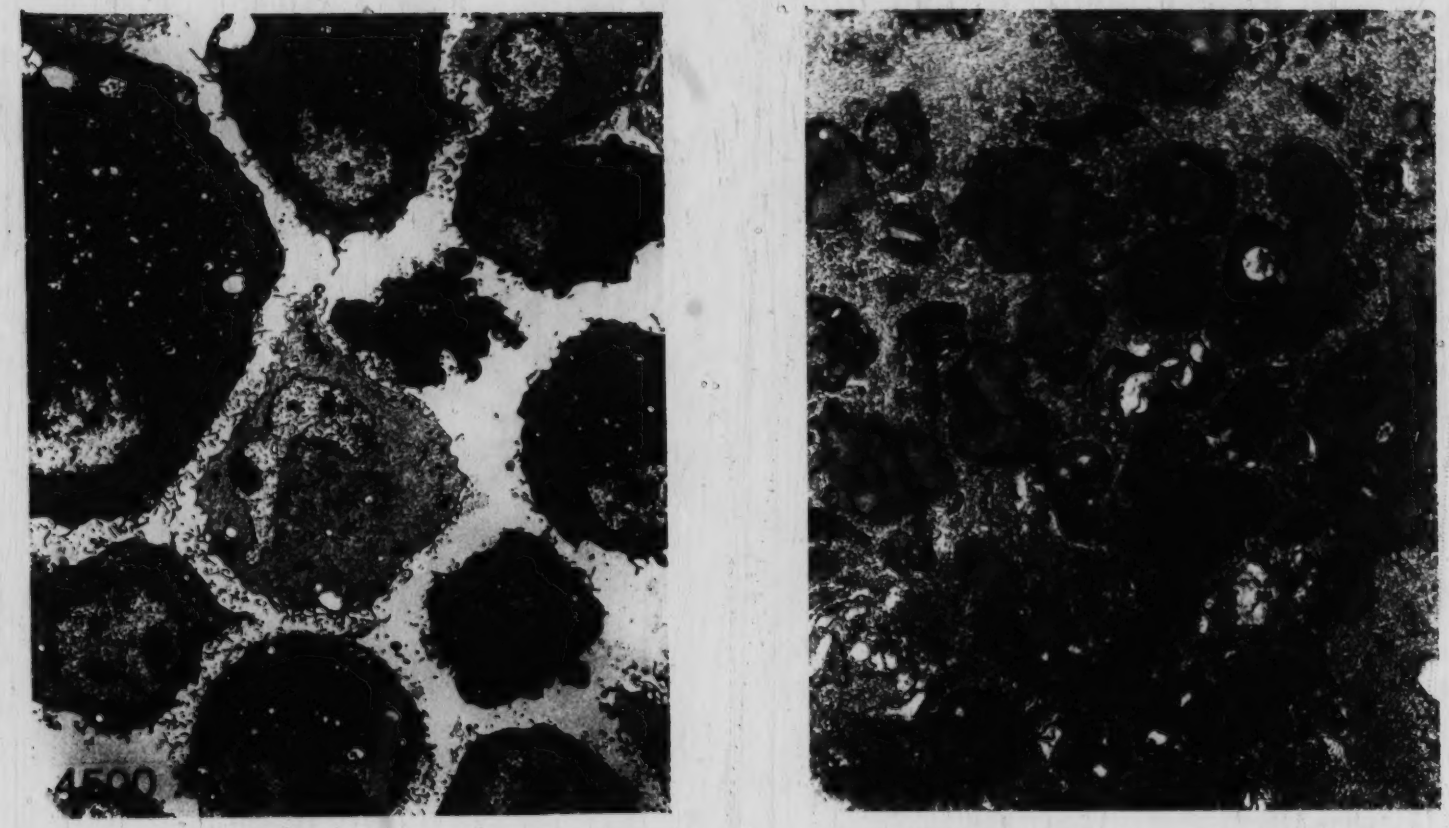


(A) (B)

Figure 5.7: Transmission electron micrographs of in-vitro R3327-AT tumor cells treated with PDT to 3.0 J/cm$^2$. (A) At low power the mitochondria appear very dense. (B) Examination of the same cells at higher power reveals matrix photo-coagulation of the mitochondria.

**5.4 DISCUSSION**

This histopathological study demonstrates PDT-induced changes in both vascular and tumor cells of the Dunning R3327-AT tumor model. Together with the perfusion studies, the data reveal that infarction is an early event resulting in tumor necrosis and sloughing. Contrary to the hypothesis of Ben-Hur *et al.* (1988), the negative fibrin staining studies revealed that the clotting cascade is not involved in the early events of infarction. If it were involved, fibrin deposition should have been noted with Martius-Scarlet-Blue stain. This is in keeping with recent reports that non-steroidal anti-inflamatory drugs (NSAIDs), which inhibit platelet aggregation, can protect against the tumoricidal effects (Ferrario and Gomer, 1990; Fingar *et al.*, 1990). This protection suggests that platelet clotting is involved with vascular stasis. One can envision damage to the endothelial cell surface resulting in activation of platelet aggregation which is dependent on thromboxane $A_2$ for the "release reaction". NSAIDs inhibit cyclo-oxygenase, thereby inhibiting thromboxane $A_2$ production and platelet aggregation. Platelet aggregation is also enhanced in the presence of high levels of ADP, which would increase if mitochondrial oxidative phosphorylation was disrupted by a direct effect as noted by EM in the *in-vitro* treated cells and other studies (Salet and Moreno, 1981; Sandberg *et al.*, 1982; Berns *et al.*, 1982). However the red blood cells (RBCs) themselves may cause vascular stasis by plugging the

vessel lumen as a result of membrane alteration resulting in swollen and rigid RBCs (Bellnier and Dougherty, 1982).

The most notable structural alteration by EM is cell and mitochondrial swelling. The EM changes noted *in-vivo* could result indirectly from ischemia (Ghadially, 1975). However, since similar EM findings were found in cells lased *in-vitro* a direct mechanism is implied. Energy level changes have been shown to produce reversible mitochondrial changes including matrix swelling (Hackenbrock, 1966). However matrix photo-coagulation is not reversible. Thus the mitochondrial changes observed *in-vivo* most likely result from both indirect and direct means. Microspectrofluorometric studies have localized HPD to lysosomes and mitochondria (Reyftmann *et al.*, 1986; Berns *et al.*, 1982). Initially porphyrins are taken up into the cell via coated-pits with LDL and deposited in lysosomes and mitochondria (Candide *et al.*, 1988). The localization of porphyrin to mitochondria is most likely related to the mitochondrial synthesis of heme from the precursor 5-aminolevulinic acid (5-ALA) and coproporphyrinogen III. Therefore mitochondria become a sensitive target by concentration of the photosensitizer.

Why then do cells treated *in-vivo* survive when explanted immediately to tissue culture and cells treated *in-vitro* succumb when they manifest similar ultrastructural changes post-PDT? Henderson and Fingar (1989) performed a unique

experiment to examine this. They studied the relationship between levels of *in-vivo* accumulated photosensitizer ($P_{II}$), photodynamic cell inactivation upon *in-vitro* or *in-vivo* illumination and variable tumor oxygenation in the RIF tumor model. They concluded that direct kill *in-situ* was limited by oxygen as a result of the rapid infarction during *in-vivo* PDT. Therefore the mitochondrial changes observed by EM in the *in-vivo* tissue specimen may result from ischemia, whereas the changes observed in the *in-vitro* specimens result from direct damage to these organelles from photo-oxidative damage. Alternatively there could be localized superheating in the mitochondria, however, with current technology this would not be possible to prove.

## 5.5 CONCLUSIONS

The results reported in this chapter confirm that PDT induced cellular damage is rapid in onset. The histological findings are consistent with previously reported findings in other tumor models (Chaudhuri *et al.*, 1987; Reed *et al.*, 1988; Nelson *et al.*, 1988; Reed *et al.*, 1989). With the observed damage both *in-vivo* and *in-vitro* the question as to why *in-vivo* treated tumors display such a large fraction of indirect cell killing needs further investigation.

# CHAPTER VI

## GENERAL DISCUSSION

The research described in this thesis shows a preponderance of indirect cell kill resulting from vascular injury after tumor PDT. Perfusion imaging studies reveal dose-dependent and time-dependent shutdown that is similar for both well and poorly perfused tumors. Hypoxia imaging studies reveal a negative correlation to perfusion and demonstrate selective targeting of BRAAs. Hypoxia imaging was a less sensitive marker of PDT effect. *In-vivo/in-vitro* clonogenic assays demonstrated the indirect nature of PDT killing and its enhancement by BRAAs. No significant difference in enhancement between the first and second generation hypoxic cytotoxins could be shown when drug is administered at equitoxic doses. Although the enhancement ratio was ~ 2.0 in this assay, BRAAs may play a significant role in mopping up hypoxic cells at the tumor periphery where cells can potentially survive as a graft post-PDT. This form of adjuvant therapy could thus spare the margin of infarcted normal tissue that appears to be required for local PDT cure. The *in-vitro* photobiology studies demonstrate the complex nature of this form of therapy with its three variables that need to be optimized for maximal effect. Partitioning of the large oligomeric components with time appears to be critical as to the cellular and subcellular tumor targets, as well as the efficacy of photo-

inactivation. Histological studies reveal ultrastructural changes to both endothelial and tumor cells. The observed mitochondrial changes are possibly reversible except for the matrix photocoagulation observed *in-vitro*.

Throughout the course of this investigation several limitations of PDT with the current available technology were evident. The first and foremost limiting factor is the currently available clinical photosensitizer $P_{II}$. This mixture of monomers and oligomers has proven over time to have marked variability and potency (Dougherty, 1982). Even with standardized commercial production of lyophilized $P_{II}$ the biological potency has been variable between different lots (Chapman *et al.*, 1991c; and unpublished data). The fact that the debate of chemical composition is still ongoing is worrisome. For knowledgeable clinical application it is necessary to precisely define both photosensitizer concentration and light dose to predict tumor response. The multiple active chemical components in $P_{II}$ and their metabolites create a further variability in an already complex process of three variables, namely oxygen, light and sensitizer.

The limitation of $P_{II}$ as a photosensitizer has been recognized by the research community for some time and criteria for the selection of new compounds have been defined (Bonnett and Berenbaum, 1990). One of these criteria

is that the new photosensitizer be a single chemical structure of known chemical composition. Promising second generation photosensitizers are phthalocyanines, purpurins and chlorins which are synthesized from porphyrins (Kreimer-Birnbaum, 1989). These compounds appear to have similar mechanisms of tumor destruction as those reported for $P_{II}$ (Spikes, 1990; Morgan *et al.*, 1988). If these newer photosensitizers continue to show vascular damage as the mechanism of tumor response then techniques for monitoring and exploiting such damage should prove useful.

The second major limiting factor evident from this investigation is the penetration of 630 nm light in tissue. The "effective" penetration depth of 3 mm greatly limits the interstitial application of PDT. The dilution and attenuation of 630 nm light from cylindrical diffusing fiber tips in air as well as in the R3327-AT and -H tumor is shown in Figure 6.1. The relative light fluence in air is inversely proportional to the distance from the center of the source and represents the dilution of light by divergence. The attenuation of light in tissue is approximately exponential and can be approximated by $e^{-\mu d}$ where d = distance from the source and $\mu$ = the attenuation coefficient, which is inversely proportional to effective penetration depth 1/e (Wilson, 1989). The attenuation of 630 nm light is mainly by hemoglobin and melanin pigments. This

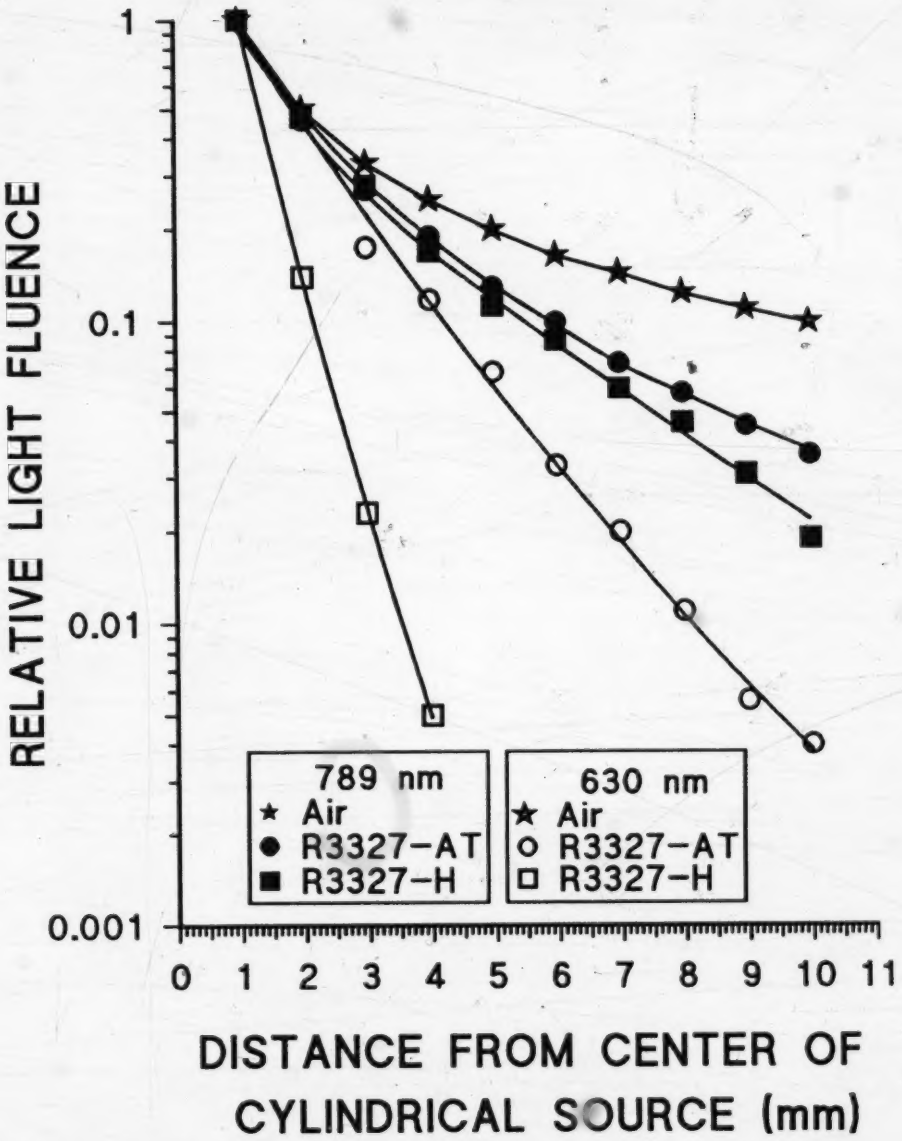


**Figure 6.1: Graph of 630 nm and 789 nm light attenuation in Dunning R3327-H and R3327-AT tumors. Penetration of 630 nm light is 2 X less in the R3327-H tumor as a result of hemoglobin absorption. Penetration of 789 nm light, which is not absorbed by hemoglobin is equal in both the R3327-AT and R3327-H tumors. The "penetrance gain" of 789 nm light over 630 nm light is 2.7 X for R3327-H and 1.4 X for R3327-AT tumor.**

* Unpublished raw data obtained from Dr. Mark Arnfield, CCI.

is clearly demonstrated when the R3327-AT tumor is compared to the R3327-H tumor, which is 1.8 X better perfused on average and has a two-fold greater attenuation. By using light with wavelengths greater than 630 nm there is less absorption by hemoglobin and therefore greater penetration. Singlet oxygen can be generated by quantum energies as low as 0.98 electron volts (1270 nm). However since excitation has to occur through the triplet state of the sensitizer, which is 0.55 electron volts below the lowest singlet state, 1.48 electron volts are required, corresponding to about 850 nm (Moan, 1990). Thus a therapeutic window for optimal tissue penetration and singlet oxygen generation is between 700 and 850 nm. Current research is thus focusing on developing lasers and photosensitizers that emit and absorb light in this part of the electromagnetic spectrum. Newer photosensitizers absorbing in this region will require larger absorption coefficients thus themselves becoming the limiting factor to light penetration (Wilson, 1989). The fact that light does not penetrate as well in the R3327-H tumor did not limit the response of this tumor to PDT relative to the more transparent R3327-AT tumor. This is most likely related to the PDT effect being dependent on the product of light fluence x sensitizer concentration. The R3327-H being better perfused would also be expected to receive more sensitizer in direct proportion to its perfusion.

The most commonly used lasers for PDT are argon pumped dye lasers. The dye lasers have the advantage of being tunable over the projected absorption spectrum for the second generation photosensitizers. However, their high capital and running costs, complexity and poor reliability make them less than desirable for clinical application. Current laser developments include diode lasers than can produce up to 1 watt of emitted light. Unfortunately this emitted light is of a fixed wavelength. The development of more powerful diode lasers is currently limited by semiconductor materials. However, diode arrays may over come this limitation. Preliminary light penetration studies with a diode laser emitting 789 nm light are encouraging (Figure 6.1). At 10% attenuation (relative fluence) there is a "penetrance gain" of 2.7 X for the R3327-H tumor and 1.4 X for the R3327-AT tumor, in the absence of a photosensitizer. The ratio of these penetrance gain (2.7/1.4) is - 1.9. Again this coincides with the difference in perfusion. As expected, the penetration of 789 nm light in the R3327-AT and -H tumors is almost equal in the absence of absorption by hemoglobin and photosensitizer. For interstitial application the gain in needle separation would be - 1.5 X. Strict placement of needles within tumors at 10-12 mm spacing may still prove to be clinically difficult. Once again the addition of BRAAs may extend the "effective limits" of PDT.

One of the major clinical limitations of PDT is the prolonged skin photosensitivity following photosensitizer administration. Second generation photosensitizers have been developed with increased hydrophilicity in an attempt to increase the excretion rate. However, *in-vivo* bioassays of these compounds have shown them to be less effective in producing photodynamic effect (Bonnett and Berenbaum, 1990).

With the currently available technology clinical PDT appears to have the greatest potential for treatment of superficial diffuse intracavitary lesions. Such lesions include; transitional cell carcinoma of the bladder and malignant mesothelioma of the pleura where the limited penetration of light is desirable. Another promising site of therapy is superficial basal and squamous cell carcinoma of the skin. Topical application of 5-aminolevulinic acid to these superficial lesions as put forward by Kennedy *et al.* (1990) would alleviate the undesired general cutaneous photosensitivity. The interstitial application of PDT for solid tumors such as prostate awaits the development of a pure single component photosensitizer with improved pharmacological and chemical properties. Such a photosensitizer in combination with accurate photodosimetry would allow precise prediction of the boundaries of photodynamic effect. With the current lack of photosensitizer selectivity for tumor or minimal selectivity this becomes extremely important since the current response

to PDT is not unlike surgical excision. A sharp demarcation of tissue necrosis is observed dependent upon light and photosensitizer concentration which is unlike the mitotic arrest observed with radiotherapy. With the advent of an improved photosensitizer $^{99m}Tc$ HMPAO SPECT imaging should prove useful for monitoring PDT response and adjuvant bioreductive chemotherapy with Etanidazole could potentiate tumor response.

## BIBLIOGRAPHY


ADAMS, J.E. — AHMED, I., SHELDON, P.W., STRATFORD, I.J. Radiation sensitization and chemo potentiation: RSU-1069 a compound more efficient than misonidazole in-vitro and in-vivo. Br. J. Cancer 49:571-577, 1984

ARNFIELD, M.R. — GONZALEZ, S., LEE, P., TULIP, J., McPHEE, M.S. Cylindrical irradiator fiber tip for photodynamic therapy. Lasers Surg. Med. 6:150, 1986

ARNFIELD, M.R. — TULIP, J., CHETNER, M., McPHEE, M.S. Optical dosimetry for interstitial photodynamic therapy. Med. Phys. 16:602, 1989

ARNFIELD, M.R. — TULIP, J., McPHEE, M.S. Photodynamic therapy dosimetry in postmortem and in-vivo rat tumors and an optical phantom. Photochem. Photobiol. 51(6):667-674, 1990

ATHAR, M. — MUKHTAR, H., BICKERS, D.R. Differential role of reactive oxygen intermediates in Photofrin I and Photofrin II mediated photo enhancement of lipid peroxidation in epidermal microsomal membranes. Invest. Dermatology 90:652-657, 1988

BALCHUM, O.J. — DOIRON, D.R., HUTH, G. Photoradiation therapy of endobronchial tumors using the photodynamic effect of hematoporphryin derivative. Lasers Surg. Med. 4:13-30, 1984(a)

BALCHUM, O.J. — PROFIO, A.E., DOIRON, D.R. Imaging fluorescence bronchoscopy for localizing early bronchial cancer and carcinoma in-situ. In: Porphyrin localization and treatment of tumors. (D.R. Doiron, C.J. Gomer, eds) Alan R. Liss, New York, NY, Prog. Clin. Biol. Res. 170:847-861, 1984(b)

BALLINGER, J.R. — REID, R.H., GULENCHYN, K.Y. Radiochemical purity of $^{99m}$TcHMPAO. Nuc. Med. 29:572, 1988

BAREL, A. JORI, G., PERIN, A., ROMANDINI, P., PAGNAN, A., BIFFANTI, S. Role of high, low and very low density lipoproteins and the transport and tumor delivery of hematoporphyrin in-vivo. Cancer Lett. 32:145-150, 1986

BELLNIER, D.A. DOUGHERTY, T.J. Membrane lysis in chinese hamster ovary cells treated with hematoporphyrin derivative plus light. Photochem. Photobiol. 36(1):43-47, 1982

BELLNIER, D.A. HO., Y.K., PANDEY, R.K., MISSERT, J.R., DOUGHERTY, T.J. Distribution and elimination of Photofrin II in mice. Photochem. Photobiol. 50(2):221-228, 1989

BEN-HUR, E. HELDMAN, E., CRANE, S.W., ROSENTHAL, I. Release of clotting factors from photosensitized endothelial cells: A possible trigger for blood vessel occlusion by photodynamic therapy. FEB. Lett. 236(1):105-108, 1988

BENSON Jr. R.C. Treatment of diffuse transitional cell carcinoma in-situ by whole bladder hematoporphyrin derivative photodynamic therapy. J. Urol. 134:675-678, 1985

BENSON Jr. R.C. FARROW, G.M., KINSEY, J.H., CORTESE, D.A., ZINCKE, H., URTZ, D.C. Detection and localization of in-situ carcinoma of the bladder with hematoporphyrin derivative. Mayo Clin. Proc. 57:548-555, 1982

BERENBAUM, M.C. BONNETT, R., SCOURIDES, P.A. In-vivo biological activity of the components of hematoporphyrin derivative. Br. J. Cancer 45:571-581, 1982

BERENBAUM, M.C. HALL, G.W., HOYES, A.D. Cerebral photosensitization by hematoporphyrin derivative. Evidence for endothelial site of action. Br. J. Cancer 53:81-89, 1986

| | |
|---|---|
| BERNS, M.W. | DAHLAMAN, A., JOHNSON, F.M., BURNS, R., SPERLING, D., GUILTINAN, M., SIEMENS, A., WALTER, R., WRIGHT, W., HAMMER-WILSON, M., WILE, A. In-vivo cellular effects of hematoporphyrin derivative. Cancer Res. 42:2325-2329, 1982 |
| BERTOLONI, G. | SALVATO, B., DAL'ACQUA, M., VAZZOLER, M., JORI, G. Hematoporphyrin sensitized photoinactivation of Streptococcus faecalis. Photochem. Photobiol. 39:811, 1984 |
| BIAGLOW, J.E. | VARNES, M.E., ROIZAN-TOWLE, L., CLARK, E.P. EPP, E.R., ASTOR, M.B., HALL, E.J. Biochemistry of reduction of nitroheterocycles. Biochem. Pharmacol. 35:77-90, 1986 |
| BOEGHEIM, J.P.J. | SCHOLET, H., DUBBELMAN, T.M.A.R., BEEMS, E., RAAP, A., van STEVENINCK, J. Photodynamic effects of hematoporphryin derivative on enzyme activities of murine L-929 fibroblasts. J. Photochem. Photobiol.B:Biol. 1:61-73, 1987 |
| BONNETT, R.B. | BERENBAM, M.C. HPD-A study of its components and their properties. Adv. Exp. Biol. Med. 160:241-250, 1983 |
| BONNETT, R.B. | BERENBAUM, M.C. Porphyrins as photosensitizers. Photosensitizing compounds: Their chemistry, biology and clinical use. Wiley, Chichester (Ciba Foundation Symposium 146) 40-59, 1989 |
| BONNETT, R.B. | BERENBAUM, M.C. Porphyrin sensitizers in tumor phototherapy: Novel sensitizers of the chlorin and bacteriochlorin class with amphiphilic proteins. J. Photochem. Photobiol. B:Biol. 6:29-37, 1990 |
| BRAULT, D. | Physical chemistry of porphyrins and their interactions with membranes: The importance of pH. J. Photochem. Photobiol. B:Biol. 6:79-86, 1990 |

BROWN, J.M. YU, N.Y., BROWN, D.M., LEE, W.W. SR-2508; A 2-nitroimidazole amide which should be superior to misonidazole as a radiosensitizer for clinical care. Int. J. Radiat. Oncol. Biol. Phys. 7:695-701, 1981

BUETTNER, G.R. NEED, M.J., Hydrogen peroxide and hydroxyl free radical production by hematoporphyrin derivative, ascorbate and light. Cancer Lett. 25:297-304, 1985

BYRNE, C.J. MARSHALLSAY, L.V., WARD, A.D. The compositions of Photofrin II. J. Photochem. Photobiol. B:Biol. 6:13-27, 1990

CAMPS, J.L. POWERS, S.K., BACKMAN, W.C., BROWN, J.T., WEISSMAN, R.M. Photodynamic therapy of prostate cancer: An in-vitro study. J. Urol. 134:1222-1226, 1985

CANDIDE, C. MORLIERE, P., MAZIERE, J.C., GOLDSTEIN, S., SANTUS, R., DUBERTRET, L., REYFTMANN, J.P., POLONOVSKY, J. In-vitro interaction of the photoactive anti-cancer porphyrin derivative Photofrin II with low density lipoprotein, and its delivery to cultured human fibroblasts. FEBS. Lett. 207(1):133-138, 1986

CANDIDE, C. REYFTMANN, J.P., SANTUS, R., MAZIERE, J.C., MORLIERE, P., GOLDSTEIN, S. Modification of ε-amino group of lysines, cholesterol oxidation and oxidized lipid apoprotein cross link formation by porphyrin-photosensitized oxidation of human low density lipoproteins. Photochem. Photobiol. 48(2):137-146, 1988

CASTELLANI, A. PACE, G.P., CONCIOLI, M., Photodynamic effect of hematoporphyrin on blood circulation. Path. Bact. 86:99-102, 1963

CHANG, C.T. DOUGHTERY, T.J. Photoradiation therapy: Kinetics and thermodynamics porphyrin uptake and loss in normal and malignant cells in culture. Radiat. Res. 74:498, 1978

CHAPMAN, J.D. Hypoxic sensitizers-implications for radiation therapy. New England J. Med. 301:1429, 1979

CHAPMAN, J.D. BAER, K., LEE, J. Characteristics of the metabolism-induced binding of misonidazole to hypoxic mammalian cells. Cancer Res. 43:1523-1528, 1983(a)

CHAPMAN, J.D. BLAKELY, E.A., SMITH, K.C., URTASUN, R.C. Radiobiological characterization of the inactivating events produced in mammalian cells by helium and heavy ions. Int. J. Radiat. Oncol. Biol. Phys. 3:97-102, 1977

CHAPMAN, J.D. FRANKO, A.J., SHARPLIN, J. A marker for hypoxic cells in tumors with potential clinical applicability. Br. J. Cancer 43:546-550, 1981

CHAPMAN J.D. LEE, J., MEEKER, B.E. Keynote address: Cellular reduction of nitroimidazole drugs: potential for selective chemotherapy and diagnosis of hypoxic cells. Int. J. Radiat. Oncol. Biol. Phys. 16:911-917, 1989

CHAPMAN, J.D. McPHEE, M.S., WALZ, N., CHETNER, M.P., STOBBE, C.C., SODERLINE, K., ARNFIELD, M.R., MEEKER, B.E., TRIMBLE, L., ALLEN, P.S., NMR spectroscopy and sensitizer-adduct measurement of PDT induced ischemia in solid tumors. J. Natl. Cancer Inst. (In Press), 1991(a)

CHAPMAN, J.D. NGAN-LEE, J., STOBBE, C.C., MEEKER, B.E. Radiation-induced and metabolism-induced reactions of hypoxic sensitizers with cellular macromolecules. In: "Advanced Topics on Radiosensitizers of Hypoxic Cells",(A. Breccia, C. Rimondi, G.E. Adams, eds.) Plenum Press, New York, NY 91-103, 1983(b)

CHAPMAN, J.D. STOBBE, C.C., ARNFIELD, M.R., SANTUS, R., LEE, J., McPHEE, M.S. Oxygen dependency of tumor cell killing in-vivo by light activated Photofrin II. Radiat. Res. (In Press), 1991(b)

CHAPMAN, J.D. — STOBBE, C.C., ARNFIELD, M.R., SANTUS, R., McPHEE, M.S. The effectiveness of short-term versus long-term exposure to Photofrin II in killing light activated tumor cells. Radiat. Res. (In Press), 1991(c)

CHAUDHURI, K. — KECK, R.W., SELMAN, S.H. Morphological changes of tumor microvasculature following hematoporphyrin derivative sensitized photodynamic therapy. Photochem. Photobiol. 46(5):823-827, 1987

CHOPP, M. — HETZEL, F.W., JIANKA, Q. Dose-dependent metabolic responses of mammary carcinoma to photodynamic therapy. Radiat. Res. 121:288-294, 1990

DEUTICKE, B. — HENSELEIT, U., HAEST, C.W.M., HELLER, K.B., DUBBELMAN, T.M.A.R. Enhancement of transbilayer mobility of a membrane lipid probe accompanies formation of membrane leaks during photodynamic treatment of erythrocytes. Biochimica et Biophysica Acta 982:53-61, 1988

DIAMOND, I. — GRANELLI, S., McDONAGH, A.F., NIELSEN, S., WILSON, C.B., JAENICKE, R. Photodynamic therapy of malignant tumors. Lancet 2:1175-1177, 1972

DOUGHERTY T.J. — Variability in hematoporphryin derivative preparation. Cancer Res. 42:1188, 1982

DOUGHERTY, T.J. — Photodynamic therapy (PDT) of malignant tumors. CRC Crit. Rev. Oncol. Hematol. 2:83-116, 1984(a)

DOUGHERTY, T.J. — Photosensitizers: Therapy and detection of malignant tumors. Photochem. Photobiol. 45:879-889, 1987

DOUGHERTY, T.J. — Photodynamic therapy. In: Medical radiology innovations and Radiation Oncology (H.R. Withers, L.J. Peters, eds.) Springer-Verlag, Berlin Heidelberg. 175-188, 1989

DOUGHERTY, T.J. — COOPER, M.T., MANG, G.S. Cutaneous phototoxic occurrences in patients receiving Photofrin. Lasers Med. Surg. 10(5):485-488, 1990

DOUGHERTY, T.J. GRINDEY, G.B., WEISHAUPT, K.R., BOYLE, D.G. Photoradiation therapy 2. Nat. Cancer Instit. 55:115-120, 1975

DOUGHERTY, T.J. KAUFMAN, J.E., GOLDFARB, A., WEISHAUPT, K.R., BOYLE, D.G., MITTLEMAN, A. Photoradiation therapy for the treatment of malignant tumors. Cancer Res. 38:2628-2635, 1978

DOUGHERTY, T.J. LAWRENCE, G., KAUFMAN, J.H., BOYLE, D., WEISHAUPT, K.R., GOLDFARB, A. Photoradiation in the treatment of recurrent breast carcinoma. J. Natl. Cancer. Inst. 62:231-237, 1979

DOUGHERTY, T.J. POTTER, W.R., WEISHAUPT, K.R. The structure of the active component of hematoporphyrin derivative. In: Porphyrin localization treatment of tumors. (D.R. Doiron, C.J. Gomer, eds.) Alan R. Liss Inc., New York 301-314, 1984(b)

DUBBELMAN, T.M.A.R. van STEVENINCK, J. Photodynamic effect of hematoporphyrin-derivative on transmembrane transport system of murine L-929 fibroblasts. Biochemica et Biophysica Acta 771:201-207, 1984

DUNNING, W.F. Prostate cancer in the rat. Natl. Cancer Inst. Monogram 12:351, 1963

EDELL, E.S. CORTESE, D.A. Bronchoscopic phototherapy with hematoporphyrin derivative for treatment of localized bronchogenic carcinoma: A five year experience. Mayo Clin. Proc. 62:8, 1987

FERRARIO, A. GOMER, C.J. Systemic toxicity in mice induced by localized porphyrin photodynamic therapy. Cancer Res. 50:539-543, 1990

FIGGE, F. WIELAND, G., MANGIELLO, L. Cancer detection and therapy. Affinity of neoplastic, embryonic and traumatized tissue for porphyrins and metalloporphyrins. Proc. Soc. Ex. Biol. Med. 168:640-641, 1948

FINGAR, V.H. — HENDERSON, B.W. Drug and light dose dependence of photodynamic therapy: a study of tumor and normal tissue response. Photochem. Photobiol. 46:837-841, 1987

FINGAR, V.H. — POTTER, W.R., HENDERSON, B.W. Drug and light dose dependence of photodynamic therapy: A study of tumor cell clonogenicity and histological changes. Photochem. Photobiol. 45:643, 1987

FINGAR, V.H. — WIEMANN, T.J.M, DOAK, K.W. Role of Thromboxane and Prostacyclin release on photodynamic therapy-induced tumor destruction. Cancer Res. 50:2599-2603, 1990

FOOTE, C.S. — Mechanisms of photo-oxygenation. In: Porphyrin localization and treatment of tumors (D.R. Dorin, C.G. Gomer, eds) Alan R. Liss, New York, NY, 301-334, 1984

GHADIALLY, F.N. — Ultrastructural pathology of the cell. A text and altas of physiological and pathological alterations in cell fine structure. Butterworths, London. 1975

GIDDINGS, J.C. — JARVIS, A.L., BLOOM, A.L. Differential localization and synthesis of porcine Factor VIII R:AG in vascular endothelium and endothelial cells in culture. Thrombosis Res. 29:299-312, 1983

GOMER, C.J. — DNA damage and repair in Chinese hamster ovary cells following hematoporphryin photoradiation. Cancer Lett. 11:161-167, 1980

GOMER, C.J. — DOIRON, D.R., RUCKER, N., RAZUM, N.J., FOUNTAIN, S.W. Action spectrum (620-640 nm) for hematoporphyrin derivative induced cell killing. Photochem. Photobiol. 39:365-368, 1984

GOMER, C.J. — DOUGHTERY, T.J. Determination of [$^{3}$H ($^{14}$C)] hematoporphyrin derivative distribution in malignant and normal tissue. Cancer Res. 39:146-151, 1979

GOMER, C.J. RUCKER, N., BANERJEE, A., BENEDICT, W.F. Comparison of mutagenicity and induction of sister chromatid exchanges in Chinese hamster cells exposed to hematoporphyrin derivative, photoradiation, ionizing radiation or UV irradiation. Cancer Res. 43:2622-2627, 1983

GOMER, C.J. RUCKER, N., FERRARIO, A., LIN MURPHREE, A. Expression of potentially lethal damage in Chinese hamster cells exposed to hematoporphyrin derivative photodynamic therapy. Cancer Res. 46:3348, 1986

GOMER C.J. RUCKER, N., FERRARIO, A., WONG, S. Properties and applications of photodynamic therapy. (Review) Radiat. Res. 120:1-18, 1989

GOMER, C.J. RUCKER, N., MURPHREE, A.L. Differential cell photosensitivity following porphyrin photodynamic therapy. Cancer Res. 48:4539-4542, 1988(a)

GOMER, C.J. RUCKER, N., MURPHREE, A.L. Transformation and mutagenic potential of porphyrin photodynamic therapy in mammalian cells. Int. J. Radiat. Biol. 53:651-659, 1988(b)

GONZALEZ, S. ARNFIELD, M.R., MEEKER, B.E. TULIP, J., LAKEY, W.H., CHAPMAN, J.D., McPHEE, M.S. Treatment of Dunning R3327-AT rat prostate tumors with photodynamic therapy in combination with misonidazole. Cancer Res. 46:2858, 1986

GRASCHEW, G. SHOPOVA, M. Hypoxia, misonidazole and hyperthermia in photodynamic therapy of tumors. Lasers in Med. Sci. 1:181-186, 1986

GREGORIE, H.B. HORGER, E.O., WARD, J.L., GREEN, J.F., RICHARDS, T., ROBERTSON, H.C., STEVENSON, T.B. Hematoporphyrin-derivative fluorescence in malignant neoplasms. Ann. Surg. 167:820-828, 1968

GROSSWEINER, L.I — Membrane photosensitization by hematoporphyrin and hematoporphyrin derivative. In: Porphyrin Localization and Treatment of Tumors.(C.J. Gomer, D.R. Dorion) Alan R. Liss, New York, 391-404, 1984

HACKENBROCK, C.R. — Ultrastructural bases for metabolically linked mechanical activity in mitochondria: 1. Reversible ultrastructural changes with change in metabolic steady state in isolated liver mitochondria. J. Cell Biol. 30:269-297, 1966

HAMMERSLEY, P.A.G. — McCREDY, V.R., BABICH, J.W., COGHLAN, G. 99mTc-HMPAO as a tumor blood flow agent. Eur. Nuc. Med. 13:90, 1987

HENDERSON, B.W. — BELLNIER, D.A., ZIRING, B., DOUGHERTY, T.J. Aspects of the cellular uptake and retention of hematoporphyrin derivative and their correlation with biological response to PRT in-vitro. In: Porphyrin Photosensitization, (D. Kessel, T.J. Dougherty, eds.), Plenum Press, New York, NY 129-137, 1983

HENDERSON, B.W. — DONOVAN, J.M. Release of prostaglandin $E_2$ from cells by photodynamic treatment in-vitro. Cancer Res. 49:6896-6900, 1989

HENDERSON B.W. — FINGAR, V.H. Oxygen limitation of direct tumor cell kill during photodynamic treatment of a murine tumor model. Photochem. Photobiol. 49(3):299-304, 1989

HENDERSON, B.W. — FINGAR, V.H. Relationship of tumor hypoxia and response to photodynamic treatment in an experimental mouse tumor. Cancer Res. 47:3110-3114, 1987

HENDERSON, B.W. — MILLER, A.C. Effects of scavengers of reactive oxygen and radical species on cell survival following photodynamic treatment in-vitro: Comparison to ionizing radiation. Radiat. Res. 108:196-205, 1986

HENDERSON, B.W. WALDOW, S.M., MANG, T.S., POTTER, W.R., MALONE, P.B., DOUGHERTY, T.J. Tumor destruction and kinetics of tumor cell death in two experimental mouse tumors following photodynamic therapy. Cancer Res. 45:572, 1985

HENRY, J.M. ISAACS, J.T. Synergistic enhancement of the efficacy of the bioreductively activated alkylating agent RSU-1164 in the treatment of prostate cancer by photodynamic therapy. J. Urol. 142:165, 1989

HILF, R. GIBSON, S.L., PENNEY, D.P., CECKLER, T.L., BRYANT, R.G. Early biochemical responses to photodynamic therapy monitored by NMR spectroscopy. Photochem. Photobiol. 46:809, 1987

HILF, R. MURANT, R.S., NARAYANAN, U., GIBSON, S.L. Relationship of mitochondrial function and cellular adenosine triphosphate levels to hematoporphyrin derivative-induced photosensitization in R-3230-AC mammary tumors. Cancer Res. 46:211-217, 1986

HIRSCH, B.D. WALZ, N.C., MEEKER, B.E., ARNFIELD, M.R., TULIP, J., McPHEE, M.S., CHAPMAN, J.D. Photodynamic therapy induced hypoxia in rat tumors and normal tissue. Photchem. Photobiol. 45:847, 1987

ISAACS, J.T. Development and characteristics of the available animal model systems for the study of prostate cancer. In: Current Concepts and Approaches to the Study of Prostate Cancer, (D.S. Coffey, N. Bruchovsky, W.A. Gardener, M.I. Resnick, J.P. Cur eds.) New York, Alan R. Liss, New York, 513-576, 1987

KENNEDY, J.C. POTTIER, R.H., PROSS, D.C. Photodynamic therapy with endogenous protoporphyrin IX: Basic principles and present clinical experience. Photochem. Photobiol. B:Biol. 6:143-148, 1990

KESSEL, D. Effects of photoactivated porphyrins at the cell surface of leukemia L-1210 cells. Biochem. 16(15):3443-3449, 1977

KESSEL, D. Chemical and biochemical determinants of porphyrin localization in porphyrin localization and treatment of tumors, (C.J. Gomer, D.R. Doiron, eds.) Alan R. Liss, New York, 405-418, 1984

KESSEL, D. Porphyrin-lipoprotein association as a factor in porphyrin localization. Cancer Lett. 33:183, 1986(a)

KESSEL, D. Proposed structure of the tumor localizing fraction of HPD. Photochem. Photobiol. 44:193-196, 1986(b)

KESSEL, D. CHOU, T.H. Tumor-localizing components of porphyrin preparation of hematoporphyrin derivative. Cancer Res. 43:1994-1999, 1983

KINSEY, J.H. CORTESE, D.A., NEEL, H.B. Thermal considerations in murine tumor killing using hematoporphyrin derivative phototherapy. Cancer Res. 43:1562-1567, 1983

KLAUNIG, J.E. SELMAN, S.H., SHULOK, J.R., SCHAFER, P.J., BRITTON, S.L., GOLDBLATT, P.J. Morphological studies of bladder tumors treated with hematoporphyrin derivative photochemotherapy. Am. J. Pathol. 119(2):236-243, 1985

KREIMER-BIRNBAUM, M. Modified porphyrins, chlorins, phthalocyanines and purpurins: Second-generation photosensitizers for photodynamic therapy. Seminars in Hematology 26:157-173,1989

LAM, S. MULLER, N.L., MILLER, R.R., KOSTASHUK, E.C., SZASZ, I.J., LeRICHE, J.C., LEE-CHUY, E. Predicting the response of obstructive endobronchial tumors to photodynamic therapy. Cancer Res. 58:2298-2306, 1986

LI, J. GUO, Z., GIN, M., ZHAO, F., CAI, W., GAO, M., SHU, M., ZOU, J. Photodynamic therapy in the treatment of malignant tumors: An analysis of 540 cases. J. Photochem. Photobiol. B:Biol. 6:149-155, 1990

| | |
|---|---|
| LIPSON, R.L. | BALDES, E.J. OLSEN, E.M. The use of a derivative of hematoporphyrin in tumor detection. Nat. Cancer. Instit. 26:1-12, 1961 |
| LOFGREN, L. | LARSSON M., THANING, L., HALLGREN, S. Transthoracic endoscopic photodynamic treatment of malignant mesotheliomas. Lancet. 337(8737):359, 1991 |
| MADOR, D. | RITCHIE, B., MEEKER, B., MOORE, R.B., ELLIOTT, F.G., McPHEE, M.S., CHAPMAN, J.D., LAKEY, W.H. Response of the Dunning R3327-H prostate adenocarcinoma to radiation and various chemotherapeutic drugs. Cancer Treatment Report 66:1837-1843, 1982 |
| MANNAN, R.H. | SOMAYAJI, V.V., LEE, J., MERCER, J.R., CHAPMAN, J.D., WIEBE, L.I. Radioiodinated 1-(5-iodo-5'-deoxy-D-arabinofuranosyl)-2-nitroimidazole (Iodoazomycin Arabinoside: IAZA); a novel marker for tissue hypoxia. J. Nuc. Med. (Submitted), 1991 |
| MATHESON, I.B.C. | ETHERIDGE, R.D, KRATOWICH, N.R., LEE, J. The quenching of singlet oxygen by amino acids and proteins. Photochem. Photobiol. 21:165-171, 1975 |
| McCAUGHAN, J.S. | GUY, J.T., HICKS, W., LAUFMAN, L., NIMS, S.T.A., WALKER, J. Photodynamic therapy for cutaneous and subcutaneous malignant neoplasms. Arch. Surg. 124:211-216, 1989 |
| McPHEE, M.S. | THORNDYKE, C.W., THOMAS, G., TULIP, J., CHAPMAN, J.D., LAKEY, W.H. Interstitial applications of laser irradiation in hematoporphyrin derivative-photosensitized Dunning R-3327 prostate cancers. Lasers Surg. Med. 4:93-98, 1984 |

MERCER, J.R. — MANNAN, R.H., SOMAYAJI, V.V., LEE, J., CHAPMAN, J.D., WIEBE, L.I. Sugar-coupled 2-nitroimidazoles: Novel in-vivo markers for hypoxic tumor tissue. In: "Advances in Radiopharmacology", Proc. 6th Int. Sym. Radiopharm., Wollongong, Australia. (D.J. Maddalena, G.M. Snowdon, G.R. Boniface, eds.) Wollongong University Press 104-113, 1990

MEYER-BETZ, F. — Investigation on the biological (photodynamic) action of hematoporphyrin and other derivatives of blood and bile pigments. Deutsch Arch. Klin. Med. 112:476-503, 1913

MILLER, A.C. — HENDERSON, B.W. The influence of cellular glutathione content on cell survival following photodynamic treatment in-vitro. Radiat. Res. 107:83:94, 1986

MITCHELL, J.B. — McPHERSON, S., DeGRAFF, W., GAMSON, J., ZABELL, A., RUSSO, A. Oxygen dependence of hematoporphyrin derivative induced photoinactivation of Chinese hamster cells. Cancer Res. 45:2008, 1985

MOAN, J. — Photofrin photosensitization and phototherapy. Photochem. Photobiol. 43:681-690, 1986

MOAN, J. — Properites for optimal PDT sensitizers. J. Photochem. Photobiol. B:Biol. 5:521-524, 1990

MOAN, J. — CHRISTENSEN, T., SOMMER, S. The main photosensitizing components of hematoporphyrin derivative. Cancer Lett. 15:161-166, 1982

MOAN, J. — SOMMER, S. Oxygen dependence of photosensitizing effect of hematoporphyrin derivative in NHIK-3025 cells. Cancer Res. 45:1608-1610, 1985

MOAN, J. — STEEN, H.B., FEREN, D., CHRISTENSEN, T. Uptake of hematoporphryin derivative and sensitized photoinactivation of C3H cells with different oncogenic potential. Cancer Lett. 14:291-296, 1981

MORGAN, A.R. GARBO, G.N., KECK, R.W., SELMAN, S.H. New photosensitizers for photodynamic therapy: Combined effect of metallopurpurins and light on transplantable bladder tumors. Cancer Res. 48:194-198, 1988

MOSSMAN, B.T. GRAY, M.J., SILBERMAN, L., LIPSON, R.L. Identification of neoplastic versus normal cells in human cervical cell culture. Obst. Gync. 43:635-639, 1974

NEIRINCKX, R.D. CANNING, L.R., PIPER, I.M., NOWOTNIK, D.P., PICKETT, R.D., HOLMES, R.A., VOLKERT, W.A., FORSTER, A.M., WEISNER, P.S., MARRIOTT, J.A., CHAPLIN, S.B. Technetium 99m d,1-HM-PAO: A new radiopharmaceutical for SPECT imaging of regional cerebral blood perfusion. J. Nucl. Med. 28:191-202, 1987

NELSON, S. LIH-HUEI LIAW, ORENSTEIN, A., ROBERTS, W.G., BERNS, M.W. Mechanism of tumor destruction following photodynamic therapy with hematoporphyrin derivative, Chlorine, and Phthalocyanine. J. Nat. Cancer Instit. 80:1599-1605, 1988

NSEYO, U.O. DOUGHERTY, T.J., SULLIVAN L. Photodynamic therapy in the management of resistant lower urinary tract carcinoma. Cancer Res. 60:3113-3119, 1987

PANDEY, R.K. BELLNIER, D.A., SMITH, K.M., DOUGHTERY, T.J. Chlorine and porphyrin derivatives as potential photosensitizers and photodynamic therapy. Photochem. Photobiol. 53(1):65-72, 1991

PANDEY, R.K. DOUGHTERY, T.J. Synthesis and photosensitizing activity of porphyrins joined by ester linkages. Cancer Res. 49:2042-2047, 1989

PARAMSOTHY, M. ZAINUDDIN, J., LOW, K.S. In-vivo nuclear imaging studies of uptake and retention of Technetium 99 labelled HPD in murine tumor. Lasers Med. Sci. 14:205, 1989

PARLIAMENT, M.B. — CHAPMAN, J.D., URTASUN, R.C, McEWAN, A.J., GOLBERG, L., MERCER, J.R., MANNAN, R.H., WIEBE, L.I. Non-invasive assessment of human tumor hypoxia with $^{123}$I-Iodoazomycin arabinoside: Preliminary report of a clinical study. Br. J. Cancer (Submitted), 1991

PASS, H.I. — TOCHNER, Z., DELANEY, T., SMITH, P., FRIAUF, W., GLATSTEIN, E., TRAVIS, W. Intraoperative photodynamic therapy for malignant mesothelioma. Ann. Thoracic Surg. 50:687, 1990

PERLIN, D.S. — MURANT, R.S., GIBSON, S.L., HILF, R. Effects of photosensitization by hematoporphyrin derivative on mitochondrial adenosine triphosphatase-mediated proton transport and membrane integrity of R-3230-AC mammary adenocarcinoma. Cancer Res. 45:653-658, 1985

PRINSZE, C. — DUBBELMAN, T.M.A.R., van STEVENINCK, J. Protein damage, induced by small amounts of photodynamically generated singlet oxygen or hydroxyl radicals. Biochimica et Biophysica Acta, 1038:152-157, 1990

PROUT Jr. G.R. — LIN, C.W., BENSON, R., UNJIME, O., DALY, J.J., GRIFFIN, P.P., KINSEY, J., MAO-EN, T., LAO, Y.H., MIAN, Y.Z., CHEN, X., REN, F.M., QIAO, S.J. Phototherapy with hematoporphyrin derivative in the treatment of superficial transitional cell carcinoma of the bladder. New England J. Med. 317:1251-1255, 1987

RAAB, C. — Uber Die Wirkung Fluoreszierender Stoffe auf Infusoria Z. Biol. 39:524-526, 1900

RAUTH, A.M. — MILLIGAN, J.R., ZAMPERONI, R., McCLELLAND, R.A. 2-Nitroimidazole-glutathione reactions lead to DNA strand breaks. (Abstr) The 37th Radiation Research Society Meeting, Seattle 140, 1989

REED, M.W.R. — MILLER, F.N., WIEMAN, T.J. Microcirculatory effects of photo-activation of dihematoporphyrin ether. Excerpta Med. 825-826, 1987

REED, M.W.R. — MILLER, F.N., WIEMAN, T.J., TSENG M.T., PIETSCH, C.G. The effect of photodynamic therapy on the microcirculation. J. Surg. Res. 45:452-459, 1988

REED, M.W.R., — WIEMAN, T.J., SCHUSCHKE, D.A., TSENG, M.T., MILLER, F.N. A comparison of the effects of photodynamic therapy on normal and tumor blood vessels in the rat microcirculation. Rad. Res. 119:542-552, 1989

REYFTMANN, J.P. — KOHEN, E., MORLIERE, P., SANTUS, R., KOHEN, C., MANGEL, W.F., DUBERTRET, L., HIRSCHBERG, J.G. A microspectro-fluorometric study of porphyrin-photosensitized single living cells -1. Membrane alterations. Photochem. Photobiol. 44:461-469, 1986

RICCHELLI, F. — JORI, G. Factors influencing the distribution pattern of porphyrins in cell membranes. J. Photochem. Photobiol. B:Biol. 6:69-77, 1990

ROSENTHAL, I. — MURALI KRISHNA, C., RIESZ, P., BEN-HUR, E. The role of molecular oxygen in photodynamic effect of phthalocyanines. Radiat. Res. 107:136-142, 1986

ROWELL, N.P. — McCREADY, V.R., TAIT, D. FLOWER, M.A., CRONIN, B., ADAMS, G.E., HORWICH, A. Technetium-99m HMPAO and SPECT in the assessment of blood flow in human lung tumors. Br. J. Cancer 59:135, 1989

RYAN, U.S. — Endothelial cells. Vol. 1,2,3. CR Press Inc., Boaca Raton, Fl. 1988

RYAN, U.S. — WHITE, L., LOPEZ, M., RYAN, J.W. Use of micro-carriers to isolate and culture pulmonary microvascular endothelium. Tissue and Cell 14:597-606, 1982

SALET, C. MORENO, G. Photodynamic effects of hematoporphyrin on respiration and calcium uptake in isolated mitochondria. Int. J. Radiat. Biol. 39:227-230, 1981

SANDBERG, S. ROMSLO, I., HOVDING, G., BJORNDAL, T. Porphyrin induced photodamage as related to the subcellular localization of porphyrins. Acta Dermata Suppl. 100:75, 1982

SANTUS, R. KOHEN, C., KOHEN, E., REYFTMANN, J.P., MORLIERE, P., DUBERTRET, L., TOCCI, P.M. Permeation of lyosomal membranes in the course of photosensitization with methylene blue and hematoporphyrin: Study of cellular microspectrofluorometry. Photochem. Photobiol. 38(1):71-77, 1983

SANTUS, R. STOBBE, C.C., McPHEE, M.S, CHAPMAN, J.D. Protection against light-activated Photofrin II killing of tumor cells by nitroimidazoles. Radiat. Res. (Submitted), 1991

SCOURIDES, P.A. BOHMER, R.M., KAYE, A.H., MORSTYN, G. Nature of the tumor localizing components of hematoporphyrin derivative. Cancer Res. 47:3439-3445, 1987

SELMAN, S.H. KREIMER-BIRNABAUM, M., GOLDBLATT, P.J., ANDERSON, T.S., KECK, R.W., BRITTON, S.L. Jejunal blood flow after exposure to light in rats injected with hematoporphyrin derivative. Cancer Res. 45:6424, 1985

SELMAN, S.H. KREIMER-BIRNBAUM, M., KLAUNIG, J.E., GOLDBLATT, P.J., KECK, R.W., BRITTON, S.L. Blood flow in transplantable bladder tumors treated with hematoporphyrin derivative and light. Cancer Res. 44:1924-1927, 1984

SHULOK, J.R. KLAUNIG, J.E., SELMAN, S.H., SCHAFER, P.J., GOLDBLATT, P.J. Cellular effects of hematoporphyrin derivative photodynamic therapy on normal and neoplastic rat bladder cells. Amer. J. Path. 122:277-283, 1986

| | |
|---|---|
| SHUMAKER, B.P. | HETZEL, F.W. Clinical laser photodynamic therapy in the treatment of bladder cancer. Photochem. Photobiol. 46(5):899-901, 1987 |
| SINGH, G. | JEEVES, W.P., WILSON, B.C., JANG, D. Mitochondrial photosensitization by Photofrin II. Photochem. Photobiol. 46:645, 1987 |
| SPIKES, J.D. | New trends in photobiology (Invited review): Chlorins as photosensitizers in biology and medicine. J. Photochem. Photobiol. B:Biol. 6:259-274, 1990 |
| SPIKES, J.D. | JORI, G. Photodynamic therapy of tumors and other diseases using porphyrins. Lasers Med. Sci. 2(3):3-15, 1986 |
| SPRIK, S.A. | SULLIVAN, M.J., CAREY, T.E. In-vitro photosensitization of human head and neck squamous cells by dihematoporphyrin ether. Otolaryngology, Head and Neck Surgery 99:28-37, 1988 |
| STAR, W.M. | MARIJNISSEN, H.P.A., van den BERG-BLOK, A.E., VERSTEEG, J.A.C., FRANKEN, K.A.P., REINHOLD, H.S. Destruction of rat mammary tumor and normal tissue microcirculation by hematoporphyrin derivative photoradiation observed in-vivo in sandwich observation chambers. Cancer Res. 46:2532-2540, 1986 |
| STOZHKOVA, I.N. | MIRSKII, V.M. Model damage to cell membranes during photodynamic therapy: Photosensitization of planar lipid bilayer by hematoporphyrin dimethalester. Plenum Publishing Corporation. Bivll: Eksp. Biol. Med. 110(7):45-46, 1990 |
| SUTHERLAND, R.M. | Selective chemotherapy of non-cycling cells in an in-vitro tumor model. Cancer Res. 34:3501-3503, 1974 |
| THOMAS, J.P. | GIROTTI, A.W. Role of lipid peroxidation in hematoporphyrin derivative-sensitized photokilling of tumor cells: Protective effects of glutathione peroxydase. Cancer Res. 49:1682-1686, 1989 |

| | |
|---|---|
| THORNDYKE, C. | MEEKER, B.E., THOMAS, G., LAKEY, W.H., McPHEE, M.S., CHAPMAN, J.D. The radiation sensitivities of R3327-H and R3327-AT rat prostatic adenocarcinomas. J. Urol. 134:191, 1985 |
| TIETZE, F. | Enzymatic method for quantitative determination of nanogram amounts of total and oxidized glutathione: Applications to mammalian blood and other tissues. Annal. Biochem. 27:502-522, 1969 |
| TORINUKI, W. | MIURA, T., SEIJI, M. Lyosome destruction and lipid peroxide formation due to active oxygen generated from hematoporphyrin and UV radiation. Brit. J. Dermat. 102:17, 1980 |
| TROMBERG, B.J. | ORENSTEIN, A., KIMEL, S., BARKER, S.J., HYATT, J., NELSON, J.S., BERNS, M.W. Tumor oxygen tension during photodynamic therapy. J. Photochem. Photobiol. B:Biol. 5:121, 1990 |
| TSENG, M.T. | REED, M.W.R, ACKERMANN, D.M., SCHUSCHKE, D.A., WIEMAN, T.J., MILLER, F.N. Photodynamic therapy induced ultrastructural alterations in microvasculature of the rat cremaster muscle. Photochem. Photobiol. 48(5):675-681, 1988 |
| URTASUN, R.C. | CHAPMAN, J.D., FELDSTEIN, M.L., BAND, R.P., RABIN, H.R., WILSON, A.F., MARYNOWSKI, B., STARVELD, E., SHNITKA, T. Peripheral neuropathy related to misonidazole: Instance in pathology. Br. J. Cancer 37 (Suppl. 3):271-275, 1978 |
| URTASUN, R.C. | COLEMAN, C.N., WASSERMAN, T.H., PHILLIPS, T.L. Clinical trials with hypoxic cell sensitizers: Time to retrench or time to push forward. Int. J. Radiat. Oncol. Biol. Phys. 10:1691-1696, 1984 |
| VAN LEENGOED, E. | VERSTEEG, J., VAN-DER-VEEN, N. Tissue localizing properties of some photosensitizers studied by in-vivo fluorescence imaging. J. Photochem. Photobiol. B:Biol. 6:111-119, 1990 |

| | |
|---|---|
| VINDELOV, L.L. | CHRISTENSEN, I.J., NISSEN, N.I. Detergent-trypsin method for the preparation of nuclei for flowcytometric DNA analysis. Cytometry 3(6):323-327, 1983 |
| VOLDEN, G. | CHRISTENSEN, T., MOAN, J. Photodynamic membrane damage of hematoporphyrin derivative treated NHIK 3025 cells in-vitro. Photochem. Photobiophysics 3:105, 1981 |
| WALDOW, S.M. | DOUGHERTY, T.J. Interaction of hyperthermia and photoradiation therapy. Radiat. Res. 97:380-385, 1984 |
| WEISHAUPT, K.R. | GOMER. C.J., DOUGHERTY, T.J. Identification of singlet oxygen as a cytotoxic agent in photoinactivation of a murine tumor. Cancer Res. 36:2326-2329, 1976 |
| WEST C.M.L. | WEST, D.C., KUMAR, S., MOORE, J.V. A comparison of the sensitivity to photodynamic treatment of endothelial and tumor cells in different proliferative states. Int. J. Radiat. Biol. 58(1):145-156, 1990 |
| WHITEMORE, G.F. | VARGHESE, A.J. The biological properties of reduced nitroheterocycles and possible underlying biochemical mechanisms. Biochem. Pharmacol. 35:97-103, 1986 |
| WIEMAN, T.J. | MANG, T.S., FINGAR, V.H., HILL, T.G., REED, W.R., COREY, T.S., NGUYEN, V.Q., RENDER, E.R. Effect of photodynamic therapy on blood flow in normal and tumor vessels. Surgery 104:512-517, 1988 |
| WILKINSON, F. | BRUMMER, J.G. Rate constants for the decay and reactions of the lowest electronically excited singlet state of molecular oxygen in solution. Phys. Chem. Ref. Dat. 10:809, 1981 |

WILSON, B.C. — Photodynamic therapy: Light delivery and dosage for second generation photosensitizers. In photosensitizing compounds: Their chemistry, biology and clinical use. Wiley Chichester (Ciba Foundation Symposium 146) 60-77, 1989

WILSON, B.C. — JEEVES, W.P., LOWE, D.M. In-vivo and postmortem measurements of the attenuation spectra of light in mammalian tissues. Photochem. Photobiol. 42(2):153-162, 1985

WILSON, B.C. — PATTERSON, M.S., BURNS, D.M. Effect of photosensitizer concentration in tissue on the penetration depth of photoactivating light. Lasers Med. Sci. 1:235-244, 1986

WINTHER, J. — OVERGAARD, J. EHLERS, N. The effect of photodynamic therapy alone and in combination with misonidazole or x-rays for management of retinoblastoma-like tumor. Photochem. Photobiol. 47(3):419-423, 1988

WU, Q.Y. — DROUET, L., CARRIER, J.L., ROTHCHILD, C., BERARD, M., ROUALT, C., CAEN, J.P., MEYER, D. Different distribution of Von Willebrand factor in endothelial cells: Comparison between normal pigs and pigs with Von Willebrand disease. Arteriosclerosis 7(1):47-54, 1987

ZEMAN, E.M. — BROWN, J.M., LEMMON, M.J., HIRST, V.K., LEE, W.W. SR-4233 A new bioreductive agent with high selective toxicity for hypoxic mammalian cells. Int. J. Radiat. Oncol. Biol. Phys. 12:1239-1242, 1986

# VITA

| | |
|---|---|
| Name: | **Ronald Brian Moore** |
| Place of Birth: | Edmonton, Alberta, Canada. |
| Date of Birth: | July 1, 1958 |
| Martial Status: | Married, Wife: Jo-Anne Marie<br>Three Children: Thomas, 6<br>Sarah, 4<br>Nathan, 2 |

Education:

| | |
|---|---|
| 1989 - 1991 | Graduate Studies<br>PhD Experimental Surgery<br>Urology Research<br>University of Alberta |
| 1989 - 1990 | Postgraduate Medical Education PG-4<br>Urology Residency R3<br>Urology Research<br>Cross Cancer Institute |
| 1989 | Royal College of Physicians and Surgeons<br>Principles of Surgery |
| 1988 - 1989 | Postgraduate Medical Education PG-3<br>Urology Residency R2<br>University of Alberta |
| 1987 - 1988 | Postgraduate Medical Education PG-2<br>General Surgery Residency R1<br>University of Alberta |
| 1986 - 1987 | Postgraduate Medical Education PG-1<br>Rotating Internship St. Paul's Hospital<br>Vancouver, British Columbia |
| 1986 | L.M.C.C. |
| 1982 - 1986 | Faculty of Medicine<br>University of Alberta |
| 1980 - 1982 | Faculty of Science<br>(Biochemistry/Genetics)<br>University of Alberta |
| 1977 - 1980 | B.Sc. General<br>University of Alberta |

Awards:

Dr. C.T. Wolan Award 1991
Prairie Urologic Association

American College of Radiology Jr. Investigator Award 7th International Conference on Chemical Modifiers in Cancer Treatment Clearwater FL. 1991

Alberta Heritage Foundation For Medical Research Full-Time Fellowship Award

Dr. C.T. Wolan Award 1990
Prairie Urologic Association

Alberta Cancer Board
McCartney Research Fellowship 1989
Declined

Dr. C.T. Wolan Award 1989
Prairie Urologic Association

M.D. Honors First Class Standing
Faculty of Medicine 1986

Conn Memorial Medal in Obstetrics and Gynecology 1986

First Class Honors in Research
(Ph.D. in Medical Sciences Committee) 1985

Donald A. Stafford Memorial Scholarship in Cancer Research 1983

Michael Emery Memorial Fund Award
Student Research 1983

Alberta Heritage Foundation for Medical Research Summer Studentship 1981, 1982, 1983.

Scientific Publications:

Moore, R.B.; Chapman, J.D.; Mercer, J.R.; Mannan, R.H.; Wiebe, L.I.; McEwan, A.J.; McPhee, M.S.: Measurement of Photodynamic therapy induced hypoxia in the Dunning prostatic tumor model by $^{123}$I-Iodoazomycin arabinoside. Int. J. Rad. Oncol. Biol. Phys. (Submitted) 1991

Moore, R.B.; Chapman, J.D.; Mokrzanowski, A.D.; Arnfield, M.R., McPhee, M.S.; McEwan, A.J.: Non-invasive monitoring of photodynamic therapy with $^{99}$Technetium HMPAO scintigraphy. (Submitted) 1991

Mador, D.; Ritchie, B.; Meeker, B.; Moore, R.; Elliott, F.G.; McPhee, M.S.; Chapman, J.D.; Lakey, W.H.: Response of the Dunning R3327H Prostatic Adenocarcinoma to Irradiation and Various Chemotherapeutic Drugs. Journal of Cancer Research 1982

McPhee, M.S.; Mador, D.R.; Tulip, J.; Ritchie, B.; Moore, R.B.; Lakey, W.H.: Segmental Irradiation of the Bladder with Neodymium Y.A.G. Laser Irradiation. Journal of Urology 1982.

Presentations:

Moore, R.B.; Chapman, J.D.; McPhee, M.S.; McEwan, A.J.: Measurement and Exploitation of Hypoxia induced by Photodynamic Therapy. 7th International Conference on Chemical Modifiers of Cancer Treatment. February, 1991 (Recipient of ACR Junior Investigator Award)

Moore, R.B.; Chapman, J.D.; McPhee, M.S.: An in-vitro Tumor Model for Prostatic Carcinoma: Radiobiological Response of R3327-AT Single Cells and Multicellular Spheroids. Prairie Urological Association, Lake Louise, Alberta, March 1991 (Recipient C.T. Wolan Award).

Moore, R.B.; Chapman, J.D.; Mokrzanowski, A.D.; Meeker, B.E.; Stobbe, C.C.; McEwan, A.J.; McPhee, M.S.: Potentiation of Photodynamic Therapy by Bioreductive Chemotherapy, International Photodynamic Association 3rd Biennial Meeting, Buffalo, New York, July 1990

Moore, R.B.; Tulip, J.; McPhee, M.S.: Calculi Photofragmentation with a New Long-Wavelength Nd:Yag Laser Canadian Urological Association, Vancouver, B.C., June 1990

Moore, R.B.; Chapman, J.D.; McPhee, M.S.; McEwan, A.J.: Measurement and Exploitation of Photodynamic Therapy Induced Vascular Damage. Radiation Research Society 38th Annual Meeting, New Orleans, Louisiana, April 1990

Moore, R.B.; Mokrzanowski, A.D.; Stobbe, C.C.; Chapman, J.D.; McPhee, M.S.; McEwan, A.J.: Measurement and Exploitation of Vascular Damage Induced by Photodynamic Therapy. Prairie Urological Association, Lake Louise, Alberta, March 1990 (Recipient C.T. Wolan Award).

Moore, R.B.; Lakey, W.H.; Mador, D.: Continent Total Bladder Replacement Following Radical Cystoprostatectomy; Small versus Large Bowel Substitution. Prairie Urologic Association Meeting. Kananaskis, Alberta, 1989 (Recipient C.T. Wolan Award).

Moore, R.B.; McPhee, M.S.: Biodistribution of Tritium Labelled Hematoporphyrin Derivative (3H-HpD) in the Dunning R3327-AT Rat Prostatic Cancer Model. Sixteenth Annual Students Research Day, 1982 (Recipient of the Michael Emery Memorial Award).